Oxygen, metabolism, and population growth across marine fishes

by

Sarah Gravel

B.Sc. (Biology, Hons.), McGill University, 2018

Thesis Submitted in Partial Fulfillment of the
Requirements for the Degree of
Master of Science

in the
Department of Biological Sciences
Faculty of Science

SIMON FRASER UNIVERSITY
Summer 2023

Declaration of Committee

Name:	**Sarah Gravel**
Degree:	**Master of Science**
Title:	**Oxygen, metabolism, and population growth across marine fishes**
Committee:	**Chair:** **David J. Green** Professor, Biological Sciences
	Nicholas K. Dulvy Supervisor Professor, Biological Sciences
	John D. Reynolds Committee Member Professor, Biological Sciences
	Amanda E. Bates Examiner Professor, Biology University of Victoria

Abstract

The maximum intrinsic rate of population increase (r_{max}) estimates population growth at low abundance, and varies with size, temperature, and depth, suggesting a metabolic basis for population dynamics. Additionally, recent advances in aquatic ecophysiology have highlighted that oxygen supply constrains metabolic traits. Yet, little is understood of how r_{max} relates to metabolic rate across fishes, and how both are shaped by environmental oxygen. In this thesis, I conducted a comparative analysis of metabolic rate, r_{max}, and environmental oxygen for sharks and teleosts. First, I investigated the relationship between metabolic rate and r_{max}, finding that species with lower metabolic rates also had lower r_{max}. Next, I tested how metabolic rate and r_{max} are related to environmental oxygen, and found that both increased with oxygen availability. My findings support that species with slower metabolism (e.g., sharks, or low-oxygen inhabitants) exhibit slower population growth, and hence are more intrinsically sensitive to overfishing.

Keywords: Bayesian phylogenetic regression; environmental oxygen limitation; life-history theory; oxygen demand; population dynamics; speed-of-life continuum

Acknowledgements

I am grateful beyond words for the love and support I have received from family, friends, and collaborators over the past three years. Needless to say that this thesis would not have been possible without these folks, but I'm going to say it anyway.

First, a massive thank you to my primary supervisor Nick Dulvy, for inviting me to join your lab all those years ago and for granting me this life-changing opportunity. Thank you for challenging me to do my best and for helping me to accomplish more than I ever thought I'd be capable of. I'm grateful for these projects we've built up together over the years, and for the creative freedom you gave me to pursue my ideas for this thesis. I have learned so much from you and my time in the Dulvy Lab has really taught me a lot about myself, both as a scientist and as a person. A big thank you also to John Reynolds for being so generous with your time and wisdom in committee meetings, which I always left with lifted spirits.

Huge thank yous to my collaborators for contributing their skills and insightful perspectives to this work, and for their constant encouragement and support throughout. Jenny Bigman – I don't know how I would have completed this work without your expertise and big heart. I'm very grateful to have had the pleasure to know and work with you despite not overlapping much during our degrees at SFU. Big thanks also to Seb Pardo for your contributions to this work and for being a kindred spirit and fast friend. I am so thankful for our long chats about complex topics in ecology, R coding issues, and anything else going on in life. And thanks to Serena Wong for being the first person to help me open the huge can of worms that is metabolic scaling theory. I really appreciated those whiteboard drawings and your patient explanations in the early days. I also want to thank the graduate students, postdocs, and research assistants of the past and present Dulvy Lab for their kind support and stellar feedback: Wade, Samm, Tanya, Danielle, Helen, Rachel, Nathan, Jess, Ellen, Maryam, and Amanda. And thanks to the Dulvy Lab research assistants Anthony, Eric, and Jay for being great conference and "field work" buddies, and for the fond memories of inside jokes and uninhibited laughter as we tried to stomach the smell of 100something-year-old preserved sharks.

Thanks to my day 1 E2O buddies and favourite salmon enthusiasts Anna and Nico around whom I immediately felt like I belonged in this new city, and Sara for making me

feel like I never left Quebec. And thanks to my favourite “bird person” Lena, for bringing me along birding, biking, or slacklining around the neighborhood. And also thanks to all of the other exceedingly bright scientists and big hearts in E2O and the department. I feel very privileged to have been a part of such a wonderful collective.

Thank you to my friends outside of academia who have been with me on this journey: Etia, Lara, Sarah & baby Mila, Gab, Helene, Myriam, Diana, John, Lysanne, Nader, Clarissa, Jeff, Dave, Raina, Leanne, Hannah, Logan, Guillaume, Laurianne, and many others I am fortunate to have felt close to. I love you all so much and want to thank you for more laughs and video calls than I can count. Thank you for being a constant reminder of how much more to life there is than grad school. And a special thanks to my roommate Diana for being a good friend, support system, shoulder to cry on, and source of entertainment since I first arrived in Vancouver before my ‘pandemic master’s’. Thanks for being my rock all through grad school. And thank you to my partner Marçal, for accepting me in all my forms and for being a daily source of relief, happiness, colourfulness, and love.

And above all, I want to thank my family. Words cannot fully describe how grateful I am for you every day and what you mean to me, but I will do my best to elaborate a bit. Thank you to my mother Donna for being a constant source of light, comfort, and love for me and all those who are blessed to have you in their lives. Thanks to my dad Eric for teaching me so much of what I know, and for always being there to fill in the gaps when I don’t know how. And thank you to my sister Dominique for being the most kind-hearted, vibrant, and inspiring little sister in the world. Every moment in your presence I feel better off than I was before. I love you all so much and thank you for your unconditional love, generosity, and support in all things I do, always.

Table of Contents

List of Tables

List of Figures

Chapter 1.

The metabolic basis of population growth in marine fishes

1.1. Abstract

The maximum intrinsic rate of population increase (r_{max}) represents a population's maximum capacity to replace itself and is central to fisheries management and conservation. Species with low maximum population growth rates typically have slow life histories. By extension, species with slow life histories, such as many sharks, generally have higher intrinsic sensitivity to overfishing compared to species with faster life histories, such as teleosts. Here, we posit that this difference in the speed of life histories is due to differences in metabolic rates. Specifically, we ask whether variation in r_{max}, or any of its component life-history traits, explain variation in metabolic rates (resting, maximum, and aerobic scope) across 84 shark and teleost species, while accounting for the effects of temperature, body mass, ecological lifestyle, and evolutionary history. Using an information theoretic approach, we find that species with slow population growth (lower r_{max}) generally had lower maximum metabolic rates and narrower aerobic scopes. Overall, r_{max} and the underlying time-related life history traits (age-at-maturity and maximum age) were more important in explaining variation in metabolic rates than annual reproductive output, and the connection between life histories and metabolism was stronger for maximum metabolic rate and aerobic scope compared to resting metabolic rate. Our work suggests that differences in metabolic rates between sharks and teleosts may underlie variation in the speed of life histories, and hence, explain why sharks have slower life histories and are more intrinsically sensitive to overfishing.

1.2. Introduction

Marine fishes exhibit a vast range of life histories resulting in considerable variation in their sensitivities to overfishing (Kindsvater et al. 2016, Hutchings 2021). Under the selective pressures of a given environment, life history traits evolve depending on how individuals partition resources among survival, growth, and reproduction, resulting in trait combinations that maximize fitness and underlie population dynamics

(Stearns 1992, Hutchings 2021). Consequently, these traits tend to co-evolve and cluster along at least three axes of life history variation: size-related traits (e.g., body size, length-at-maturity), time-related traits (e.g., maximum age, age-at-maturity), and reproductive allocation (Juan-Jordá et al. 2013). In general, species with faster life histories exhibit faster growth, earlier maturity, smaller maximum body size, a shorter lifespan, and invest proportionally more of their resources towards annual reproductive output (Denney et al. 2002, Hutchings 2021). Therefore, species on the fast end of the continuum have faster population growth rates than species on the slower end of the continuum (Reynolds 2003, Juan-Jordá et al. 2013). One such measure of population growth, the maximum intrinsic rate of population increase, r_{max}, is the average annual number of female spawners produced per female spawner at low population density, and hence is directly related to a species' inherent sensitivity to overfishing (Myers et al. 1997, Myers & Worm 2005, Pardo et al. 2016).

Population growth rates likely vary with body size and temperature (and hence, depth and latitude) in the ocean. Generally, populations and species in warmer (tropical and/or shallow) habitats likely have faster life histories and r_{max} compared to their deeper or higher-latitude relatives in cooler waters (Drazen & Haedrich 2012, Barrowclift-Mahon et al. 2023). However, the effect of temperature is dependent on body size: the positive relationship of r_{max} with temperature becomes negligible at larger body sizes, and r_{max} in sharks has been found to decrease with depth independently of temperature (Drazen & Haedrich 2012, Pardo & Dulvy 2022). These spatial patterns in r_{max} are consistent with the temperature-size rule and the oxygen limitation hypothesis, and suggest an underlying connection to metabolic rate, which also varies with body size and temperature (Brown et al. 2004, Savage et al. 2004).

Metabolism reflects the rate of resource uptake, transformation into available energy, and allocation to survival, growth, and reproduction (Brown et al. 2004). Metabolic rates are well-known to scale with body size and temperature across species, as well as relate to life histories and population dynamics (Brown et al. 2004, Savage et al. 2004, White et al. 2022). However, not all life history traits have been consistently linked to metabolic rate, and recent work has suggested that integrative traits (i.e., those that account for a trade-off between individual life history traits) are more related to overall fitness and, therefore, metabolic rate (Pettersen et al. 2016). For example, Wong et al. (2021) found that growth performance (a trait that integrates the trade-off between

somatic growth rate and maximum size) explained more variation in resting metabolic rate than these traits alone across 104 fishes. Indeed, variation in r_{max} among determinate-growing vertebrates, including mammals, has also been linked to metabolic rate (Savage et al. 2004, Duncan et al. 2007). However, it remains to be determined whether there is a broadscale, interspecific relationship between metabolic rate and r_{max} in fishes that grow indeterminately throughout their life.

The resting metabolic rate (RMR) of an organism has become the default measure used in metabolic theory and comparative life history analyses due to its widespread availability (White et al. 2013, Brown et al. 2004). The costs associated with activity, growth, and reproduction are all above maintenance costs, however, and are best approximated by other measures of metabolic rate, such as the maximum metabolic rate (MMR) or the difference between maximum and resting metabolic rate, known as the absolute aerobic scope (AS=MMR-RMR; Clark et al. 2013). Indeed, previous work has identified that MMR and AS are more related to life history and fitness compared to RMR (Clavijo-Baquet & Bozinovic 2012, Auer et al. 2017, Arnold et al. 2021). Thus, while using RMR is potentially limiting to our understanding of how metabolic rate relates to life histories and population dynamics, relatively few studies have examined the interrelationships among types of metabolic rate, life histories, and population growth rate, particularly for fishes (Auer et al. 2017, Clark et al. 2013, Killen et al. 2016).

Here, we examine whether variation in RMR, MMR, and AS relates to variation in r_{max} and its component life history traits (i.e., age-at-maturity, maximum age, and reproductive output) across 84 fishes, comprising 47 teleosts and 37 chondrichthyans (24 sharks, 12 rays, and 1 chimaera, hereafter referred to as “sharks”), whilst accounting for body mass, temperature, and evolutionary history. Further, because pelagic species are generally more active than benthic species, we also consider the effect of “ecological lifestyle”, where species were categorized as either pelagic, benthopelagic, or benthic (Bigman et al. 2018, Killen et al. 2016). Specifically, we ask two questions: (1) do fishes with lower metabolic rates have slow life histories (late maturation, long lifespan, and low reproductive output), and (2) do fishes with lower metabolic rates have lower r_{max} (a composite of these life history traits)?

As RMR, MMR and AS are biological rates, we expect these to be better associated with time-related traits (the age-at-maturity or maximum age) than with reproductive traits (in this case, reproductive output; Juan-Jordá et al. 2013). We also predict that metabolic rate will be best related with the integrative trait r_{max} compared to its component traits (Wong et al. 2021). More specifically, we predict that species with higher metabolic ceilings (MMR) and larger energetic budgets (AS) will generally exhibit higher r_{max}. Additionally, due to the inevitable maintenance costs (RMR) incurred to support high MMR (Killen et al. 2016), we also expect RMR to exhibit shallower (but still positive) scaling with r_{max} compared to MMR and AS.

1.3. Methods

To assess whether life histories and r_{max} explained variation in metabolic rate, we collated data for resting and maximum metabolic rate (RMR and MMR, respectively), along with the measurement body mass and measurement temperature associated with each metabolic rate estimate, for marine fishes. Aerobic scope (AS) was then calculated as MMR minus RMR if not reported directly in the study (Clark et al. 2013, Killen et al. 2016). Next, we collated the life history traits necessary to calculate population-specific maximum intrinsic population growth (r_{max}) values for the same species that had metabolic data.

We matched metabolic rate and life history data at the population scale. Specifically, data were considered to be from the same population if both the life history and metabolic rate data were collected from individuals from the same stock, from a nearby location, or, at the very least, within the same marine ecoregion province (Spalding et al. 2007; see Supplementary Methods ‘SM’ in Appendix A for more information on the population matching of metabolic rate, life history, and stock-recruitment data). When metabolic rate data and life history data could not be population-matched, values were preferred for inclusion in our dataset based on geographic proximity. Below, we detail the specifics regarding the metabolic rate and life history data collection.

1.3.1. Metabolic rate data collation, selection, and aggregation

For both RMR and MMR, we collated raw and mean estimates of population-specific metabolic rates, supplementing pre-existing RMR and MMR datasets from recent meta-analyses (Wong et al. 2021, Auer et al. 2017, Killen et al. 2017). We searched for studies reporting metabolic rates for marine fishes using Google Scholar using search terms that included “fish” followed by “maximum”/“active” or “resting”/“standard” AND “metabolic rate”, “oxygen uptake”, or “oxygen consumption”, OR other keywords such as “energetics” and “respirometry”. We limited the scope of this study to marine fishes, including brackish or anadromous species (i.e., where part of the range is in the marine environment), for which we favoured metabolic studies conducted in saltwater.

We created criteria for inclusion in our dataset due to the breadth of body sizes and temperatures at which metabolic rate is estimated across ectothermic, indeterminately growing fishes, and the type of metabolic rate (i.e., whether the metabolic rate is categorized as resting, maximum, etc.). First, we retained metabolic rate data from a given study for older stages (i.e., no embryos or larvae) only if the associated body mass of the individual/species and measurement temperature were reported. If only a range of masses or temperature was given, the median was used. Second, we ensured each metabolic rate estimate adhered to the standard conditions for measuring the respective type of metabolic rate. For RMR, we retained only those data measured in undisturbed, quiescent, and fasted fish displaying little to no movement in the respirometry chamber, and in the absence of potential stressors (e.g., minimizing auditory or visual stimuli, no salinity, oxygen or temperature stress, allowing sufficient acclimation time in the respirometer, etc.; Chabot et al. 2016). For highly active or obligate ram-ventilating species that swim continuously, RMR estimates are approximated by extrapolating a metabolic rate–swimming speed relationship to a speed of zero (commonly referred to as the immobile metabolic rate, ‘IMR’; Brill 1987). MMR was included from those studies that used an exercise or air exposure protocol and measured in actively swimming organisms or during the recovery period following exertion (Killen et al. 2017, Auer et al. 2017). When several methods were implemented within the same study, the method eliciting the highest MMR values was preferred.

For analysis, all metabolic rate data were averaged by study to generate a species-mean value. Only one study per species was chosen to avoid giving undue weight to species with multiple studies over species with fewer data points and preference was given to the metabolic study using individuals sourced from the same population as the available life history data, or in the case for teleosts the spatial domain of the stock-recruitment data (required for the calculation of r_{max} for teleosts; see Methods section 2.2.2. below). If a given study repeated measurements on individuals at different temperatures, data were averaged within the temperature treatment (i.e., for repeated metabolic rate measurements on individuals at multiple temperature treatments, metabolic rate data was averaged for a given treatment; Killen et al. 2016, Wong et al. 2021). A correction factor of 3.5˚C was added to the measurement temperature of all partial endothermic species (i.e., lamnid sharks and tunas; Pardo & Dulvy 2022). Because sample size and temperature treatments varied across studies, we created two datasets, one where a study was included based on the temperature treatment closest to 15˚C ('temperature dataset') and one with the largest sample size ('sample size dataset'). Overall, the results of the analyses were not sensitive to the choice of dataset used, and therefore we present the results based on the dataset with the largest sample size (for results based on the mean temperature dataset, see Tables A.2-4 in Appendix A).

1.3.2. Life history data collation and selection at the population level

For sharks, r_{max} was calculated from species-mean estimates of age-at-maturity, maximum age, and reproductive output (Pardo et al. 2016). Age-at-maturity is the age by which 50% of the individuals have reached maturity. Maximum age was taken as the maximum observed (validated) rather than theoretical maximum age, where possible. These traits were collated from stock assessments and other primary literature, and online databases such as The IUCN Red List of Threatened Species (Dulvy et al. 2021, IUCN 2022), FishBase (Froese & Pauly 2019) and Sharkipedia (Mull et al. 2022). For teleosts, stock-recruitment time series data were compiled from the RAM Legacy Stock Assessment Database (hereafter, 'RAM'; Ricard et al. 2012), which were population-matched to the metabolic rate data (see the SM in Appendix A for more detail). Once stocks had been matched at the finest possible spatial scale, mean life history parameter estimates (age-at-maturity, maximum age), length-weight regressions, and von

Bertalanffy growth parameters required for the calculation of r_{max} (section 1.3.3 below and SM section A.1.4) were collated from RAM when available, and otherwise, from stock assessments, the primary literature, or databases (IUCN Red List and FishBase). Teleost annual reproductive output was calculated based on estimates of maximum spawners per spawner used in the calculation of r_{max} and estimates of the survival to maturity.

For inclusion in our life history trait dataset, we prioritized (in order): (1) population-matched data (of the metabolic rate), (2) when no match was available, life history data was mined for the nearest population with available data, (3) data from females, otherwise, estimates were taken for both sexes combined, (4) the year of the study, where the most recent was included, and (5) studies with larger sample sizes and body size ranges (for length–weight regressions and von Bertalanffy parameters).

1.3.3. Calculation of the maximum intrinsic rate of population increase r_{max}

We calculated r_{max} for all sharks and teleosts in our dataset for which the required population-specific life history data on reproductive output, maximum age, and age-at-maturity were available. Sharks and teleosts differ in their life histories and population dynamics and, as such, r_{max} is calculated slightly differently for each group (Hutchings et al. 2012, Pardo et al. 2016). Below, we define shark- and teleost-specific methods (where required) based on standard practices (Cortés 2016, Pardo et al. 2016).

Shark r_{max}

We calculated r_{max} for sharks following Pardo et al. (2016) and Cortés (2016), based on four traits: age-at-maturity, maximum age, litter size, and breeding interval (i, in years). Annual reproductive output b (number of daughters) was calculated as $b = 0.5 * f/i$, where fecundity f is equivalent to the average litter size (average number of pups, uterine embryos, or egg cases, depending on the reproductive mode of the species and data available), and the sex ratio is assumed to be 1:1 to calculate the number of females per litter. More details on the calculation of r_{max} for sharks can be found in the SM for Appendix A.

Teleost r_{max}

For teleosts, the relationship between fecundity and female size is nearly universally positive (and therefore, fecundity cannot be assumed to be constant), and density dependence is an important component of population dynamics (Myers et al. 1997). For these species, we calculated r_{max} following standard practices outlined in Myers et al. (1997, 2001), Denney et al. (2002), and Goodwin et al. (2006), based on estimates of age-at-maturity, maximum age, stock spawner-recruitment time series data (from RAM; Ricard et al. 2012), and any required conversion relationships (length-weight and von Bertalanffy equations). See Appendix A for more details on the calculation of r_{max} and estimation of annual reproductive output b for teleosts.

1.3.4. Statistical analyses

We used a phylogenetic Bayesian modeling framework and an information-theoretic approach to assess whether life histories and r_{max} explain variation in metabolic rate across fishes. For all models, measurement body mass was converted to grams, measurement temperature was converted to inverse temperature, and metabolic rate was converted to Watts (Joules·s^{-1}) following Grady *et al.* (2014). The inverse temperature was parameterized as the Boltzmann-Arrhenius formulation, $-\mathrm{E}/\mathrm{kT}$, following Gillooly *et al.* (2001), where E is the activation energy, k is the Boltzmann constant (8.617×10^{-5} eV) and T is the temperature in Kelvin. All covariates (with the exception of temperature) and the response variable (metabolic rate) were natural log-transformed, following which all covariates were centered and scaled (i.e., standardized) using the function *scale* in R. All models included a phylogenetic random effect to account for phylogenetic non-independence among residuals because of the evolutionary relatedness between species. We constructed a supertree from a molecular chondrichthyan tree (Stein et al. 2018) and a teleost tree from the Fish Tree of Life (Rabosky et al. 2018), and only species present in the resulting phylogeny were included in our analyses. All models were fitted in Stan using the *brms* package v.2.14.4 (Bürkner 2017) in R v.4.0.5 (R Core Team 2021).

Do fishes with low metabolic rates have slower life histories?

Specifically, we tested whether variation in metabolic rate was explained by any of the life history trait components of r_{max} (age-at-maturity, maximum age, and

reproductive output), to which end we fitted 12 models. Models were parameterized building on the relationship among metabolic rate, body mass, temperature, and ecological lifestyle, the 'null model' (e.g., following Gillooly et al. 2001, Brown et al. 2004, Bigman et al. 2018). We then added in either age-at-maturity, maximum age, or reproductive output. For example, the response variable was either RMR, MMR, or AS and the covariates were body mass, temperature, ecological lifestyle (benthic, benthopelagic, pelagic), and one life history trait.

We then used model selection to identify the model(s) with most support for each metabolic rate type. Specifically, we used the LOO information criterion value (looic) implemented in the *loo* package (Vehtari et al. 2017), where all models within looic < 2 of the top-ranked model (lowest looic value) have similar support.

Do fishes with low metabolic rates have lower r_{max}?

We fitted three additional models to examine whether the integrative trait r_{max} explained variation in metabolic rate (for RMR, MMR, and AS). As above, models were parameterized building on the relationship among metabolic rate, body mass, temperature, ecological lifestyle, and then adding r_{max}. To assess whether r_{max} better explained variation in metabolic rate compared to its composite life history traits (or null model, if top model), we compared these models (with r_{max}) to the model(s) with the most support for each metabolic rate type from the previous question.

1.4. Results

We compiled population-specific metabolic rate and life history data required for the calculation of r_{max} for 84 marine fish species (37 sharks and 47 teleosts). The maximum intrinsic rate of population increase, r_{max}, ranged from 0.04 to 0.57 in sharks (in the Greenland shark, *Somniosus microcephalus*, and the nursehound, *Scyliorhinus stellaris*, respectively) and 0.04 to 2.25 in teleosts (in the bigeye tuna, *Thunnus obesus*, and the lesser sandeel, *Ammodytes tobianus*, respectively). Overall, the r_{max} of sharks was less than half that of teleosts (median for sharks = 0.29 ±0.03 SE [standard error of the median]; teleosts = 0.61 ±0.07 SE; fig. 1). Although there are inevitable nuances in the methods by which r_{max} is calculated for sharks and teleosts (namely, in the estimation of natural mortality and of the maximum annual reproductive rate $\tilde{\alpha}$, which we highlight in the Methods and the SM of Appendix A), the lower r_{max} of sharks relative to

teleosts is likely due to their later age-at-maturity (median for sharks = 7.5 ±0.73 SE; teleosts = 2.9 ±0.19 SE), greater maximum age (median for sharks = 20 ±1.80 SE; teleosts = 17 ±1.73 SE), and lower reproductive output (median for sharks = 3 ±0.46 SE; teleosts = 18.7 ±3.74 SE). However, to ensure that the shark and teleost r_{max} methods produced reasonably comparable values of r_{max}, we also calculated r_{max} values using both reproductive traits from the literature (shark r_{max} method) and stock-recruitment time series data (teleost r_{max} method; see SM in Appendix A) for 5 shark species for which spawner-recruit time series were available. Both methods yielded similar values of r_{max} for the 5 species (see Supplementary Results section A.2).

For all models, the addition of ecological lifestyle as a fixed factor (intercept effect) accounted for a great deal of variation in RMR, MMR, and AS, where pelagic species had higher metabolic rates than benthopelagic species, which, in turn, had higher metabolic rates than benthic species (Table 1.3). Thus, we present only the results based on models including ecological lifestyle (see Table A.1 for comparisons of models with and without ecological lifestyle).

Do fishes with low metabolic rates have slower life histories?

Overall, metabolic rates were better explained by time-related traits compared to annual reproductive output, where species with lower metabolic rates were relatively later-maturing and longer-lived (Figure 1.1, Table 1.1, Figures A.3-5). For RMR, the model with age-at-maturity ranked highest (looic=152.0) and performed slightly better than the model with just mass and temperature (looic=155.8; Table 1.1, Figure 1.1a), further evidenced by a negative slope of -0.25 (95% BCI: -0.47 to -0.02, 100% of the posterior distribution < 0; Table 1.3). For MMR, no models with single life history traits explained more variation than the model with just mass and temperature (Table 1.1b). Although it is worth noting the considerable (negative) effect size of age-at-maturity on MMR (mean slope = -0.32, 95% BCI: -0.52 to -0.10, 100% of the posterior distribution < 0; Table 1.3), the inclusion of this trait appeared to reduce the amount of variation explained by temperature and was less parsimonious than the model with just mass and temperature (Table 1.1b). Similarly, AS scaled with age-at-maturity with a negative slope of -0.38 (95% BCI: -0.63 to -0.10, 100% of the posterior distribution < 0; Table 1.3). Although the AS model with age-at-maturity ranked higher (looic=75.3) than the model

with just mass and temperature (looic=77.0), the model with just mass and temperature was the more parsimonious of the two (Table 1.1c).

Do fishes with low metabolic rates have lower r_{max}?

Species with lower maximum metabolic rates (MMR) and narrower aerobic scopes (AS) also had slower population growth rates (lower r_{max} values) after accounting for body mass, temperature, ecological lifestyle, and phylogenetic relatedness (Table 1.2, Figure 1.1dhl, and Figure A.2). For example, the pelagic skipjack tuna, *Katsuwonus pelamis*, had relatively higher r_{max} and MMR than the similarly-sized benthopelagic Pacific spiny dogfish, *Squalus suckleyi*, even after accounting for differences in body mass, temperature, and ecological lifestyles (Figure 1.2). Similarly, looking at the smaller end of the body size range, the r_{max} and MMR of the pelagic Peruvian Anchoveta, *Engraulis ringens*, was greater than that of the similarly-sized benthic Epaulette Shark, *Hemiscyllium ocellatum*, after accounting for the effects of body mass, temperature, and ecological lifestyle (Figure 1.2). Overall, the model with measurement body mass, measurement temperature, and r_{max} was the highest ranking and best model for both MMR and AS (Table 1.2bc). Specifically, the MMR model with r_{max} had significantly more support (looic=36.7) than the model with just mass and temperature (looic=46.4), evidenced by a positive slope of 0.43 (95% BCI: 0.26 to 0.60, 100% of the posterior distribution > 0; Table 1.2b, Table 1.3). Similarly, the AS model including r_{max} had more overall support (looic=64.5) than the models without (looic=77.0 and 75.3 for the null and age-at-maturity models, respectively; Table 1.2c), where AS increased with r_{max} with a positive slope of 0.51 (95% BCI: 0.28 to 0.73, 100% of the posterior distribution > 0; Table 1.3). For RMR, there was considerable support for a positive relationship with r_{max}, as 96% of the posterior distribution was greater than zero (mean slope=0.16, 95% BCI: -0.02 to 0.33; Table 1.3). However, the model with age-at-maturity had slightly more support (looic=165.1) than the model with r_{max} (looic=168.3; Table 1.2a).

1.5. Discussion

Overall, we found that species with slower life histories (with low r_{max} and late age-at-maturity) had lower metabolic rates. Specifically, maximum metabolic rate (MMR) and absolute aerobic scope (AS) were positively related to r_{max}, while resting metabolic rate (RMR) was less strongly (but positively) related to r_{max}. Additionally, metabolic rates

were negatively related to the age-at-maturity, a time-related component of r_{max}. Next, we consider (1) why metabolic rates were generally better explained by time-related traits (r_{max} and age-at-maturity), (2) why the integrative trait of r_{max} was generally more closely related to metabolic rate than its component life history traits, (3) why MMR and AS were more strongly related to r_{max} than RMR, (4) the conservation implications of our findings.

Our findings are consistent with the speed-of-life continuum, which posits that species with faster life histories (e.g., early maturity, short-lived, faster population growth) have faster metabolic rates (Auer et al. 2018, Pettersen et al. 2016, Wong et al. 2021). Specifically, metabolic rates were found to be better associated with time-related traits (r_{max} and age-at-maturity) than size and reproductive traits (this study, Wong et al. 2021). Indeed, metabolic rate is often itself viewed as the most fundamental biological rate in ecology (Brown et al. 2004). And although maximum body size is most commonly associated with r_{max} in life history and risk assessments (primarily for sharks), age-at-maturity has been found to be better (negatively) correlated with r_{max}, while size or reproductive traits, such as maximum body size and fecundity, have been found to be less well related to r_{max} across fishes (Hutchings et al. 2012, Juan-Jordá et al. 2013).

In addition to being a time-related trait, r_{max} is an integrative population estimate of mean fitness, which accounts for the trade-off between survival and the onset of reproduction (Hutchings 2021, Stearns 1992, Clavijo-Baquet & Bozinovic 2012). Thus, it is unsurprising that metabolic rate was more strongly related to r_{max} than component traits that do not account for such a trade-off and may only partially relate to fitness (Pettersen *et al.* 2016, Juan-Jordá et al. 2013, Arnold *et al.* 2021). Indeed, we found that MMR and AS were better explained by r_{max} than its component traits (age-at-maturity, maximum age, and reproductive output). This is consistent with a recent interspecific study across 104 fishes, which determined that growth performance (encompassing a trade-off between growth and maximum body size) better explained variation in whole-organism RMR than other single life history traits, such as the growth coefficient k, generation length (calculated from age-at-maturity and maximum age), or maximum body size (Wong et al. 2021).

Our study supports the hypothesis that higher r_{max} is related to higher MMR and AS across fishes, and to a lesser extent, higher RMR (Table 1.2). While the optimization

of MMR or AS represent clear benefits to fitness, the evolutionary advantages of an elevated RMR are less apparent (Brill 1987). Indeed, selection upon daily energy expenditure or MMR will inevitably 'pull-up' RMR, while also broadening AS (as RMR scales < 1 with MMR across fishes, whereby a species' AS increases as its MMR increases; Auer. et al. 2017, Killen et al. 2016). For example, we found that species with higher MMR (such as pelagic species) also had wider AS, despite the heightened maintenance costs (RMR) required to achieve such high MMR. Here, our findings support the idea that fitness-related traits (in this case, r_{max}) are more related to MMR or AS than RMR across fishes, as has been found in rodents (Clavijo-Baquet & Bozinovic 2012). This may elucidate why several studies have found conflicting results when testing the relationship between RMR and fitness-related traits (Pettersen et al. 2016, Arnold et al. 2021). Our results suggest that comparative analyses of metabolic rate and population dynamics would greatly benefit from the consideration of MMR and AS (in addition to RMR), as these data become more available.

Sharks are one of the most threatened vertebrate groups with more than one-third of species (37.5%) threatened or predicted to be threatened with extinction (Dulvy et al. 2021). This stems from the combination of their slow life histories coupled with fishing mortality levels better suited to target species with faster life histories, such as tunas (Dulvy et al. 2021, Juan-Jordá et al. 2022). Here, we have demonstrated how sharks' slower population growth rates (and, thus, resulting heightened intrinsic sensitivity to overfishing) may be underpinned by lower metabolic rates and, resultantly, lower aerobic scopes relative to teleost fishes. To the best of our knowledge, this is the first extensive study of population-paired r_{max} and metabolic rate (RMR, MMR, and AS) across fishes. Here, we found that the integrative, time-related trait r_{max} explained variation in MMR and AS (and to a lesser extent, RMR) above that explained by body mass and temperature. Our analysis supports the existence of a metabolic rate pace-setting of life history and population growth rates, which is the first step towards understanding the physiological basis of population dynamics and, by extension, recovery potential. We hypothesize that additional variation in metabolic rates across species can be explained by environmental oxygen availability, oxygen uptake capacity across the gills and activity levels, as indexed by Caudal Fin Aspect Ratio (Pauly 2010, Rubalcaba et al. 2020, Bigman et al. 2021, Bigman et al. 2022). Future work, combined with the evolutionary (interspecific) relationship between metabolic rate and r_{max}

examined in this paper, may provide insight as to how population dynamics are linked to the morphological, ecological, and environmental features shaping metabolic rates, and may ultimately help us predict the population-level consequences of overfishing in a changing climate.

1.6. Tables

Table 1.1. Comparison of models testing whether the component life history traits of r_{max} (age at maturity 'amat', maximum age 'amax', and reproductive output 'RO') explain variation in (a) resting metabolic rate RMR, (b) maximum metabolic rate MMR and (c) absolute aerobic scope AS (MMR – RMR) across marine fishes, while accounting for the effect of measurement temperature ('invtemp'), measurement body mass ('M') and ecological lifestyle ('LS'). The metabolic rate dataset was based on largest sample size (see Methods). Models were fit in *brms* using R version 4.0.5. Metabolic rates (Watts), reproductive output (no. of offspring), age-at-maturity (years), maximum age (years), and body mass (grams) were natural log-transformed, while measurement temperature was parameterized as the inverse temperature (see Methods). All explanatory variables were standardized. All models within 2 looic of the highest-ranking model (emboldened) are highlighted in grey.

a) RMR models (N = 82)		p_{loo}	looic	$elpd_{loo}$	se_elpd_{loo}	$elpd_{diff}$	weight
RMR_null	$stdlog(M) + std(invtemp) + LS$	20.0	167.8	-83.9	13.0	-1.4	0.012
RMR_amat	$\boldsymbol{stdlog(M) + std(invtemp) + stdlog(amat) + LS}$	**18.0**	**165.1**	**-82.6**	**12.9**	**0.0**	**0.964**
RMR_amax	$stdlog(M) + std(invtemp) + stdlog(amax) + LS$	18.9	167.3	-83.7	13.5	-1.1	0.023
RMR_RO	$stdlog(M) + std(invtemp) + stdlog(RO) + LS$	19.7	169.8	-84.9	13.0	2.3	0.000
b) MMR models (N = 49)							
MMR_null	$\boldsymbol{stdlog(M) + std(invtemp) + LS}$	**30.7**	**46.4**	**-23.2**	**3.9**	**0.0**	**0.929**
MMR_amat	$stdlog(M) + std(invtemp) + stdlog(amat) + LS$	15.3	51.9	-26.0	4.5	-2.8	0.071
MMR_amax	$stdlog(M) + std(invtemp) + stdlog(amax) + LS$	27.8	51.9	-25.9	4.5	-2.8	0.000
MMR_RO	$stdlog(M) + std(invtemp) + stdlog(RO) + LS$	30.0	50.1	-25.1	4.0	-1.9	0.000
c) AS models (N = 45)							
AS_null	$stdlog(M) + std(invtemp) + LS$	17.8	77.0	-38.5	7.1	-0.9	0.246

AS_amat	$\boldsymbol{stdlog(M) + std(invtemp) + stdlog(amat) + LS}$	**12.4**	**75.3**	**-37.6**	**3.9**	**0.0**	**0.754**
AS_amax	$stdlog(M) + std(invtemp) + stdlog(amax) + LS$	17.8	79.3	-39.6	7.6	-2.0	0.100
AS_RO	$stdlog(M) + std(invtemp) + stdlog(RO) + LS$	18.0	78.8	-39.4	6.8	-1.8	0.000

Table 1.2. Comparison of models testing whether the maximum intrinsic rate of population increase, r_{max}, explained variation in (a) RMR, (b) MMR and (c) AS (MMR – RMR) across marine fishes, while accounting for the effects of measurement temperature ('invtemp'), measurement body mass ('M') and ecological lifestyle ('LS'). The metabolic rate dataset was based on largest sample size (see Methods). Models were fit in *brms* using R version 4.0.5. Metabolic rates (Watts), r_{max} (yr^{-1}), its component life history traits, and body mass were natural log-transformed, while measurement temperature was parameterized as the inverse temperature (see methods). All explanatory variables were standardized. All models within 2 looic of the highest-ranking model (emboldened) are highlighted in grey.

a) RMR models (N = 82)		p_{loo}	looic	$elpd_{loo}$	se_elpd_{loo}	$elpd_{diff}$	weight
RMR_amat	$\boldsymbol{stdlog(M) + std(invtemp) + stdlog(amat) + LS}$	18.0	165.1	-82.6	12.9	0.0	0.994
RMR_rmax	$stdlog(M) + stdinv(temp) + stdlog(r_{max}) + LS$	19.7	168.3	-84.2	13.3	-1.6	0.006
b) MMR models (N = 49)							
MMR_null	$stdlog(M) + std(invtemp) + LS$	30.7	46.4	-23.2	3.9	-4.8	0.206
MMR_rmax	$\boldsymbol{stdlog(M) + std(invtemp) + stdlog(r_{max}) + LS}$	21.7	36.7	-18.4	5.3	0.0	0.794
c) AS models (N = 45)							
AS_null	$stdlog(M) + std(invtemp) + LS$	17.8	77.0	-38.5	7.1	-6.2	0.000
AS_amat	$stdlog(M) + std(invtemp) + stdlog(amat) + LS$	12.4	75.3	-37.6	3.9	-5.4	0.000
AS_rmax	$\boldsymbol{stdlog(M) + std(invtemp) + stdlog(r_{max}) + LS}$	14.3	64.5	-32.3	6.1	0.0	1.000

Table 1.3. Coefficient means and 95% Bayesian Credible Intervals (BCI, in parentheses) for all models from the dataset with the largest sample size (see Methods). 'B' = benthic, 'BP' = benthopelagic, and 'P' = pelagic. Models (and corresponding model names) are the same as those presented in Tables 1.1 and 1.2, except here only the inverse temperature was standardized (i.e., centered and scaled; see Methods).

model	lifestyle	intercept	log_mass	std_inv_temp	log_rmax_or_trait	sigma
RMR_null	P	-6.80 (-7.20 to -6.40)	0.84 (0.75 to 0.93)	-0.57 (-0.74 to -0.41)	NA	0.59 (0.45 to 0.73)
	BP	-7.02 (-7.42 to -6.62)				
	B	-7.65 (-8.39 to -6.89)				
RMR_amat	P	-6.90 (-7.30 to -6.49)	0.90 (0.80 to 1.01)	-0.48 (-0.66 to -0.30)	-0.25 (-0.47 to -0.02)	0.59 (0.46 to 0.72)
	BP	-7.05 (-7.44 to -6.67)				
	B	-7.62 (-8.26 to -6.90)				
RMR_amax	P	-6.47 (-6.86 to -6.08)	0.87 (0.78 to 0.97)	-0.51 (-0.68 to -0.34)	-0.20 (-0.43 to 0.03)	0.60 (0.47 to 0.73)
	BP	-6.64 (-7.02 to -6.25)				
	B	-7.26 (-8.07 to -6.43)				
RMR_RO	P	-6.87 (-7.27 to -6.47)	0.84 (0.75 to 0.93)	-0.58 (-0.75 to -0.41)	0.02 (-0.06 to 0.10)	0.60 (0.45 to 0.74)
	BP	-7.10 (-7.50 to -6.69)				
	B	-7.72 (-8.46 to -6.89)				
RMR_rmax	P	-6.84 (-7.23 to -6.44)	0.87 (0.77 to 0.96)	-0.54 (-0.71 to -0.38)	0.16 (-0.02 to 0.33)	0.59 (0.46 to 0.73)
	BP	-7.08 (-7.47 to -6.67)				
	B	-7.64 (-8.33 to -6.90)				
MMR_null	P	-5.43 (-5.81 to -5.06)	0.89 (0.81 to 0.96)	-0.44 (-0.59 to -0.29)	NA	0.27 (0.10 to 0.43)
	BP	-6.26 (-6.63 to -5.89)				

	B	-6.60 (-7.40 to -5.75)				
MMR_amat	P	-5.10 (-5.42 to -4.79)	0.91 (0.84 to 0.98)	-0.30 (-0.46 to -0.16)	-0.32 (-0.52 to -0.10)	0.35 (0.22 to 0.46)
	BP	-5.86 (-6.19 to -5.52)				
	B	-6.35 (-6.93 to -5.80)				
MMR_amax	P	-5.18 (-5.56 to -4.80)	0.89 (0.82 to 0.97)	-0.41 (-0.58 to -0.25)	-0.11 (-0.32 to 0.11)	0.29 (0.13 to 0.45)
	BP	-5.98 (-6.36 to -5.60)				
	B	-6.37 (-7.28 to -5.50)				
MMR_RO	P	-5.52 (-5.91 to -5.14)	0.89 (0.81 to 0.97)	-0.45 (-0.60 to -0.30)	0.03 (-0.05 to 0.11)	0.28 (0.12 to 0.44)
	BP	-6.37 (-6.76 to -5.98)				
	B	-6.68 (-7.54 to -5.80)				
MMR_rmax	P	-5.41 (-5.69 to -5.13)	0.95 (0.89 to 1.01)	-0.33 (-0.45 to -0.21)	0.43 (0.26 to 0.60)	0.27 (0.16 to 0.38)
	BP	-6.29 (-6.58 to -6.01)				
	B	-6.62 (-7.15 to -6.09)				
AS_null	P	-5.65 (-6.14 to -5.17)	0.88 (0.77 to 0.99)	-0.44 (-0.64 to -0.24)	NA	0.45 (0.30 to 0.62)
	BP	-6.61 (-7.11 to -6.12)				
	B	-7.01 (-7.92 to -6.09)				
AS_amat	P	-5.38 (-5.79 to -4.96)	0.93 (0.82 to 1.03)	-0.31 (-0.51 to -0.12)	-0.38 (-0.63 to -0.10)	0.48 (0.35 to 0.63)
	BP	-6.27 (-6.72 to -5.82)				
	B	-6.77 (-7.49 to -6.06)				
AS_amax	P	-5.41 (-5.89 to -4.93)	0.89 (0.78 to 1.00)	-0.42 (-0.62 to -0.21)	-0.12 (-0.39 to 0.16)	0.46 (0.31 to 0.63)
	BP	-6.34 (-6.85 to -5.84)				
	B	-6.77 (-7.83 to -5.72)				

AS_RO	P	-5.80 (-6.29 to -5.32)	0.88 (0.78 to 0.99)	-0.46 (-0.67 to -0.26)	0.04 (-0.07 to 0.15)	0.45 (0.31 to 0.63)
	BP	-6.80 (-7.31 to -6.28)				
	B	-7.15 (-8.11 to -6.17)				
AS_rmax	P	-5.72 (-6.10 to -5.34)	0.97 (0.87 to 1.06)	-0.35 (-0.51 to -0.19)	0.51 (0.28 to 0.73)	0.41 (0.30 to 0.54)
	BP	-6.74 (-7.14 to -6.34)				
	B	-7.07 (-7.72 to -6.42)				

1.7. Figures

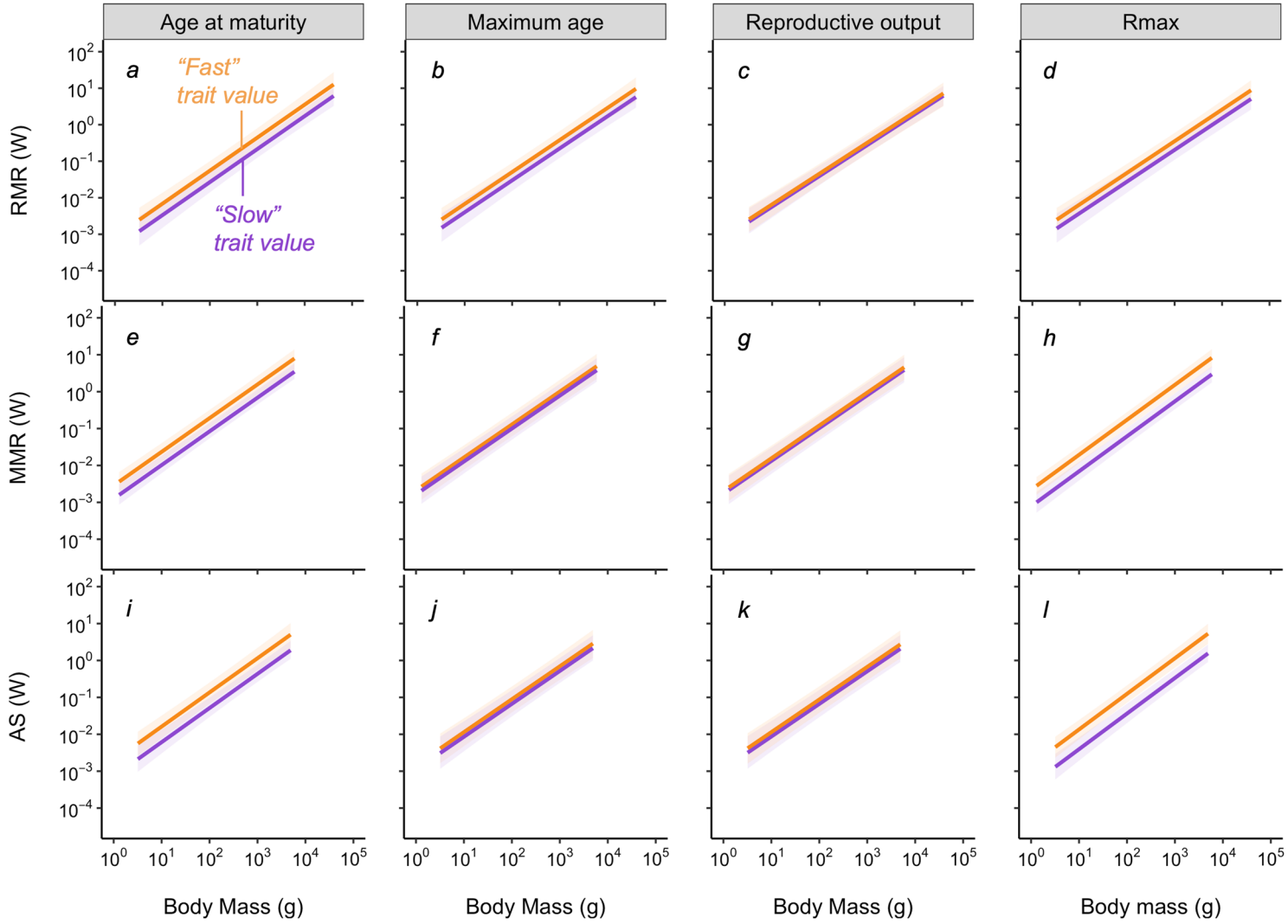
Age at maturity
Maximum age
Reproductive output
Rmax
a
b
c
d
e
f
g
h
i
j
k
l
"Fast" trait value
"Slow" trait value
RMR (W)
MMR (W)
AS (W)
Body Mass (g)
Body Mass (g)
Body Mass (g)
Body mass (g)

Figure 1.1. Time-related traits were overall better related to metabolic rates than reproductive output. Relationships between resting metabolic rate 'RMR' (N=82), maximum metabolic rate 'MMR' (N=49), or aerobic scope 'AS' (N=45) and any single one of the component life history traits of r_{max} – age-at-maturity (*a,e,i*), maximum age (*b,f,j*), or reproductive output (*c,g,k*) – or with r_{max} itself (*d,h,l*). The purple and orange fitted regression lines in all panels is the estimated metabolic rate (in Watts) scaling with body mass (in grams), fit to relatively high (95th percentile) or relatively low (5th percentile) values of the life history trait in the dataset, characteristic of either a faster or slower life history. Models fit to "fast" values of the trait are shown in orange (e.g. low age at maturity, low maximum age, high reproductive output, high r_{max}), while lines fit to "slow" trait values are in purple (e.g., high age at maturity, high maximum age, low reproductive output, low r_{max}). All models also accounted for the effects of temperature, ecological lifestyle, and evolutionary history. The maximum intrinsic rate of population increase r_{max} was the best explanatory variable for MMR and AS, while the model with age-at-maturity was preferred in the case of RMR (see Table 1.1, 1.2, and 1.3). Metabolic rates and all explanatory variables were natural log transformed, except for measurement temperature which was taken as the inverse temperature (see Methods). All explanatory variables were standardized.

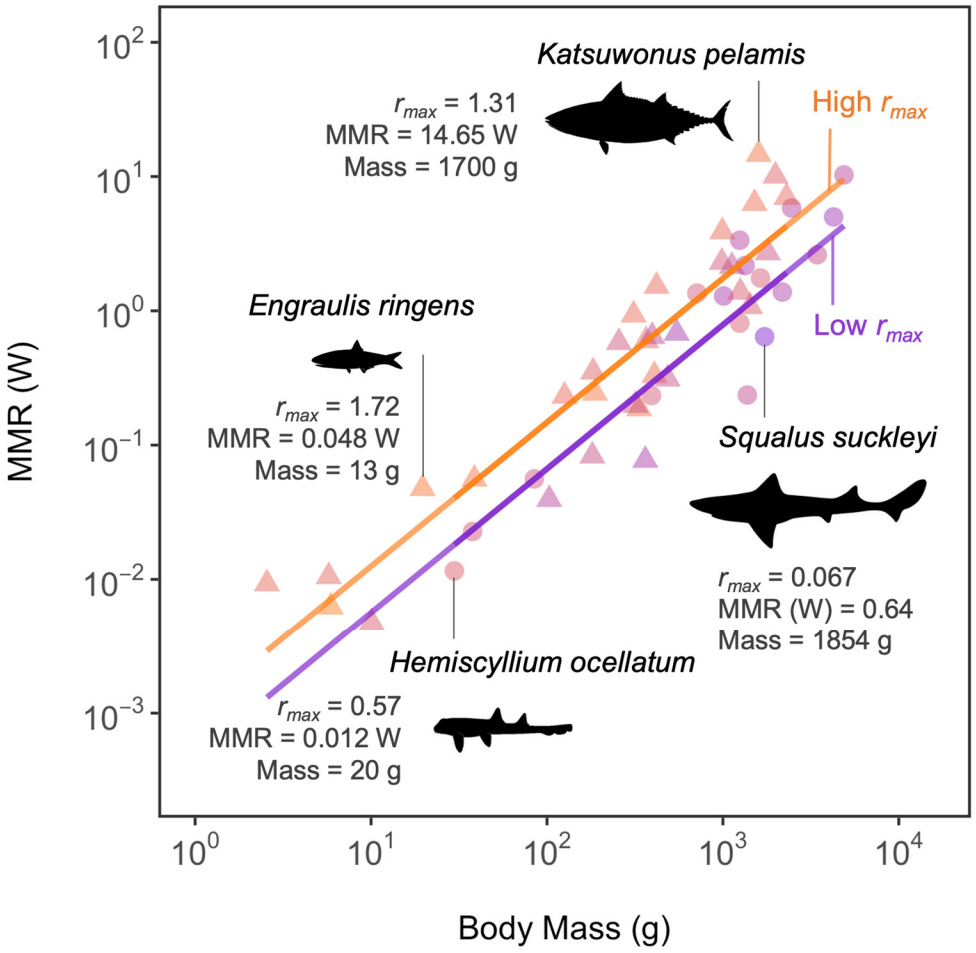

Figure 1.2. **Species with high r_{max} have higher maximum metabolic rates for their measurement body size and temperature.** Mean whole-organism maximum metabolic rate (Watts) plotted against mean measurement body mass (grams) for 49 marine fish species. Points are coloured by the magnitude of r_{max}, where orange indicates species with higher values of r_{max} and purple indicates species with lower values of r_{max}. Triangles symbolize teleost fishes, while circles symbolize sharks. Lines show the estimated maximum metabolic rate (controlling for the effect of mass, temperature, and evolutionary history) for species with relatively high (95th percentile, orange line) versus relatively low (5th percentile, purple line) values of r_{max}.

1.8. References

Arnold, P. A., Delean, S., Cassey, P., & White, C. R. (2021). Meta-analysis reveals that resting metabolic rate is not consistently related to fitness and performance in animals. *Journal of Comparative Physiology B*, *191*(6), 1097-1110.

Auer, S. K., Killen, S. S., & Rezende, E. L. (2017). Resting vs. active: A meta-analysis of the intra-and inter-specific associations between minimum, sustained, and maximum metabolic rates in vertebrates. *Functional Ecology*, *31*(9), 1728-1738.

Auer, S. K., Dick, C. A., Metcalfe, N. B., & Reznick, D. N. (2018). Metabolic rate evolves rapidly and in parallel with the pace of life history. *Nature communications*, *9*(1), 14.

Barrowclift, E., Gravel, S. M., Pardo, S. A., Bigman, J. S., Berggren, P., & Dulvy, N. K. (2023). Tropical rays are intrinsically more sensitive to overfishing than the temperate skates. *Biological Conservation*, *281*, 110003.

Bigman, J. S., Pardo, S. A., Prinzing, T. S., Dando, M., Wegner, N. C., & Dulvy, N. K. (2018). Ecological lifestyles and the scaling of shark gill surface area. *Journal of morphology*, *279*(12), 1716-1724.

Bigman, J. S., M'Gonigle, L. K., Wegner, N. C., & Dulvy, N. K. (2021). Respiratory capacity is twice as important as temperature in explaining patterns of metabolic rate across the vertebrate tree of life. *Science Advances*, *7*(19), eabe5163.

Bigman, J. S., Wegner, N. C., & Dulvy, N. K. (2022). Gills, growth and activity across fishes. *Fish and Fisheries*.

Brill, R. W. (1987). On the standard metabolic rates of tropical tunas, including the effect of body size and acute temperature change. *Fish. Bull*, *85*(1), 25-35.

Brown, J. H., Gillooly, J. F., Allen, A. P., Savage, V. M., & West, G. B. (2004). Toward a metabolic theory of ecology. *Ecology*, *85*(7), 1771-1789.

Bürkner, P. C. (2017). brms: An R package for Bayesian multilevel models using Stan. *Journal of statistical software*, *80*, 1-28.

Chabot, D., Steffensen, J. F., & Farrell, A. P. (2016). The determination of standard metabolic rate in fishes. *Journal of Fish Biology*, *88*(1), 81-121.

Clark, T. D., Sandblom, E., & Jutfelt, F. (2013). Aerobic scope measurements of fishes in an era of climate change: respirometry, relevance and recommendations. *Journal of Experimental Biology*, *216*(15), 2771-2782.

Clavijo-Baque, S., & Bozinovic, F. (2012). Testing the fitness consequences of the thermoregulatory and parental care models for the origin of endothermy. *PLoS One*, *7*(5), e37069.

Cortés, E. (2016). Perspectives on the intrinsic rate of population growth. *Methods in Ecology and Evolution*, *7*(10), 1136-1145.

Denney, N. H., Jennings, S., & Reynolds, J. D. (2002). Life–history correlates of maximum population growth rates in marine fishes. *Proceedings of the Royal Society of London. Series B: Biological Sciences*, *269*(1506), 2229-2237.

Drazen, J. C., & Haedrich, R. L. (2012). A continuum of life histories in deep-sea demersal fishes. *Deep Sea Research Part I: Oceanographic Research Papers*, *61*, 34-42.

Dulvy, N. K., Pacoureau, N., Rigby, C. L., Pollom, R. A., Jabado, R. W., Ebert, D. A., ... & Simpfendorfer, C. A. (2021). Overfishing drives over one-third of all sharks and rays toward a global extinction crisis. *Current Biology*, *31*(21), 4773-4787.

Duncan, R. P., Forsyth, D. M., & Hone, J. (2007). Testing the metabolic theory of ecology: allometric scaling exponents in mammals. *Ecology*, *88*(2), 324-333.

Forster, J., Hirst, A. G., & Atkinson, D. (2012). Warming-induced reductions in body size are greater in aquatic than terrestrial species. *Proceedings of the National Academy of Sciences*, *109*(47), 19310-19314.

Gillooly, J. F., Brown, J. H., West, G. B., Savage, V. M., & Charnov, E. L. (2001). Effects of size and temperature on metabolic rate. *science*, *293*(5538), 2248-2251.

Goodwin, N. B., Grant, A., Perry, A. L., Dulvy, N. K., & Reynolds, J. D. (2006). Life history correlates of density-dependent recruitment in marine fishes. *Canadian Journal of Fisheries and Aquatic Sciences*, *63*(3), 494-509.

Grady, J. M., Enquist, B. J., Dettweiler-Robinson, E., Wright, N. A., & Smith, F. A. (2014). Evidence for mesothermy in dinosaurs. *Science*, *344*(6189), 1268-1272.

Hutchings, J. A., Myers, R. A., García, V. B., Lucifora, L. O., & Kuparinen, A. (2012). Life-history correlates of extinction risk and recovery potential. *Ecological Applications*, *22*(4), 1061-1067.

Hutchings, J. A. (2021). *A primer of life histories: ecology, evolution, and application*. Oxford University Press.

Juan-Jordá, M. J., Mosqueira, I., Freire, J., & Dulvy, N. K. (2013). Life in 3-D: life history strategies in tunas, mackerels and bonitos. *Reviews in Fish Biology and Fisheries*, *23*, 135-155.

Juan-Jordá, M. J., Murua, H., Arrizabalaga, H., Merino, G., Pacoureau, N., & Dulvy, N. K. (2022). Seventy years of tunas, billfishes, and sharks as sentinels of global ocean health. *Science*, *378*(6620), eabj0211.

Killen, S. S., Glazier, D. S., Rezende, E. L., Clark, T. D., Atkinson, D., Willener, A. S., & Halsey, L. G. (2016). Ecological influences and morphological correlates of resting and maximal metabolic rates across teleost fish species. *The American Naturalist*, *187*(5), 592-606.

Killen, S. S., Norin, T., & Halsey, L. G. (2017). Do method and species lifestyle affect measures of maximum metabolic rate in fishes?. *Journal of Fish Biology*, *90*(3), 1037-1046.

Kindsvater, H. K., Mangel, M., Reynolds, J. D., & Dulvy, N. K. (2016). Ten principles from evolutionary ecology essential for effective marine conservation. *Ecology and Evolution*, *6*(7), 2125-2138.

Mull, C. G., Pacoureau, N., Pardo, S. A., Ruiz, L. S., García-Rodríguez, E., Finucci, B., ... & Dulvy, N. K. (2022). Sharkipedia: a curated open access database of shark and ray life history traits and abundance time-series. *Scientific Data*, *9*(1), 559.

Myers, R. A. (2001). Stock and recruitment: generalizations about maximum reproductive rate, density dependence, and variability using meta-analytic approaches. *ICES Journal of Marine Science*, *58*(5), 937-951.

Myers, R. A., Hutchings, J. A., & Barrowman, N. J. (1997). Why do fish stocks collapse? The example of cod in Atlantic Canada. Ecological applications, 7(1), 91-106.

Myers, R. A., & Worm, B. (2005). Extinction, survival or recovery of large predatory fishes. *Philosophical Transactions of the Royal Society B: Biological Sciences*, *360*(1453), 13-20.

Pardo, S. A., Kindsvater, H. K., Reynolds, J. D., & Dulvy, N. K. (2016). Maximum intrinsic rate of population increase in sharks, rays, and chimaeras: the importance of survival to maturity. *Canadian journal of fisheries and aquatic sciences*, *73*(8), 1159-1163.

Pardo, S. A., & Dulvy, N. K. (2022). Body mass, temperature, and depth shape the maximum intrinsic rate of population increase in sharks and rays. *Ecology and Evolution*, *12*(11), e9441.

Pauly, D., Kinne, O., & Jorgensen, B. B. (2010). Gasping fish and panting squids: oxygen, temperature and the growth of water-breathing animals.

Pettersen, A. K., White, C. R., & Marshall, D. J. (2016). Metabolic rate covaries with fitness and the pace of the life history in the field. *Proceedings of the Royal Society B: Biological Sciences*, *283*(1831), 20160323.

R Core Team (2021). R: A language and environment for statistical computing. R Foundation for Statistical Computing, Vienna, Austria. URL https://www.R-project.org/.

Rabosky, D. L., Chang, J., Title, P. O., Cowman, P. F., Sallan, L., Friedman, M., ... & Alfaro, M. E. (2018). An inverse latitudinal gradient in speciation rate for marine fishes. *Nature*, *559*(7714), 392-395.

Reynolds, J. D. (2003). Life histories and extinction risk. *Macroecology. Blackwell Publishing, Oxford, UK*, 195-217.

Ricard, D., Minto, C., Jensen, O. P., & Baum, J. K. (2012). Examining the knowledge base and status of commercially exploited marine species with the RAM Legacy Stock Assessment Database. *Fish and fisheries*, *13*(4), 380-398.

Rubalcaba, J. G., Verberk, W. C., Hendriks, A. J., Saris, B., & Woods, H. A. (2020). Oxygen limitation may affect the temperature and size dependence of metabolism in aquatic ectotherms. *Proceedings of the National Academy of Sciences*, *117*(50), 31963-31968.

Savage, V. M., Gillooly, J. F., Brown, J. H., West, G. B., & Charnov, E. L. (2004). Effects of body size and temperature on population growth. *The American Naturalist*, *163*(3), 429-441.

Spalding, M. D., Fox, H. E., Allen, G. R., Davidson, N., Ferdaña, Z. A., Finlayson, M. A. X., ... & Robertson, J. (2007). Marine ecoregions of the world: a bioregionalization of coastal and shelf areas. *BioScience*, *57*(7), 573-583.

Stearns, S. C. (1992). *The evolution of life histories* (Vol. 249, p. xii). Oxford: Oxford university press.

Stein, R. W., Mull, C. G., Kuhn, T. S., Aschliman, N. C., Davidson, L. N., Joy, J. B., ... & Mooers, A. O. (2018). Global priorities for conserving the evolutionary history of sharks, rays and chimaeras. *Nature ecology & evolution*, *2*(2), 288-298.

Vehtari, A., Gelman, A., & Gabry, J. (2017). Practical Bayesian model evaluation using leave-one-out cross-validation and WAIC. *Statistics and computing*, *27*, 1413-1432.

White, C. R., & Kearney, M. R. (2013). Determinants of inter-specific variation in basal metabolic rate. *Journal of Comparative physiology B*, *183*, 1-26.

White, C. R., Alton, L. A., Bywater, C. L., Lombardi, E. J., & Marshall, D. J. (2022). Metabolic scaling is the product of life-history optimization. *Science*, *377*(6608), 834-839.

Wong, S., Bigman, J. S., & Dulvy, N. K. (2021). The metabolic pace of life histories across fishes. *Proceedings of the Royal Society B*, *288*(1953), 20210910.

Chapter 2.

Oxygen and the scaling from individual metabolic rate to the dynamics of fish populations

2.1. Abstract

The maximum intrinsic rate of population increase (r_{max}) is an estimate of population-scale turnover rate at low adult abundance, and hence reflects the average fitness across the individuals in a population. There is increasing evidence of a metabolic basis for variation in r_{max} along environmental gradients in temperature with latitude, and with depth, suggesting oxygen availability may also be an underlying driver. Yet, little is understood of how oxygen and temperature effects upon metabolic rates scale up to the dynamics of populations. We bridge from the individual to population scales using an information theoretic approach to assess how metabolic rate (resting, maximum, and aerobic scope) and r_{max} are shaped by environmental oxygen and temperature across 35 chondrichthyan and 140 teleost species. We use population-matched metabolic and life history traits, as well as species distribution maps from Aquamaps and environmental data from the World Ocean Atlas. We found that environmental oxygen, body mass, and temperature best explained variation in metabolic rates and r_{max}, where MMR, AS, and r_{max} showed stronger (positive) scaling with oxygen partial pressure than RMR. Additionally, oxygen proved to be better associated with r_{max} than body mass or temperature. Our work highlights the central role of oxygen availability as metabolic habitat for aquatic ectotherms, and hence population dynamics.

2.2. Introduction

Marine fish populations are experiencing historically unprecedented mortality rates from overfishing, compounded by the effects of habitat loss and degradation due to climate change (Dulvy et al. 2021, Harley et al. 2006). The geographic distribution of marine ectotherms will become progressively squeezed between the increased metabolic demands of a warming ocean and deoxygenation limiting the oxygen supply required to meet their energetic needs (Pörtner & Knust 2007, Deutsch et al. 2015).

Consequently, ocean warming and deoxygenation will significantly reduce the available habitat suitable for many species, potentially causing increased susceptibility to overfishing by shifting distributions into areas without regulation or narrowing the depth range of populations, potentially causing greater overlap with the depth range of fishing gears (Penn & Deutsch 2022, Spijkers & Boonstra 2017, Vedor et al. 2021). Aside from habitat compression, those species unable to move or keep track of their preferred isotherms risk population decline as a result of the physiological consequences upon fitness-related performance traits such as growth rate, locomotion, and reproductive capacity (Pörtner & Knust 2007). For example, the non-migratory population of common eelpout, *Zoarces viviparus*, was effectively trapped in the Wadden Sea and unable to track the northward-shifting isotherms, and therefore suffered reduced physiological and growth performance from warming, resulting in population decline (Brodte et al. 2008, Pörtner & Knust 2007). Yet, we lack a unified physiological and ecological understanding as to whether and how oxygen and temperature effects upon physiological performance scale up to influence population dynamics (Ern 2019, Wilson et al. 2020).

The maximum intrinsic rate of population increase (r_{max}) estimates population growth at low population sizes, in the absence of density-dependent processes (Cortés 2016, Myers et al. 1997, Pardo et al. 2016). Thus, r_{max} is also an indicator of a population's resilience to overfishing (Dulvy et al. 2004, Myers & Worm 2005, Hutchings 2021). Across the ocean, r_{max} exhibits a positive relationship with environmental temperature and decreases with body size, in addition to decreasing with depth independently of temperature (Drazen & Haedrich 2012, Pardo & Dulvy 2022). In sharks however, temperature and size effects on r_{max} were found to be interdependent, where the relationship between r_{max} and body size breaks down with decreasing water temperature, consistent with the temperature-size rule and oxygen limitation hypothesis (Pardo & Dulvy 2022, Forster et al. 2012). Thus, r_{max} exhibits similar dependencies on mass and temperature as metabolic rate (Drazen & Haedrich 2012, Pardo & Dulvy 2022, Savage et al. 2004). Indeed, r_{max} and somatic growth have been directly linked to the speed of metabolism in fishes (see Chapter 1, Wong et al. 2021). Hence, there is growing interest in applying metabolic principles to understand and predict the patterning of population dynamics across environmental gradients in the ocean (Bernhardt et al. 2018, Drazen & Haedrich 2012, Pardo & Dulvy 2022).

Metabolic theory is founded largely on estimates of metabolic rates from animals at rest (i.e., resting metabolic rate, RMR). Metabolic rate, which reflects the speed of energetic cycling of an organism, is well-known to scale with environmental temperature and body mass across species (Clarke & Johnston 1999, Brown et al. 2004, Rubalcaba et al. 2020). While the RMR encompasses the maintenance costs of an organism, the maximum metabolic rate (MMR) and aerobic scope (AS=MMR-RMR) reflect maximum rates of energetic cycling and the energy available for fitness-enhancing activities, such as locomotion, growth, and reproduction (Pörtner & Knust 2007). Concomitantly, studies in mammals and fishes have found MMR and AS to be better related to r_{max} than RMR (see Chapter 1, Clavijo-Baquet & Bozinovic 2012). However, as MMR and AS are less commonly measured than RMR, metabolic scaling theory and principles have thus been founded on the exponential relationship of RMR with body mass and temperature (primarily for terrestrial endotherms), and subsequently used in its ecological applications (Brown et al. 2004, Savage et al. 2004, Pardo & Dulvy 2022).

Resting and maximal metabolic rates vary widely across fishes even after accounting for the effects of body size and temperature, exceeding that observed for endotherms (Killen et al. 2016). Environmental oxygen is thought to be limiting to the metabolic rate of water-breathing organisms, particularly to MMR, which is less responsive to temperature than RMR (Rubalcaba et al. 2020). Intraspecific studies have shown the effects of oxygen on metabolic rate (e.g., testing the effects of hypoxia in a lab setting; Whiteley & Taylor 2015), but the interspecific variation of metabolic rate across environmental oxygen gradients is relatively unknown. To date, there is no direct test of the connection between the environmental oxygen where a population is geographically distributed with experimental measures of metabolic rate of that population.

Here, we conduct a meta-analytic comparative analysis of marine fish metabolic rates, r_{max}, and environmental temperature and oxygen. To do this, we used laboratory measures of metabolic rate and calculated population-matched estimates of r_{max}, and utilize new methods for extracting the routine environmental oxygen and temperature experienced by species across their core distributions (Pardo & Dulvy 2022). We ask two questions: (1) Do marine fishes living in cooler or low-oxygenated habitats have lower metabolic rates than those in warm or well-oxygenated habitats? (2) Do marine fishes living in cooler or low-oxygenated habitats have lower r_{max} than fishes living in

warm or well-oxygenated habitats? Specifically, we model metabolic rate (RMR, MMR, and AS) with environmental oxygen availability and environmental temperature, whilst accounting for measurement body size, ecological lifestyle, and evolutionary history. Next, we explore these same relationships for r_{max}, accounting for the effects of body size using the maximum documented body mass. Based on previous findings and models proposed by Rubalcaba et al. (2020) and Pardo & Dulvy (2022), we also test for interactions between (i) mass or temperature and oxygen, and (ii) mass and temperature on metabolic rates and r_{max}. We predict that whole-organism metabolic rates (particularly MMR and AS) and r_{max} will scale positively with both environmental oxygen and temperature.

2.3. Methods

First, we collated data for resting and maximum metabolic rate (RMR and MMR, respectively), along with the measurement body mass and measurement temperature associated with each metabolic rate estimate. Aerobic scope (AS) was calculated as MMR minus RMR if not reported directly in the study (Clark et al. 2013). Second, we collated the life history traits necessary to calculate population-specific maximum intrinsic rate of population increase (r_{max}) for all populations with metabolic data. Third, we collated the maximum body mass to account for the effect of body size on r_{max}. Fourth, we used species distribution maps and environmental data from the World Ocean Atlas (2018) to estimate the routinely-experienced, species-specific environmental temperature and oxygen at depth for each species.

2.3.1. Metabolic rate data collation, selection, and aggregation

We conducted an extensive meta-analysis of the literature on fish metabolic rates. We collated data on RMR and MMR for all marine fishes we could find, along with the measurement body mass and measurement temperature of the metabolic rate, based on standard practices and selection criteria (e.g., detailed in Chapter 1, Bigman et al. 2021, Wong et al. 2021). In summary, only one study per species was used to avoid giving undue weight to species with multiple studies over species with fewer data points. If a given study repeated measurements on individuals at different temperatures, data were averaged within the temperature treatment (i.e., for repeated metabolic rate

measurements on individuals at multiple temperature treatments, metabolic rate data was averaged for a given treatment; Clarke & Johnston 1999, Killen et al. 2016, Wong et al. 2021). See Chapter 1 Methods for more information.

To examine the variation of metabolic rates with environmental temperature across fishes (which are ectothermic, where the internal body temperature corresponds to the ambient temperature), we selected metabolic rates measured at a temperature closest to the estimated mean environmental temperature (see Methods section 2.3.4). Across metabolic rate datasets, the experimental measurement temperature of the metabolic rate was highly correlated with the estimated environmental temperature (Pearson's $r \geq 0.95$). Thus, experimental measurement temperature was subsequently used in metabolic rate analyses and hereafter referred to as "environmental temperature".

2.3.2. Maximum body size and r_{max}-related life history trait data collation and selection

As previously described in Chapter 1, we required several life history traits for the calculation of r_{max}, such as age-at-maturity, maximum age, and reproductive output (the latter of which was calculated from estimates of litter size and interbreeding interval for sharks, or stock-recruitment data and length-weight and von Bertalanffy equation parameters for teleosts). Additionally, to account for the effects of size on r_{max}, we collated the maximum body mass of the species, which was taken as the maximum observed body mass for the population in question when available, and otherwise as the largest body mass recorded for the species. When the largest observed body size was only reported in units of length, it was converted to body mass using length-weight relationships. All traits and conversion equations were collated from online databases such as The IUCN Red List of Threatened Species (Dulvy et al. 2021, IUCN 2022), FishBase (Froese & Pauly 2019), Sharkipedia (Mull et al. 2022), the RAM Legacy Stock Assessment Database (2018), stock assessments, and other primary literature. Teleost stock-recruitment time series data were compiled from the RAM Legacy Stock Assessment Database (2018). See Chapter 1 and Appendix A for more information on population-specific life history data collation and selection.

2.3.3. Calculation of r_{max}

Shark r_{max}

We calculated r_{max} for sharks following Pardo et al. (2016) and Cortes (2016), based on four traits: age-at-maturity, maximum age, litter size, and interbreeding interval, detailed in Chapter 1 and the SM in Appendix A.

Teleost r_{max}

For teleosts, the relationship between fecundity and female size is nearly universally positive (and therefore, fecundity cannot be assumed constant), and density dependence is an important component of population dynamics (Myers et al. 1997). For these species, we calculated r_{max} following standard practices outlined in Myers *et al.* (1997, Myers 2001), based on estimates of age-at-maturity, maximum age, stock spawner-recruitment timeseries data (RAM Legacy Stock Assessment Database, 2018) and any other required conversion relationships (length-weight and von Bertalanffy equations). See Chapter 1 and Appendix A for more details on the derivation of r_{max}.

2.3.4. Estimation of environmental oxygen and temperature

To estimate the average environmental temperature and oxygen routinely experienced by each species, we extracted temperature and oxygen data across the core geographic distribution of each species at its median "usual" depth, following methods from Pardo & Dulvy (2022). To this end, we collected species distribution maps and depth ranges, and ocean temperature and oxygen data at depth from the World Ocean Atlas (2018) as we next describe.

Species geographic distributions and depth ranges

We used probability of occurrence maps for each species, available from Aquamaps (Kaschner et al. 2019), where the map entries represented individual grid cells corresponding to a geographic coordinate (latitude and longitude, with 0.5° grid resolution) and the probability of the species occurring within a given cell. The grid cells making up the distribution of a given species were then filtered to reflect its "core range", corresponding to the portion of the species' range where it has ≥90% probability of occurring (Kaschner et al. 2019, Pardo & Dulvy 2022).

We then collated the “usual” (or “preferred”) depth range observed for adult individuals of each species, representing the range of depths most often occupied. The usual depth range was obtained from Fishbase, and otherwise from the IUCN or mined from the literature. The usual depth range was often inferred from data on habitat use and catch depth for adult life stages (e.g., where specimens spent >50% of their time, or where >50% of the specimens were typically caught). For species exhibiting seasonal or diurnal variation in their usual depth range, the total usual range was considered (extreme upper and lower limits) across the year. When different populations showed significant latitudinal variation in usual depth range, depth information from the population in question (from which the metabolic and population data was sourced) was preferred. In some cases, we took the mean depth when this information was available, and otherwise we took the median of the usual depth range, which was subsequently used to determine estimates of the mean oxygen and temperature experienced by each species in its environment (detailed in the next section).

We also considered the median of the species’ full observed depth range (i.e., between the shallowest and deepest depth observed) from Fishbase (Froese & Pauly 2019) and/or the IUCN Red List (Dulvy et al. 2021), supplemented with primary literature when information from these databases was conflicting or unavailable. For data-poor species with no available usual range information, the median of the full observed range was taken. As species missing usual depth range information were typically very shallow-water or very deep-sea organisms, the oxygen and temperature conditions at the median of the full observed depth range was generally a fairly good proxy of the conditions experienced at usual depth range median (see example provided in Figure B.1).

Mean environmental oxygen and temperature at depth

Environmental data files were obtained from the World Ocean Atlas (WOA 2018), representing the statistical annual mean oxygen and temperature (averaged across decade years) at a given depth level and geographic coordinate, with a 1° degree grid resolution. Oxygen concentrations at depth (μmol/kg) were converted to partial pressures (atm) following standard methods (Clarke et al. 2021, T. M. Clarke pers. comm.), which required environmental temperature, density, salinity, and depth data for each oxygen value’s corresponding grid cell, all of which were also obtained from the

WOA (2018). A correction factor of 3.5˚C was added to all partial endothermic species (i.e., tunas and lamnid sharks; Pardo & Dulvy 2022).

For each species, data was then extracted as close as possible to its usual depth (i.e., at the depth level nearest its usual depth, discussed in the previous section). To this end, species core distributions (Aquamaps) were overlaid on the gridded environmental data using the *sp* package in R to obtain all of the oxygen and temperature values at the usual depth of each species across its core distribution, where the mean of these values was taken as the "usual" oxygen and temperature experienced by each species (see Figure B.1 and the SM in Appendix B).

2.3.5. Statistical analyses

We used a phylogenetic Bayesian modeling framework and an information theoretic approach to assess whether environmental oxygen, temperature, and body mass explained variation in metabolic rate and r_{max} across fishes. For all models, body mass was converted to grams, temperature was converted to inverse temperature, and metabolic rate was converted to Watts (Joules·s^{-1}) following Grady et al. (2014). The inverse temperature was parameterized as the Boltzmann-Arrhenius formulation, using the Boltzmann constant (8.617×10^{-5} eV) and temperature in Kelvin, and was then standardized (Gillooly et al. 2001). All covariates (with the exception of temperature) and the response variable (metabolic rate or r_{max}) were natural log-transformed, following which all covariates were centered and scaled (i.e., standardized) using the function *scale* in R. All models included a phylogenetic random effect to account phylogenetic non-independence among residuals for the evolutionary relatedness between species. We constructed a supertree from a molecular chondrichthyan tree (Stein et al. 2018) and the teleost tree from the Fish Tree of Life (Rabosky et al. 2018) and only species also present in these phylogenies were used in our analyses. All model analyses were fitted in Stan with the *brms* package v.2.14.4 (Burkner 2017) using R v.4.0.5 (R Core Team 2021).

We used model selection to identify the model(s) with the most support for each metabolic rate type and r_{max}. Specifically, we used the LOO information criterion value (looic) implemented in the loo package (Vehtari et al. 2022), where all models within looic < 2 of the top-ranked model (lowest looic value) have similar support.

Inevitably, there is a significant amount of collinearity between environmental oxygen and temperature, as cooler waters in the mixed layer hold more dissolved oxygen than warm water. However, the correlations were lower than the threshold of $|r| > 0.7$, where collinearity may result in the misrepresentation or severe distortion of model estimates (Pearson's $|r| \leq 0.5$ across metabolic rate datasets, and $|r| < 0.2$ for the r_{max} dataset; Dormann et al. 2013, Pardo & Dulvy 2022). We also ensured that estimates of the effect of temperature on metabolic rate and r_{max} were not significantly affected by the inclusion of oxygen in the models.

Additionally, ecological lifestyle is known to be an important determinant of activity and metabolic rate across marine fishes, where species from pelagic habitats generally have higher metabolic rates than benthopelagic species, which in turn have higher metabolic rates than benthic species (see Chapter 1, Killen et al. 2016, 2017). Thus, we added ecological lifestyle as an intercept effect (i.e., a fixed factor with three levels, where species were categorized as 'Benthic', 'Benthopelagic', or 'Pelagic') to all metabolic rate models (RMR, MMR, and AS).

Do fishes living in cooler or low-oxygenated habitats have lower metabolic rates than fishes living in warm or well-oxygenated habitats?

Specifically, we tested whether variation in metabolic rate (RMR, MMR, and AS) was explained by environmental oxygen in addition to environmental temperature and measurement body size, to which end we fitted 24 models. Models were parameterized building on the relationship between metabolic rate and body mass, temperature, and ecological lifestyle, the 'null model' (e.g., following Gillooly et al. 2001, Brown et al. 2004, Bigman et al. 2018), and then adding in environmental oxygen. However, we also parameterized models without temperature, including only body mass and environmental oxygen as covariates. We also tested for any interactions between (i) mass and temperature, (ii) mass and oxygen, and (iii) oxygen and temperature. For example, the response variable was either RMR, MMR, or AS and the covariates were measurement body mass, environmental temperature, and environmental oxygen availability, with an interaction between temperature and body mass.

Do fishes living in cooler or low-oxygenated habitats have lower rmax than fishes living in warm or well-oxygenated habitats?

We fitted 9 additional models to examine whether environmental oxygen explained variation in r_{max}, building on the relationship between r_{max} and maximum body mass (e.g., following Pardo & Dulvy 2022, Barrowclift-Mahon et al. 2023). We then added in environmental oxygen and temperature, and tested any interactions between mass, temperature, and oxygen, as described above. For example, the response variable was r_{max} and the covariates were the maximum observed body mass, environmental temperature, and environmental oxygen, including an interaction between temperature and oxygen. As we did for the metabolic rate models, we also parameterized models without temperature, including only maximum body mass and environmental oxygen as covariates.

Sensitivity analyses

The range of environmental temperature and oxygen encountered by an organism within its 'usual' distribution may vary greatly across species (Schwieterman et al. 2020). Therefore, we also ran our analyses using the lower (deeper) depth limit of the usual depth range. Additionally, although the oxygen partial pressure is a more biologically relevant metric than dissolved oxygen concentration, the latter may be more widely available, considering the method by which we convert from concentration to partial pressure within each grid cell (which requires additional data on water density, salinity, depth, and temperature; see Clarke et al. 2021 and Appendix B Supplementary Methods). Therefore, we also ran our analyses using environmental dissolved oxygen concentrations. As the above choices of method had very little effect on our results, we only present the results based on the models using environmental oxygen partial pressure and temperature at the median of the usual depth range (see Tables B.1-4 in Appendix B for results based on models using oxygen concentration and alternative depths).

2.4. Results

We collated metabolic rate and environmental data for 175 marine fishes (comprising 35 chondrichthyans and 140 teleosts) from a wide range of habitats, spanning environmental temperatures from -1 to 31˚C and oxygen partial pressures from

0.009 to 0.208 atm (i.e., 22.2 to 366.4 μmol/kg in dissolved oxygen concentration). Of the species for which we were able to calculate r_{max} (i.e., 80 species), environmental temperature and oxygen spanned similar oxygen and temperature ranges (3 to 28˚C and 0.009 to 0.152 atm, respectively).

Do fishes living in cooler or low-oxygenated habitats have lower metabolic rates than fishes living in warm or well-oxygenated habitats?

Overall, we found that species living in cool or low-oxygen habitats exhibited relatively lower metabolic rates than species living in warm, well-oxygenated habitats (Table 2.1, Figure 2.1). Metabolic rate (RMR, MMR, and AS) scaled positively with measurement body mass, environmental temperature, and environmental oxygen partial pressure, although oxygen was better related to MMR and AS than to RMR (Table 2.3, Figure B.2).

Specifically, for RMR, the model with oxygen, mass, and temperature had more overall support (looic=253.7) than the model with just mass and temperature (looic=261.3; Table 2.1a). Thus, RMR scaled positively with oxygen even after accounting for the effects of mass, temperature, ecological lifestyle, and evolutionary history, evidenced by a slope of 0.16 (95% BCI: 0.08 to 0.25; Table 2.3, Figure B.2). Similarly, the model including mass, temperature, and oxygen explained more variation in MMR (looic=109.9) and AS (looic=141.9) than the model with just mass and temperature (looic=154.8 and 149.5 for MMR and AS, respectively; Table 2.1bc), evidenced by strong positive scaling with environmental oxygen (mean standard slope = 0.34, 95% BCI: 0.24 to 0.43 for MMR, and mean standard slope = 0.26, 95% BCI: 0.10 to 0.42 for AS; Table 2.3, Figure 2.1). Further, even the model with just oxygen and body mass was preferred for MMR (looic=140.8) and AS (looic=145.1) over the model with just temperature and body mass (Table 2.1bc). Additionally, the top ranking model for AS included an interaction between mass and temperature, where AS was less sensitive to changes in body mass (i.e., scaled more shallowly with mass) at higher temperatures (Table 2.3). Although this model also ranked highly for MMR (looic=110.0, nearly the same score as the top model), it was less parsimonious than the model without interaction.

Do fishes living in cooler or low-oxygenated habitats have lower r_{max} than fishes living in warm or well-oxygenated habitats?

Species in relatively cooler or low-oxygen habitats also exhibited slower population growth rates (lower r_{max} values) than species living in warm, well-oxygenated habitats (Table 2.2, Figure 2.2). The model with maximum body mass, environmental temperature, and environmental oxygen partial pressure was the highest ranking model and had significantly more support (looic=166.2) than a model with just maximum body mass and temperature (looic=185.2). Specifically, r_{max} declined with increasing maximum body mass and increased with increasing environmental temperature and with increasing oxygen availability (Table 2.4). Environmental oxygen was the best explanatory factor for r_{max}, as evidenced by the absolute relative effect size (standard mean slope = 0.40, 95% BCI: 0.25 to 0.56) exceeding that of environmental temperature (standard mean slope = -0.27, 95% BCI: -0.48 to -0.06) and maximum body mass (standard mean slope = -0.37, 95% BCI: -0.55 to -0.19) in the top-ranked model (Table 2.4, Figure B.2). Similar to MMR and AS, even the model with just environmental oxygen and maximum body mass also had more support (looic=173.2) than the model with just environmental temperature and maximum body mass (looic=185.2; Table 2.2).

2.5. Discussion

In this study, we found that species from habitats with relatively lower oxygen availability not only had slower metabolism (lower RMR, MMR, and AS) but also exhibited slower population growth rates (lower r_{max}) than species living at higher oxygen availability, after accounting for the effects of temperature, body mass, ecological lifestyle, and evolutionary history. Our findings support the hypothesis that environmental oxygen places a significant constraint on the individual metabolic rate of marine fishes (particularly MMR and AS), with consequences that scale up to the level of their population dynamics. Next, we discuss how (1) our study expands upon previous investigations of constraints on oxygen supply in aquatic habitats (specifically, an external constraint – environmental oxygen availability), (2) the implications of metabolic oxygen limitation for population growth, (3) the geography of intrinsic sensitivity to overfishing, and (4) some concluding thoughts in the context warming and deoxygenation in aquatic ecosystems.

Constraints on oxygen supply are hypothesized to fundamentally shape metabolic traits across marine fishes, and are an increasingly popular avenue for exploration in an era of climate change (Bigman et al. 2021, Clarke et al. 2021, Daufresne et al. 2009, Forster et al. 2012, Pörtner & Knust 2007, Rubalcaba et al. 2020). Inherently, the extraction of oxygen from the surrounding water poses unique challenges and limitations to the metabolism of water-breathing ectotherms. Obstacles to oxygen supply can arise at any given step along the oxygen uptake pathways, from the environment (organism interface at the gill surface) to the mitochondria of the organism (Rubalcaba et al. 2020). Aside from the geometric constraints inherent to the fractal circulatory system of organisms (Brown et al. 2004), the metabolic demands of aquatic ectotherms have been proposed to be limited by the capacity of the gills to supply oxygen (the *gill oxygen limitation theory*, 'GOLT'), in conjunction with limitations imposed by environmental oxygen availability (the *oxygen limitation hypothesis*; Forster et al. 2012, Pauly 2010, Pörtner & Knust 2007, Rubalcaba et al. 2020). These constraints on oxygen supply, whether intrinsic (e.g., gill surface area) or extrinsic (e.g., environmental oxygen availability), are thought to underpin a significant portion of the observed variation in metabolic rate across water-breathing ectotherms, and by extension, the life history strategies of species.

Although environmental oxygen availability has long been considered to act as a selective factor on metabolic rate and to modulate the scaling of metabolic rates with mass, temperature, and activity levels across aquatic species (Rubalcaba et al. 2020), it has been relatively unexplored compared to the recent attention received by intrinsic geometric constraints on oxygen uptake through the gills (Brown et al. 2004, Gillooly et al. 2001, Bigman et al. 2021, Killen et al. 2016). Rubalcaba et al. (2020) theoretically derived and implemented intrinsic and extrinsic constraints on oxygen supply into metabolic rate models, and supported their expectations with real observations of the scaling of metabolic rate with mass, temperature, and activity level across aquatic ectotherms. Congruently, we found evidence of the (extrinsic) constraint on oxygen supply imposed by oxygen availability within the habitats of marine fishes. Overall, species from low-oxygen habitats had inferior maximal aerobic capacity (MMR) and narrower energetic budgets for fitness-related activities (AS) than species from well-oxygenated environments. We also found evidence of an interactive effect between mass and temperature on AS, where AS was more sensitive to (i.e., scaled more steeply

with) body mass at cooler temperatures than in warm waters, in accordance with what was proposed by Rubalcaba et al. (2020). For MMR however, this model was ranked second to the model without interaction, although it performed equally well (Table 2.1). We also found RMR to be positively related with environmental oxygen availability, which is unsurprising given that higher maintenance costs (RMR) are an inevitable consequence of high MMR. It is noteworthy that despite a relative lack of MMR data for deep-sea, "sluggish" species compared to RMR, we observed a strong positive effect of environmental oxygen availability on MMR and AS, exceeding that for RMR.

From an ecological standpoint, any confines placed on physiological performance (MMR and AS) by oxygen are expected to have downstream consequences for the fitness and population dynamics of aquatic ectotherms (Pörtner & Knust 2007). Indeed, there is a growing body of literature proposing ecological frameworks on the basis of models of metabolic rate and oxygen availability (e.g., the "metabolic niche framework" and energetics-performance frameworks; Ern 2019, Brownscombe et al. 2022). At the population scale, r_{max} approximates mean fitness, where an individual's realized annual fitness is its contribution to population growth (Coulson et al. 2005). Although the evolution of the mean life history of a species maximizes r_{max} (McNab 1980, Lande 1982), fitness strategies develop within the confines of phylogenetic, physiological, and ecological constraints. Accordingly, our most significant finding is that fish population growth rates (r_{max}) are strongly positively related to environmental oxygen availability, even more so than to mass and temperature (Table 2.4, Figure B.2). Our results are in agreement with previous investigations of the scaling of r_{max} with mass, temperature, and depth in sharks (Pardo & Dulvy 2022), which found that r_{max} declined with depth independently of environmental temperature, and may be related to the decline in oxygen availability despite the relatively constant, cool temperatures at intermediate to deeper depths. Given that species with higher metabolic rates (particularly MMR and AS) generally exhibit higher r_{max} (see Chapter 1, Clavijo-Baquet & Bozinovic 2012, Savage et al. 2004), and our finding of a strong positive relationship between MMR (and AS) and environmental oxygen availability, it is unsurprising but important that we found r_{max} to increase with oxygen availability.

Crucially, the observed relationship between r_{max} and oxygen availability implies that species living in low-oxygen conditions or routinely-exposed to hypoxia may be more intrinsically sensitive to overfishing (and hence, would have lower fishing limits and

recovery potential) than species from well-oxygenated habitats. For example, cool-water benthic skates generally exhibit higher r_{max} than warm-water benthic rays, which is counterintuitive given the expected positive relationship between r_{max} and temperature (Barrowclift-Mahon et al. 2023). Aside from obvious differences in the reproductive modes of these two groups, most skates live in cool well-oxygenated environments, while warm-water coastal stingrays live in relatively lower oxygen or may periodically experience hypoxia (this study, Schwieterman et al. 2019). As most marine species (particularly sharks) are data poor, our findings may directly inform the basis of geographic models which predict r_{max} and intrinsic sensitivity to overfishing, despite a lack of life history trait data required to calculate these essential population metrics.

Our findings clearly indicate that environmental oxygen availability and temperature underlie MMR (and hence, AS) and the maximum intrinsic population growth rates of aquatic species. Climate change is shifting and expanding warmer isotherms and decreasing oxygen availability in the ocean. Ideally, we would like to understand how these abiotic variables influence the range of population growth from r_0 to r_{max} for individual species, and hence the spatial extents of populations. Nevertheless, our findings forewarn that climate change will affect individual fitness, which will in turn have repercussions for the population dynamics and geographic distributions of marine species.

2.6. Tables

Table 2.1. Comparison of models testing the effects of environmental oxygen partial pressure, environmental (measurement) temperature, and measurement body mass on metabolic rate (RMR, MMR, or AS) across marine fishes, whilst accounting for evolutionary history and ecological lifestyle. Environmental oxygen and temperature were estimated at the median usual depth for each species across grid cells overlapping with its core distribution. Models were fit in brms using R version 4.0.5. Whole organism metabolic rate (Watts), measurement body mass (grams), and environmental oxygen (atm) were natural log transformed, while measurement temperature was taken as the inverse temperature (see Methods). All explanatory variables were standardized. All models within 2 looic of the highest-ranking model (emboldened) are highlighted in grey.

a) RMR models **(N=169)**		p_{loo}	looic	$elpd_{loo}$	se_elpd_{loo}	$elpd_{diff}$	weight
RMR_mt	$stdlog(M) + std(invtemp) + LS$	36.2	261.3	-130.7	12.8	-3.8	0.333
RMR_mxt	$stdlog(M) * std(invtemp) + LS$	32.9	264.9	-132.4	12.6	-5.6	0.000
RMR_mo	$stdlog(M) + stdlog(PO2) + LS$	52.4	327.7	-163.9	10.1	-37.0	0.000
RMR_mxo	$stdlog(M) * stdlog(PO2) + LS$	53.4	322.8	-161.4	10.7	-34.6	0.037
RMR_mto	$\boldsymbol{stdlog(M) + std(invtemp) + stdlog(PO2) + LS}$	**32.8**	**253.7**	**-126.8**	**12.0**	**0.0**	**0.630**
RMR_mxto	$stdlog(M) * std(invtemp) + stdlog(PO2) + LS$	31.1	256.8	-128.4	11.9	-1.6	0.000
RMR_mxot	$stdlog(M) * stdlog(PO2) + std(invtemp) + LS$	35.9	255.3	-127.7	12.1	-0.8	0.000
RMR_mtxo	$stdlog(M) + std(invtemp) * stdlog(PO2) + LS$	31.8	255.6	-127.8	12.2	-1.0	0.000
b) MMR models **(N=100)**							
MMR_mt	$stdlog(M) + std(invtemp) + LS$	30.7	154.8	-77.4	15.9	-22.5	0.057
MMR_mxt	$stdlog(M) * std(invtemp) + LS$	34.1	155.2	-77.6	15.3	-22.6	0.000
MMR_mo	$stdlog(M) + stdlog(PO2) + LS$	60.9	140.8	-70.4	7.3	-15.5	0.000
MMR_mxo	$stdlog(M) * stdlog(PO2) + LS$	60.5	141.0	-70.5	7.1	-15.6	0.106
MMR_mto	$\boldsymbol{stdlog(M) + std(invtemp) + stdlog(PO2) + LS}$	**22.9**	**109.9**	**-54.9**	**8.0**	**0.0**	**0.495**

MMR_mxto	$stdlog(M) * std(invtemp) + stdlog(PO2) + LS$	24.4	110.0	-55.0	8.0	0.0	0.342
MMR_mxot	$stdlog(M) * stdlog(PO2) + std(invtemp) + LS$	23.8	112.2	-56.1	8.0	-1.1	0.000
MMR_mtxo	$stdlog(M) + std(invtemp) * stdlog(PO2) + LS$	23.4	112.3	-56.1	8.0	-1.2	0.000
***c) AS models* (N=80)**							
AS_mt	$stdlog(M) + std(invtemp) + LS$	31.8	149.5	-74.7	13.4	-3.8	0.000
AS _mxt	$stdlog(M) * std(invtemp) + LS$	36.2	145.5	-72.7	12.8	-1.8	0.000
AS _mo	$stdlog(M) + stdlog(PO2) + LS$	57.4	145.1	-72.5	9.7	-1.6	0.283
AS _mxo	$stdlog(M) * stdlog(PO2) + LS$	61.3	148.6	-74.3	9.4	-3.3	0.000
AS _mto	$stdlog(M) + std(invtemp) + stdlog(PO2) + LS$	24.6	144.7	-72.4	14.8	-1.4	0.000
AS _mxto	$\boldsymbol{stdlog(M) * std(invtemp) + stdlog(PO2) + LS}$	**28.8**	**141.9**	**-70.9**	**15.3**	**0.0**	**0.717**
AS _mxot	$stdlog(M) * stdlog(PO2) + std(invtemp) + LS$	24.8	146.7	-73.4	14.6	-2.4	0.000
AS _mtxo	$stdlog(M) + std(invtemp) * stdlog(PO2) + LS$	25.5	145.7	-72.8	14.9	-1.9	0.000

Table 2.2. Comparison of models testing the effects of environmental oxygen partial pressure, environmental temperature, and maximum body mass on population growth rate r_{max} across marine fishes, whilst accounting for evolutionary history. Environmental oxygen and temperature were estimated at the median usual depth for each species across grid cells overlapping with its core distribution. Models were fit in brms using R version 4.0.5. The maximum intrinsic rate of population increase r_{max} (yr^{-1}), maximum body mass (grams), and environmental oxygen (atm) were natural log transformed, while measurement temperature was taken as the inverse temperature (see Methods). All explanatory variables were standardized. All models within 2 looic of the highest-ranking model (emboldened) are highlighted in grey.

r_{max} models **(N = 80)**		p_{loo}	looic	$elpd_{loo}$	se_elpd_{loo}	$elpd_{diff}$	weight
rmax_m	$stdlog(M)$	14.5	197.0	-98.5	8.6	-15.4	0.000
rmax_mt	$stdlog(M) + std(invtemp)$	19.2	185.2	-92.6	8.8	-9.5	0.000
rmax_mxt	$stdlog(M) * std(invtemp)$	19.9	187.2	-93.6	8.9	-10.5	0.000
rmax_mo	$stdlog(M) + stdlog(PO2)$	13.6	173.2	-86.6	7.7	-3.5	0.000
rmax_mxo	$stdlog(M) * stdlog(PO2)$	14.7	175.1	-87.5	7.8	-4.5	0.000
rmax_mto	$\boldsymbol{stdlog(M) + std(invtemp) + stdlog(PO2)}$	**16.3**	**166.2**	**-83.1**	**7.9**	**0.0**	**0.480**
rmax_mxto	$stdlog(M) * std(invtemp) + stdlog(PO2)$	16.4	167.0	-83.5	7.7	-0.4	0.000
rmax_mxot	$stdlog(M) * stdlog(PO2) + std(invtemp)$	17.3	167.5	-83.8	8.1	-0.7	0.145
rmax_mtxo	$stdlog(M) + std(invtemp) * stdlog(PO2)$	19.8	167.9	-84.0	7.7	-0.9	0.374

Table 2.3. Coefficient means and 95% Bayesian Credible Intervals (BCI, in parentheses) for all metabolic rate models presented in Table 2.1. Ecological lifestyles 'LS' were 'B' = benthic, 'BP' = benthopelagic, and 'P' = pelagic.

model	LS	intercept	std_log_mass	std_inv_temp	std_log_oxygen	interaction	sigma
RMR_mt	P	-2.65 (-2.95 to -2.35)	2.25 (2.14 to 2.35)	-0.57 (-0.69 to -0.46)	NA	NA	0.46 (0.39 to 0.54)
	BP	-3.02 (-3.25 to -2.79)					
	B	-3.50 (-4.04 to -2.94)					
RMR_mxt	P	-2.66 (-2.96 to -2.37)	2.26 (2.15 to 2.37)	-0.58 (-0.70 to -0.47)	NA	-0.06 (-0.15 to 0.03)	0.47 (0.40 to 0.56)
	BP	-3.01 (-3.24 to -2.78)					
	B	-3.51 (-4.01 to -3.00)					
RMR_mo	P	-2.63 (-3.03 to -2.23)	2.24 (2.11 to 2.37)	NA	0.08 (-0.03 to 0.19)	NA	0.52 (0.44 to 0.61)
	BP	-2.91 (-3.22 to -2.61)					
	B	-3.66 (-4.52 to -2.75)					
RMR_mxo	P	-2.59 (-2.99 to -2.20)	2.23 (2.10 to 2.36)	NA	0.06 (-0.05 to 0.16)	0.18 (0.06 to 0.29)	0.51 (0.43 to 0.60)
	BP	-2.85 (-3.15 to -2.65)					
	B	-3.65 (-4.49 to -2.79)					
RMR_mto	P	-2.61 (-2.90 to -2.33)	2.27 (2.16 to 2.37)	-0.60 (-0.71 to -0.50)	0.16 (0.08 to 0.25)	NA	0.46 (0.39 to 0.53)
	BP	-3.03 (-3.25 to -2.82)					
	B	-3.53 (-4.00 to -3.05)					

RMR_mxto	P	-2.62 (-2.90 to -2.35)	2.28 (2.17 to 2.38)	-0.61 (-0.72 to -0.51)	0.16 (0.07 to 0.24)	-0.05 (-0.13 to 0.04)	0.47 (0.40 to 0.54)
	BP	-3.03 (-3.24 to -2.82)					
	B	-3.54 (-3.99 to -3.09)					
RMR_mxot	P	-2.60 (-2.89 to -2.31)	2.26 (2.16 to 2.36)	-0.59 (-0.70 to -0.48)	0.15 (0.07 to 0.24)	0.06 (-0.04 to 0.15)	0.45 (0.38 to 0.53)
	BP	-3.02 (-3.24 to -2.79)					
	B	-3.53 (-4.02 to -3.04)					
RMR_mtxo	P	-2.64 (-2.93 to -2.36)	2.28 (2.18 to 2.39)	-0.59 (-0.70 to -0.49)	0.09 (-0.06 to 0.24)	0.07 (-0.06 to 0.20)	0.46 (0.39 to 0.54)
	BP	-3.05 (-3.27 to -2.83)					
	B	-3.53 (-3.99 to -3.07)					
MMR_mt	P	-1.42 (-1.90 to -0.97)	1.89 (1.77 to 2.02)	-0.51 (-0.65 to -0.37)	NA	NA	0.44 (0.34 to 0.54)
	BP	-1.88 (-2.26 to -1.52)					
	B	-2.15 (-2.76 to -1.50)					
MMR_mxt	P	-1.41 (-1.89 to -0.95)	1.88 (1.76 to 2.00)	-0.50 (-0.64 to -0.36)	NA	0.10 (-0.02 to 0.23)	0.43 (0.32 to 0.54)
	BP	-1.89 (-2.27 to -1.52)					
	B	-2.17 (-2.79 to -1.48)					
MMR_mo	P	-1.23 (-1.74 to -0.73)	1.91 (1.77 to 2.05)	NA	0.31 (0.20 to 0.43)	NA	0.32 (0.18 to 0.45)
	BP	-1.74 (-2.16 to -1.33)					
	B	-2.60 (-3.73 to -1.47)					

MMR_mxo	P BP B	-1.23 (-1.74 to -0.72) -1.77 (-2.20 to -1.34) -2.59 (-3.70 to -1.45)	1.92 (1.78 to 2.07)	NA	0.26 (0.10 to 0.42)	-0.07 (-0.20 to 0.06)	0.33 (0.17 to 0.46)
MMR_mto	P BP B	-1.12 (-1.47 to -0.81) -1.78 (-2.05 to -1.52) -2.36 (-2.80 to -1.93)	1.84 (1.74 to 1.94)	-0.56 (-0.67 to -0.45)	0.34 (0.24 to 0.43)	NA	0.37 (0.29 to 0.45)
MMR_mxto	P BP B	-1.13 (-1.47 to -0.79) -1.80 (-2.07 to -1.53) -2.38 (-2.84 to -1.95)	1.84 (1.74 to 1.93)	-0.55 (-0.66 to -0.44)	0.33 (0.24 to 0.42)	0.06 (-0.04 to 0.16)	0.36 (0.29 to 0.45)
MMR_mxot	P BP B	-1.12 (-1.47 to -0.79) -1.78 (-2.06 to -1.51) -2.36 (-2.81 to -1.94)	1.84 (1.74 to 1.94)	-0.56 (-0.67 to -0.45)	0.34 (0.21 to 0.46)	-0.00 (-0.10 to 0.10)	0.37 (0.29 to 0.45)
MMR_mtxo	P BP B	-1.12 (-1.46 to -0.78) -1.78 (-2.05 to -1.51) -2.36 (-2.81 to -1.94)	1.84 (1.74 to 1.94)	-0.57 (-0.68 to -0.45)	0.36 (0.19 to 0.53)	-0.02 (-0.14 to 0.10)	0.37 (0.29 to 0.45)
AS_mt	P BP B	-1.13 (-1.67 to -0.61) -2.00 (-2.45 to -1.56) -2.40 (-3.21 to -1.58)	1.76 (1.60 to 1.92)	-0.45 (-0.62 to -0.28)	NA	NA	0.50 (0.29 to 0.66)

AS_mxt	P BP B	-1.11 (-1.66 to -0.59) -1.98 (-2.43 to -1.55) -2.39 (-3.23 to -1.49)	1.75 (1.60 to 1.90)	-0.44 (-0.60 to -0.26)	NA	0.12 (-0.02 to 0.27)	0.47 (0.23 to 0.65)
AS_mo	P BP B	-0.99 (-1.65 to -0.34) -1.90 (-2.47 to -1.35) -2.64 (-3.99 to -1.29)	1.83 (1.63 to 2.02)	NA	0.10 (-0.07 to 0.28)	NA	0.40 (0.12 to 0.63)
AS_mxo	P BP B	-1.00 (-1.67 to -0.34) -1.91 (-2.48 to -1.36) -2.65 (-3.98 to -1.34)	1.83 (1.62 to 2.04)	NA	0.10 (-0.08 to 0.28)	-0.00 (-0.14 to 0.14)	0.40 (0.11 to 0.64)
AS_mto	P BP B	-0.99 (-1.49 to -0.52) -1.89 (-2.31 to -1.50) -2.50 (-3.13 to -1.91)	1.74 (1.59 to 1.90)	-0.55 (-0.72 to -0.38)	0.25 (0.08 to 0.41)	NA	0.51 (0.35 to 0.64)
AS_mxto	P BP B	-0.98 (-1.46 to -0.51) -1.89 (-2.29 to -1.50) -2.53 (-3.21 to -1.92)	1.74 (1.60 to 1.88)	-0.54 (-0.70 to -0.36)	0.26 (0.10 to 0.42)	0.15 (0.01 to 0.29)	0.49 (0.31 to 0.63)
AS_mxot	P BP	-0.98 (-1.48 to -0.53) -1.88 (-2.29 to -1.48)	1.73 (1.59 to 1.89)	-0.55 (-0.72 to -0.38)	0.26 (0.09 to 0.42)	0.04 (-0.09 to 0.16)	0.52 (0.36 to 0.65)

	B	-2.50 (-3.10 to -1.93)					
AS_mtxo	P	-0.95 (-1.45 to -0.49)	1.74 (1.59 to 1.89)	-0.56 (-0.74 to -0.38)	0.28 (0.09 to 0.46)	-0.05 (-0.19 to 0.09)	0.51 (0.35 to 0.64)
	BP	-1.87 (-2.27 to -1.48)					
	B	-2.48 (-3.15 to -1.86)					

Table 2.4. Coefficient means and 95% Bayesian Credible Intervals (BCI, in parentheses) for all r_{max} models presented in Table 2.2.

model	intercept	std_log_mass	std_inv_temp	std_log_oxygen	interaction	sigma
rmax_m	-1.07 (-1.68 to -0.40)	-0.37 (-0.58 to -0.15)	NA	NA	NA	0.75 (0.61 to 0.92)
rmax_mt	-1.06 (-1.79 to -0.27)	-0.39 (-0.60 to -0.18)	-0.37 (-0.63 to -0.11)	NA	NA	0.67 (0.53 to 0.84)
rmax_mxt	-1.07 (-1.81 to -0.26)	-0.39 (-0.60 to -0.17)	-0.36 (-0.63 to -0.10)	NA	-0.05 (-0.25 to 0.15)	0.68 (0.53 to 0.85)
rmax_mo	-1.11 (-1.60 to -0.58)	-0.34 (-0.52 to -0.15)	NA	0.43 (0.27 to 0.59)	NA	0.65 (0.53 to 0.79)
rmax_mxo	-1.11 (-1.62 to -0.58)	-0.34 (-0.52 to -0.15)	NA	0.41 (0.24 to 0.58)	-0.06 (-0.22 to 0.11)	0.65 (0.53 to 0.80)
rmax_mto	-1.11 (-1.66 to -0.52)	-0.37 (-0.55 to -0.19)	-0.27 (-0.48 to -0.06)	0.40 (0.25 to 0.56)	NA	0.61 (0.49 to 0.75)

rmax_mxto	-1.13 (-1.67 to -0.56)	-0.36 (-0.54 to -0.18)	-0.24 (-0.46 to -0.03)	0.41 (0.25 to 0.57)	-0.08 (-0.25 to 0.09)	0.61 (0.49 to 0.75)
rmax_mxot	-1.12 (-1.67 to -0.54)	-0.37 (-0.55 to -0.19)	-0.27 (-0.49 to -0.06)	0.37 (0.20 to 0.54)	-0.07 (-0.22 to 0.09)	0.61 (0.49 to 0.75)
rmax_mtxo	-1.13 (-1.72 to -0.51)	-0.34 (-0.53 to -0.16)	-0.30 (-0.52 to -0.08)	0.70 (0.22 to 1.19)	-0.25 (-0.62 to 0.13)	0.60 (0.48 to 0.74)

2.7. Figures

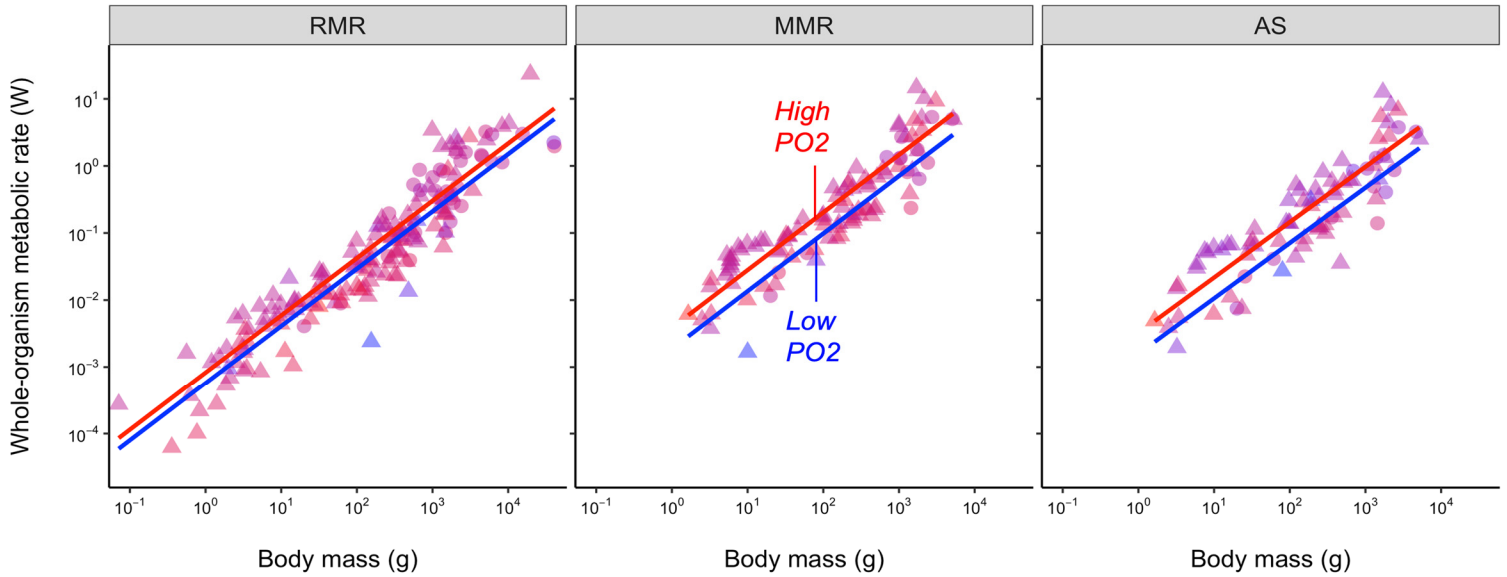

Figure 2.1. **Species from relatively high oxygen habitats have higher metabolic rates than species from habitats with low oxygen.** Models of resting metabolic rate 'RMR' (N=169, left), maximum metabolic rate 'MMR' (N=100, center), and aerobic scope 'AS' (N=80, right) scaling with measurement body mass, "environmental" temperature (closest measurement temperature), and environmental oxygen. Datapoints are coloured by the magnitude of the oxygen partial pressure at the usual median depth of the species, where red indicates high oxygen and blue indicates low oxygen. Triangles symbolize teleost fishes, while circles symbolize sharks. The fitted regression lines in all panels is the metabolic rate (Watts) scaling with body mass (grams), estimated for species living at relatively high (95th percentile of the dataset, in red) versus relatively low (5th percentile of the dataset, in blue) oxygen partial pressure values whilst accounting for measurement temperature, ecological lifestyle, and evolutionary history. Metabolic rate and all explanatory variables were natural log-transformed, with the exception of measurement temperature which was taken as the inverse temperature (see Methods).

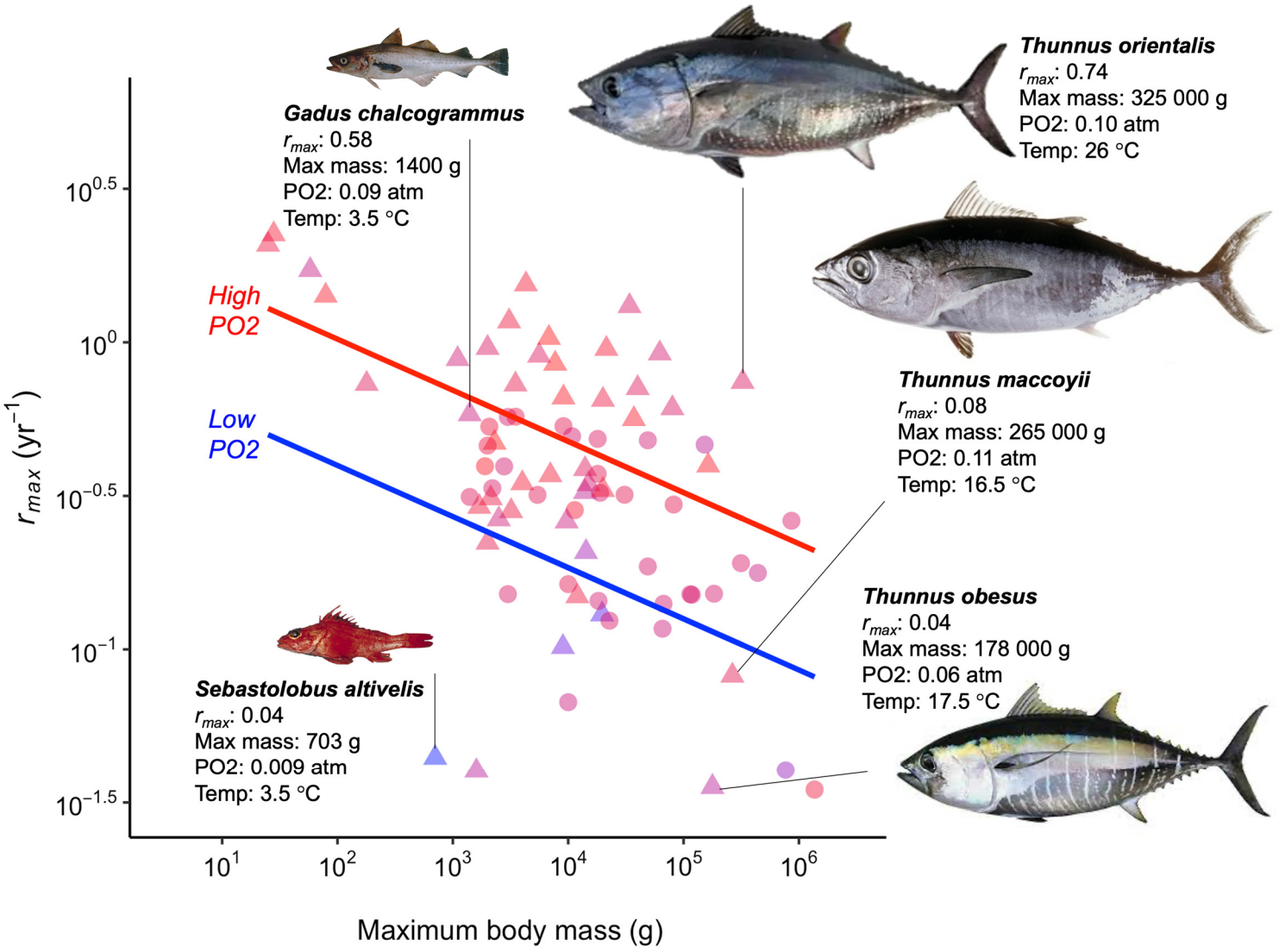
Gadus chalcogrammus
r_{max}: 0.58
Max mass: 1400 g
PO2: 0.09 atm
Temp: 3.5 °C
Thunnus orientalis
r_{max}: 0.74
Max mass: 325 000 g
PO2: 0.10 atm
Temp: 26 °C
Thunnus maccoyii
r_{max}: 0.08
Max mass: 265 000 g
PO2: 0.11 atm
Temp: 16.5 °C
Thunnus obesus
r_{max}: 0.04
Max mass: 178 000 g
PO2: 0.06 atm
Temp: 17.5 °C
Sebastolobus altivelis
r_{max}: 0.04
Max mass: 703 g
PO2: 0.009 atm
Temp: 3.5 °C
High PO2
Low PO2
r_{max} (yr^{-1})
$10^{0.5}$
10^{0}
$10^{-0.5}$
10^{-1}
$10^{-1.5}$
10^{1}
10^{2}
10^{3}
10^{4}
10^{5}
10^{6}
Maximum body mass (g)

Figure 2.2. **Species from relatively high oxygen habitats exhibit faster population growth than species from low-oxygen habitats.** Maximum intrinsic rate of population increase (r_{max}) plotted against maximum body mass for 80 marine fish species. Points are coloured by the magnitude of the oxygen partial pressure at the usual median depth of the species, where red indicates high oxygen levels and blue indicates lower oxygen levels. Triangles symbolize teleost fishes, while circles symbolize sharks. Fitted lines show the scaling of r_{max} (year^{-1}) with maximum body mass (grams), estimated for species living at relatively high (95th percentile, red line) versus relatively low (5th percentile, blue line) oxygen partial pressure values in the dataset, while controlling for the effect of environmental temperature and evolutionary history. The r_{max} of species increased with increasing environmental oxygen availability, where environmental oxygen explained more variation in r_{max} relative to environmental temperature and maximum body mass.

Photos for *S. altivelis* and *G. chalcogrammus* were sourced from the Archipelago Marine Research Ltd. (via Fishbase), photo of *T. obesus* taken by David Itano, photo of *T. orientalis* taken from the website of the Smithsonian Institution, and photo of *T. maccoyii* taken from https://fishesofaustralia.net.au/home/species/732.

2.8. References

Barrowclift, E., Gravel, S. M., Pardo, S. A., Bigman, J. S., Berggren, P., & Dulvy, N. K. (2023). Tropical rays are intrinsically more sensitive to overfishing than the temperate skates. Biological Conservation, 281, 110003.

Bernhardt, J. R., Sunday, J. M., & O'Connor, M. I. (2018). Metabolic theory and the temperature-size rule explain the temperature dependence of population carrying capacity. The American Naturalist, 192(6), 687-697.

Bigman, J. S., Pardo, S. A., Prinzing, T. S., Dando, M., Wegner, N. C., & Dulvy, N. K. (2018). Ecological lifestyles and the scaling of shark gill surface area. Journal of morphology, 279(12), 1716-1724.

Bigman JS, M'Gonigle L, Wegner NC and Dulvy NK. (2021) Respiratory capacity is twice as important as temperature in driving patterns of metabolic rate across the vertebrate tree of life. Science Advances 7, eabe5163.

Brodte, E., Graeve, M., Jacob, U., Knust, R., & Pörtner, H. O. (2008). Temperature-dependent lipid levels and components in polar and temperate eelpout (Zoarcidae). Fish Physiology and Biochemistry, 34, 261-274.

Brown, J. H., Gillooly, J. F., Allen, A. P., Savage, V. M., & West, G. B. (2004). Toward a metabolic theory of ecology. Ecology, 85(7), 1771-1789.

Brownscombe, J. W., Raby, G. D., Murchie, K. J., Danylchuk, A. J., & Cooke, S. J. (2022). An energetics–performance framework for wild fishes. Journal of Fish Biology, 101(1), 4-12.

Bürkner, P. C. (2017). brms: An R package for Bayesian multilevel models using Stan. Journal of statistical software, 80, 1-28.

Clark, T. D., Sandblom, E., & Jutfelt, F. (2013). Aerobic scope measurements of fishes in an era of climate change: respirometry, relevance and recommendations. Journal of Experimental Biology, 216(15), 2771-2782.

Clarke, A., & Johnston, N. M. (1999). Scaling of metabolic rate with body mass and temperature in teleost fish. Journal of animal ecology, 68(5), 893-905.

Clarke, T. M., Wabnitz, C. C., Striegel, S., Frölicher, T. L., Reygondeau, G., & Cheung, W. W. (2021). Aerobic growth index (AGI): An index to understand the impacts of ocean warming and deoxygenation on global marine fisheries resources. Progress in Oceanography, 195, 102588.

Clavijo-Baque, S., & Bozinovic, F. (2012). Testing the fitness consequences of the thermoregulatory and parental care models for the origin of endothermy. PLoS One, 7(5), e37069.

Cortés, E. (2016). Perspectives on the intrinsic rate of population growth. Methods in Ecology and Evolution, 7(10), 1136-1145.

Denney, N. H., Jennings, S., & Reynolds, J. D. (2002). Life–history correlates of maximum population growth rates in marine fishes. Proceedings of the Royal Society of London. Series B: Biological Sciences, 269(1506), 2229-2237.

Deutsch, C., Ferrel, A., Seibel, B., Pörtner, H. O., & Huey, R. B. (2015). Climate change tightens a metabolic constraint on marine habitats. Science, 348(6239), 1132-1135.

Dormann, C. F., Elith, J., Bacher, S., Buchmann, C., Carl, G., Carré, G., ... & Lautenbach, S. (2013). Collinearity: a review of methods to deal with it and a simulation study evaluating their performance. Ecography, 36(1), 27-46.

Drazen, J. C., & Haedrich, R. L. (2012). A continuum of life histories in deep-sea demersal fishes. Deep Sea Research Part I: Oceanographic Research Papers, 61, 34-42.

Dulvy, N. K., Pacoureau, N., Rigby, C. L., Pollom, R. A., Jabado, R. W., Ebert, D. A., ... & Simpfendorfer, C. A. (2021). Overfishing drives over one-third of all sharks and rays toward a global extinction crisis. Current Biology, 31(21), 4773-4787.

Ern, R. (2019). A mechanistic oxygen-and temperature-limited metabolic niche framework. Philosophical Transactions of the Royal Society B, 374(1778), 20180540.

Forster, J., & Hirst, A. G. (2012). The temperature-size rule emerges from ontogenetic differences between growth and development rates. Functional Ecology, 26(2), 483-492.

Froese, R., and Pauly, D. 2019. FishBase World Wide Web electronic publication. www.fishbase.org (Accessed 9 January 2019).

Gillooly, J. F., Brown, J. H., West, G. B., Savage, V. M., & Charnov, E. L. (2001). Effects of size and temperature on metabolic rate. science, 293(5538), 2248-2251.

Grady, J. M., Enquist, B. J., Dettweiler-Robinson, E., Wright, N. A., & Smith, F. A. (2014). Evidence for mesothermy in dinosaurs. Science, 344(6189), 1268-1272.

Harley, C. D., Randall Hughes, A., Hultgren, K. M., Miner, B. G., Sorte, C. J., Thornber, C. S., ... & Williams, S. L. (2006). The impacts of climate change in coastal marine systems. Ecology letters, 9(2), 228-241.

Hutchings, J. A., Myers, R. A., García, V. B., Lucifora, L. O., & Kuparinen, A. (2012). Life-history correlates of extinction risk and recovery potential. Ecological Applications, 22(4), 1061-1067.

Kaschner, K., Kesner-Reyes, K., Garilao, C., Rius-Barile, J., Rees, T., & Froese, R. (2016). AquaMaps: Predicted range maps for aquatic species. World wide web electronic publication, www. aquamaps. org, Version, 8, 2016.

Killen, S. S., Glazier, D. S., Rezende, E. L., Clark, T. D., Atkinson, D., Willener, A. S., & Halsey, L. G. (2016). Ecological influences and morphological correlates of resting and maximal metabolic rates across teleost fish species. The American Naturalist, 187(5), 592-606.

Lande, R. (1982). A quantitative genetic theory of life history evolution. *Ecology*, *63*(3), 607-615.

McNab, B. K. (1980). Food habits, energetics, and the population biology of mammals. *The American Naturalist*, *116*(1), 106-124.

Mull, C. G., Pacoureau, N., Pardo, S. A., Ruiz, L. S., García-Rodríguez, E., Finucci, B., ... & Dulvy, N. K. (2022). Sharkipedia: a curated open access database of shark and ray life history traits and abundance time-series. Scientific Data, 9(1), 559.

Myers, R. A. (2001). Stock and recruitment: generalizations about maximum reproductive rate, density dependence, and variability using meta-analytic approaches. ICES Journal of Marine Science, 58(5), 937-951.

Myers, R. A., Hutchings, J. A., & Barrowman, N. J. (1997). Why do fish stocks collapse? The example of cod in Atlantic Canada. Ecological applications, 7(1), 91-106.

Myers, R. A., & Worm, B. (2005). Extinction, survival or recovery of large predatory fishes. Philosophical Transactions of the Royal Society B: Biological Sciences, 360(1453), 13-20.

Pardo, S. A., Kindsvater, H. K., Reynolds, J. D., & Dulvy, N. K. (2016). Maximum intrinsic rate of population increase in sharks, rays, and chimaeras: the importance of survival to maturity. Canadian journal of fisheries and aquatic sciences, 73(8), 1159-1163.

Pardo, S. A., & Dulvy, N. K. (2022). Body mass, temperature, and depth shape the maximum intrinsic rate of population increase in sharks and rays. Ecology and Evolution, 12(11), e9441.

Pauly, D. (2010). Gasping Fish and Panting Squids: Oxygen. Temperature and the Growth of Water-Breathing Animals (Excellence in Ecology Series, International Ecology Institute, ed. 2, 2019), 22.

Penn, J. L., & Deutsch, C. (2022). Avoiding ocean mass extinction from climate warming. Science, 376(6592), 524-526.

Pörtner HO and Knust R. (2007) Climate change affects marine fishes through the oxygen limitation of thermal tolerance. Science 315, 95-97.

R Core Team. (2021). R: A language and environment for statistical computing. Published online 2020.

Rabosky, D. L., Chang, J., Title, P. O., Cowman, P. F., Sallan, L., Friedman, M., ... & Alfaro, M. E. (2018). An inverse latitudinal gradient in speciation rate for marine fishes. Nature, 559(7714), 392-395.

RAM Legacy Stock Assessment Database (2018). “RAM Legacy Stock Assessment Database v4.44.” doi:10.5281/zenodo.2542919

Rubalcaba, J. G., Verberk, W. C., Hendriks, A. J., Saris, B., & Woods, H. A. (2020). Oxygen limitation may affect the temperature and size dependence of metabolism in aquatic ectotherms. Proceedings of the National Academy of Sciences, 117(50), 31963-31968.

Savage, V. M., Gillooly, J. F., Brown, J. H., West, G. B., & Charnov, E. L. (2004). Effects of body size and temperature on population growth. The American Naturalist, 163(3), 429-441.

Spijkers, J., & Boonstra, W. J. (2017). Environmental change and social conflict: the northeast Atlantic mackerel dispute. Regional Environmental Change, 17, 1835-1851.

Stein, R. W., Mull, C. G., Kuhn, T. S., Aschliman, N. C., Davidson, L. N., Joy, J. B., ... & Mooers, A. O. (2018). Global priorities for conserving the evolutionary history of sharks, rays and chimaeras. Nature ecology & evolution, 2(2), 288-298.

Schwieterman, G. D., Crear, D. P., Anderson, B. N., Lavoie, D. R., Sulikowski, J. A., Bushnell, P. G., & Brill, R. W. (2019). Combined effects of acute temperature change and elevated p CO2 on the metabolic rates and hypoxia tolerances of clearnose skate (Rostaraja eglanteria), summer flounder (Paralichthys dentatus), and thorny skate (Amblyraja radiata). Biology, 8(3), 56.

Vedor, M., Queiroz, N., Mucientes, G., Couto, A., Costa, I. D., Santos, A. D., ... & Sims, D. W. (2021). Climate-driven deoxygenation elevates fishing vulnerability for the ocean's widest ranging shark. Elife, 10, e62508.

Vehtari, Aki, Andrew Gelman, and Jonah Gabry. "Practical Bayesian model evaluation using leave-one-out cross-validation and WAIC." Statistics and computing 27 (2017): 1413-1432.

Verberk WCEP, Bilton DT, Calosi P, Spicer JI (2011) Oxygen supply in aquatic ectotherms: Partial pressure and solubility together explain biodiversity and size patterns. Ecology 92(8):1565–1572.

Whiteley, N. M., & Taylor, E. W. (2015). Responses to environmental stresses: oxygen, temperature, and pH. The natural history of the Crustacea, 4, 320-358.

Wilson, M. W., Ridlon, A. D., Gaynor, K. M., Gaines, S. D., Stier, A. C., & Halpern, B. S. (2020). Ecological impacts of human-induced animal behaviour change. Ecology letters, 23(10), 1522-1536.

Wong, S., Bigman, J. S., & Dulvy, N. K. (2021). The metabolic pace of life histories across fishes. Proceedings of the Royal Society B, 288(1953), 20210910.

World Ocean Atlas: Boyer, Tim P.; Garcia, Hernan E.; Locarnini, Ricardo A.; Zweng, Melissa M.; Mishonov, Alexey V.; Reagan, James R.; Weathers, Katharine A.; Baranova, Olga K.; Seidov, Dan; Smolyar, Igor V. (2018). World Ocean Atlas 2018. [Data subsets for environmental oxygen, temperature, density, and salinity (all decade statistical annual means)]. NOAA National Centers for Environmental Information. Dataset. https://www.ncei.noaa.gov/archive/accession/NCEI-WOA18.

Chapter 3.

General Discussion

The growing body of literature on the impacts of warming and deoxygenation on fish energetics, and the high levels of uncertainty surrounding the larger-scale population responses to global change-related phenomena (e.g., overfishing and climate change) calls for the unification of bioenergetics and ecological frameworks. However, we have a limited understanding of how individual performance and population fitness are related across biological and spatial scales, which has been impeded by a lack of empirical evidence for interspecific relationships between the metabolic rate, population dynamics, and the environment of aquatic species. In this thesis, I used a combination of datamining and methods for extracting the mean ambient oxygen and temperature at depth in the ocean to conduct a comparative analysis of metabolism, population dynamics, and environment across marine fishes. In Chapter 1, I examined the relationship between population-paired estimates of metabolic rate (RMR, MMR, and AS) and the maximum intrinsic rate of population increase (r_{max}) from 37 sharks and 47 teleosts, to test whether variation in metabolic rate was related to variation in the potential for population growth. In Chapter 2, I investigated the role of environmental oxygen and temperature in shaping RMR, MMR, and AS across 175 fishes, and how these effects scale up to the dynamics of their populations (i.e., r_{max}). Here, I summarize the main findings of this research and discuss their relevance to the applications of metabolic scaling theory in aquatic species, conservation and fisheries management, and the forecasting of biological responses to global environmental change in coming years.

In Chapter 1, I revealed that fish metabolic rates were more strongly associated with time-related traits (the integrative population parameter r_{max} and its component trait, the age-at-maturity) than with reproductive output. Though previous studies have demonstrated a direct relationship between RMR and r_{max} in mammals (Hennemann 1983, Duncan et al. 2007) or similarities in the scaling of RMR and r_{max} with mass and temperature (primarily in endotherms; Savage et al. 2004, DeLong et al. 2010), my study is unique in that it reveals the link between metabolic rate (RMR, MMR and AS) and r_{max} across ectothermic, water-breathing fishes. In fish, growth is indeterminate and internal

body temperature varies with ambient temperature, thus posing challenges to the estimation of metabolic rate at a standard body size and temperature across species. I found that fishes with lower metabolic rates generally matured later and had lower r_{max} compared to species with faster metabolism after accounting for the effects of mass and temperature on metabolic rate, consistent with previous findings of a metabolic basis for the speed-of-life histories and population dynamics (Savage et al. 2004, White et al. 2022, Wong et al. 2021). Importantly, I also demonstrated that r_{max} exhibits a stronger relationship with MMR and AS than with RMR, where MMR and AS showed steeper positive scaling with r_{max}. Though few other studies have made similar comparisons, this result corroborates a similar finding in rodents (Clavijo-Baquet & Bozinovic 2012). Indeed, it has been argued that MMR is more directly related to fitness-enhancing functions because higher uptake and delivery rates of oxygen and substrates to tissues promotes somatic and gonadal growth, aerobic performance, thermogenic capacity (in endotherms), and mobility (McNab 1980, Pauly 2010, Pettersen et al. 2016). Relatedly, these results also support that the aerobic scope (AS) of energy available for expenditures surpassing survival requirements (e.g., for allocating energy to somatic growth or reproduction) is an important determinant of performance in wild fish and therefore associated with fitness-related traits (such as r_{max}), as proposed by the *oxygen-capacity-limited-thermal-tolerance hypothesis* (‘OCLTT’; Pörtner & Knust 2007). Within the confines of several physiological, phylogenetic, and environmental constraints, having higher MMR (and by extension, higher AS) is favourable for individual performance and ultimately, fitness-related traits, despite the associated increase in resting costs this incurs. In the concluding remarks of Chapter 1, I speculated that the strong relationship between r_{max} with MMR and AS compared to RMR might be capturing variation due environmental oxygen availability, which is proposed by oxygen limitation theory to be a key constraint on MMR in water-breathing ectotherms (Pörtner & Knust 2007, Rubalcaba et al. 2020).

In Chapter 2, I found that species from cooler or low-oxygen habitats had lower metabolic rate and lower r_{max} than species from warmer or well-oxygenated habitats. Furthermore, the effect of oxygen availability on MMR and AS was greater than its effect on RMR, and more closely resembled the effect of oxygen on r_{max} (where environmental oxygen explained more variation in r_{max} than both maximum body mass and environmental temperature). Our results corroborate the findings of a recent study by

Rubalcaba et al. (2020), in which they revealed that incorporating internal and external limitations to oxygen supply significantly improved metabolic rate models for aquatic ectotherms. From an ecological perspective, environmental oxygen limitations on oxygen supply capacity and aerobic performance would be expected to limit in turn the mean population fitness (e.g., r_{max}), as I have found in Chapter 2. Overall, these results are consistent with the longstanding hypothesis of oxygen limitation, and further evidence the consequences of the physiological effects of oxygen and temperature for population dynamics and fitness-related traits.

The key findings in this thesis inform our understanding of the relationship between fish energetics and the environment, and help to bridge the gap between physiology and the dynamics of wild populations and their susceptibilities to strong fishing pressure. For example, the empirical support of a positive relationship between metabolic rate and r_{max} across fishes presented in Chapter 1 offers insight into the mechanistic underpinnings of the relatively slow life histories and population dynamics (and subsequently heightened intrinsic sensitivities to overfishing) observed for many sharks compared to bony fishes (Dulvy et al. 2021, Juan-Jordá et al. 2022). Thus, in most cases, sharks would face greater risk of extinction if fished under similar regimes designed for teleost species (Myers & Worm 2005), which my work and others' suggests may be due in part to fundamental differences in metabolic traits (Chapter 1, Wegner 2011, Wegner et al. 2012). Additionally, the finding that r_{max} was better related to MMR and AS may help to elucidate the conflicting results yielded by comparative analyses of RMR and life history traits (Arnold et al. 2021). However, my findings from Chapter 2 further suggest that classical metabolic scaling theory may not be as well-suited to MMR and AS as they are to RMR (upon which they were founded) as these models do not consider the effects of oxygen limitation in aquatic habitats, which was also argued by Rubalcaba et al. (2020). The findings uncovered in Chapter 2 not only support that environmental oxygen availability is an important determinant of MMR and AS in aquatic habitats, but also a key factor shaping r_{max}. Taken together, my work implies that (1) comparative analyses of metabolism and life histories would benefit from the consideration of metabolic traits which better capture the full extent of the aerobic performance of organisms (such as MMR and AS) and therefore, better relate to fitness, and 2) energetics-performance frameworks should consider metabolic oxygen limitation as an important characteristic of life in aquatic habitats.

Here, I have demonstrated a similar dependency of r_{max} on oxygen and temperature as the MMR and AS of marine fishes, where cooler or low-oxygen habitats are expected to host low productivity species, which would therefore be inherently sensitive to overfishing. These results provide us with a better understanding of the geography of intrinsic risk, and could therefore be an asset to both fisheries management and conservation planning by facilitating the identification of 'higher risk' habitats for area-based protections. Additionally, the unveiling of these broadscale relationships could help to alleviate the need for data-intensive life history traits, which is of particular interest for marine habitats where data on these traits is lacking for most species. Reversely, there have been promising recent advances in the development and applications of imputation methods to estimate life history traits, stock-recruitment and population dynamics parameters (such as r_{max}) for all described fish species (Thorson 2020). These advances, combined with relationships such as those unveiled in my thesis, may greatly contribute to the formation of biogeographic models which are rooted in our understanding of how environmental effects scale across biological scales, from individuals to populations. In turn, we could visualize the spatial patterning of metabolic traits, life histories, population dynamics, and ultimately, the intrinsic sensitivity of species to threats from overfishing and climate change as a function of fundamental environmental correlates of metabolic physiology, such as oxygen and temperature.

There are however significant limitations to the applications this work, particularly when it comes to modelling the population-level effects of climate change. There is a vast body of literature documenting broadscale biological responses to warming and deoxygenation in water-breathing ectotherms, such as body size reductions and shifts in distribution, phenology, and productivity, varying greatly in their magnitude across species (Audzijonyte et al. 2020, Cheung et al. 2012, Sunday et al. 2012). Thus, the models presented in this thesis cannot be easily used to make direct predictions of the effects of climate change on population dynamics. Notwithstanding, studies of this kind are pivotal to forming baseline expectations which will serve as foundation for future models forecasting biological responses to climate change.

In conclusion, the results presented in Chapter 1 of this thesis support that the speed of metabolic rates is related to the speed-of-life continuum observed for time-related life history traits and population dynamics. Additionally, I found that MMR and AS were overall better associated with r_{max} than RMR, and thus may better "map" to the life

history strategies and population dynamics of species. Finally, my findings in Chapter 2 provide support for the limitation of metabolic rates by oxygen in the ocean marine fishes, and that the effects of oxygen and temperature on fish metabolism likely scale up to the dynamics of their populations. The relationships between metabolic rate, r_{max}, and environmental oxygen and temperature outlined in this thesis may ultimately contribute to the formation of geographic models for population dynamics and intrinsic risk, and can inform our baseline expectations for environmental oxygen and temperature effects on population growth in the face of an uncertain future.

3.1. References

Arnold, P. A., Delean, S., Cassey, P., & White, C. R. (2021). Meta-analysis reveals that resting metabolic rate is not consistently related to fitness and performance in animals. Journal of Comparative Physiology B, 191(6), 1097-1110.

Audzijonyte, A., Richards, S. A., Stuart-Smith, R. D., Pecl, G., Edgar, G. J., Barrett, N. S., ... & Blanchard, J. L. (2020). Fish body sizes change with temperature but not all species shrink with warming. Nature Ecology & Evolution, 4(6), 809-814.

Bernhardt, J. R., Sunday, J. M., & O'Connor, M. I. (2018). Metabolic theory and the temperature-size rule explain the temperature dependence of population carrying capacity. The American Naturalist, 192(6), 687-697.

Cheung, W. W., Sarmiento, J. L., Dunne, J., Frölicher, T. L., Lam, V. W., Deng Palomares, M. L., ... & Pauly, D. (2013). Shrinking of fishes exacerbates impacts of global ocean changes on marine ecosystems. Nature Climate Change, 3(3), 254-258.

Clavijo-Baque, S., & Bozinovic, F. (2012). Testing the fitness consequences of the thermoregulatory and parental care models for the origin of endothermy. PLoS One, 7(5), e37069.

DeLong, J. P., Okie, J. G., Moses, M. E., Sibly, R. M., & Brown, J. H. (2010). Shifts in metabolic scaling, production, and efficiency across major evolutionary transitions of life. Proceedings of the National Academy of Sciences, 107(29), 12941-12945.

Duncan, R. P., Forsyth, D. M., & Hone, J. (2007). Testing the metabolic theory of ecology: allometric scaling exponents in mammals. Ecology, 88(2), 324-333.

Dulvy, N. K., Pacoureau, N., Rigby, C. L., Pollom, R. A., Jabado, R. W., Ebert, D. A., ... & Simpfendorfer, C. A. (2021). Overfishing drives over one-third of all sharks and rays toward a global extinction crisis. Current Biology, 31(21), 4773-4787.

Duncan, R. P., Forsyth, D. M., & Hone, J. (2007). Testing the metabolic theory of ecology: allometric scaling exponents in mammals. Ecology, 88(2), 324-333.

Hennemann, W. W. (1983). Relationship among body mass, metabolic rate and the intrinsic rate of natural increase in mammals. Oecologia, 56, 104-108.

Hutchings, J. A., Myers, R. A., García, V. B., Lucifora, L. O., & Kuparinen, A. (2012). Life-history correlates of extinction risk and recovery potential. Ecological Applications, 22(4), 1061-1067.

Juan-Jordá, M. J., Murua, H., Arrizabalaga, H., Merino, G., Pacoureau, N., & Dulvy, N. K. (2022). Seventy years of tunas, billfishes, and sharks as sentinels of global ocean health. Science, 378(6620), eabj0211.

McNab, B. K. (1980). Food habits, energetics, and the population biology of mammals. The American Naturalist, 116(1), 106-124.

Myers, R. A., & Worm, B. (2005). Extinction, survival or recovery of large predatory fishes. Philosophical Transactions of the Royal Society B: Biological Sciences, 360(1453), 13-20.

Pauly, D. (2010). Gasping Fish and Panting Squids: Oxygen. Temperature and the Growth of Water-Breathing Animals (Excellence in Ecology Series, International Ecology Institute, ed. 2, 2019), 22.

Pettersen, A. K., White, C. R., & Marshall, D. J. (2016). Metabolic rate covaries with fitness and the pace of the life history in the field. Proceedings of the Royal Society B: Biological Sciences, 283(1831), 20160323.

Pörtner HO and Knust R. (2007) Climate change affects marine fishes through the oxygen limitation of thermal tolerance. Science 315, 95-97.

Rubalcaba, J. G., Verberk, W. C., Hendriks, A. J., Saris, B., & Woods, H. A. (2020). Oxygen limitation may affect the temperature and size dependence of metabolism in aquatic ectotherms. Proceedings of the National Academy of Sciences, 117(50), 31963-31968.

Savage, V. M., Gillooly, J. F., Brown, J. H., West, G. B., & Charnov, E. L. (2004). Effects of body size and temperature on population growth. The American Naturalist, 163(3), 429-441.

Sunday, J. M., Bates, A. E., & Dulvy, N. K. (2012). Thermal tolerance and the global redistribution of animals. Nature Climate Change, 2(9), 686-690.

Thorson, J. T. (2020). Predicting recruitment density dependence and intrinsic growth rate for all fishes worldwide using a data-integrated life-history model. Fish and Fisheries, 21(2), 237-251.

Wegner, N. C. (2011). Gill Respiratory Morphometrics. In Farrell, A. P. (Ed.), Encyclopedia of Fish Physiology: From Genome to Environment (Vol. 2, pp. 803–811). San Diego, CA: Academic Press.

Wegner, N. C., Lai, N. C., Bull, K. B., & Graham, J. B. (2012). Oxygen utilization and the branchial pressure gradient during ram ventilation of the shortfin mako, Isurus oxyrinchus: is lamnid shark–tuna convergence constrained by elasmobranch gill morphology? Journal of Experimental Biology, 215(1), 22-28.

White, C. R., Alton, L. A., Bywater, C. L., Lombardi, E. J., & Marshall, D. J. (2022). Metabolic scaling is the product of life-history optimization. Science, 377(6608), 834-839.

Wong, S., Bigman, J. S., & Dulvy, N. K. (2021). The metabolic pace of life histories across fishes. Proceedings of the Royal Society B, 288(1953), 20210910.

Appendix A.

Supplementary Material Chapter 1

A.1. Supplementary Methods

A.1.1. Metabolic rate data collation, selection, and aggregation

We used metabolic rates estimated from the rate of oxygen consumption of an organism over time, via respirometry methods. Different types of metabolic rate (resting, standard, routine, maximum) reflect a variety of states, according to certain conditions including activity level, digestive state, and external stimuli (Fry 1971). All metabolic rates in our study were estimated in non-reproductive, fasted, and unstressed organisms, and in the absence of external stimuli (e.g., no light or noise disturbances, "control" oxygen and salinity conditions, etc.), typically in a laboratory setting. However, due to the inherent challenges with conducting respirometry trials in-laboratory for certain species, such as very deep-sea fishes or very large species such as tunas and Greenland sharks, metabolic rates were often measured in situ or not long after the organisms were caught in the field. We collected resting metabolic rate (RMR) estimates from studies conducted on quiescent (resting) organisms, or estimates of standard metabolic rate (SMR) when this was available, for species which exhibit periods of rest characterized by little to no movement in the respirometry chamber. For highly active and obligate ram-ventilating species, RMR is typically reported as the metabolic rate at a speed of 0 (often referred to as the immobile metabolic rate 'IMR'), derived from the extrapolation of the relationship between metabolic rate and swimming speed to a speed of zero (Chabot et al. 2016). MMR estimates were collected from studies where this rate was elicited via exhaustive exercise protocols (forced swimming in swim flumes or via chase methods) or air exposure methods, depending on the species and its activity level (i.e., active, inactive). For highly active and pelagic species, MMR usually corresponds to the active metabolic rate (AMR) at the maximum sustainable swimming speed (U_{crit}), elicited under forced swimming trials in a swim flume respirometer. For less active species, MMR is usually estimated during the period immediately following exhaustive swimming (elicited via swim flume or by chasing the organism) and/or air exposure methods (Auer et al. 2017, Killen et al. 2017).

A.1.2. Ecological lifestyle classifications of species

To account for the effects of ecological lifestyle on metabolic rate, we included ecological lifestyle as a factor in all metabolic rate models. Thus, species were categorized as pelagic, benthopelagic, or benthic based on Fishbase and primary literature sources, as well as the classification criteria of Killen et al. (2016). Species which assume different lifestyles throughout ontogeny were classified based on the lifestyle assumed by mature (adult) life stages. When the primary habitat and lifestyle of a species was debated or conflicted across different literature sources, the adult stage of each species was classified into one of the three categories based on its capacity for sustained swimming and its level of interaction with the seafloor (e.g., whether it lived directly on or near the seafloor, whether its primary diet was comprised primarily of benthic species, etc.; Killen et al. 2016, 2017).

A.1.3. Population matching

We matched stock and life history trait data to our metabolic rate data to the finest possible spatial scale. At the very least, we tried to match metabolic rate, life history and stock-recruitment data to the same biogeographic provinces, defined in Spalding et al. (2007), as the life histories and population dynamics of the populations of a species living within the same biogeographic province are expected to be more alike. Furthermore, for teleosts the stock-recruitment data on RAM are specific to a particular fishing ‘stock’ (a term referring to the commercial fisheries subgrouping of a species), which is often regarded similarly to a population, as the individuals belonging to a stock are more or less isolated from other stocks of the same species. If stock-recruitment and trait data was available for a stock (or population) from an area within the same biogeographic province as the metabolic rate data, these were a “population match”. If several stocks or metabolic rate studies were available for a given species, we selected the stock and metabolic rate pair which was location-matched at the finest spatial scale possible, using population codes (for sharks) or the stock IDs (for teleosts) and associated fishing zone(s) listed on RAM, if these were within the same marine province. For example, considering a species for which we have one metabolic rate study for fish caught off the west coast of Scotland (which is within FAO Major Fishing Area 27 of the Northeastern Atlantic, which is itself divided into subareas. If stock-recruitment data was

available only for the Irish Sea, another subarea of FAO Major Fishing Area 27 (subarea 7a, where the full code at this scale would be 27.7a), it was considered a "match", as both are within biogeographic province *no. 2*. However, stock-recruitment and trait data from FAO 27.6a (i.e., the west coast of Scotland) would have been preferred if it were available (FAO 2023).

A.1.4. The calculation of r_{max}

Due to fundamental differences in the life histories and population dynamics of sharks and teleosts, the method by which r_{max} is calculated differs slightly for each group. Below, we detail a general r_{max} equation and the nuances in its application to the calculation of r_{max} for sharks and teleosts. However, to ensure the r_{max} values generated via each method were reasonably comparable, we also calculated r_{max} for 5 shark species using both the r_{max} method for sharks and the r_{max} method for teleosts (i.e., using spawner-recruitment data, which was available for 5 shark stocks in the RAM Database; see Supplementary Results section A.2 below).

A.1.4.1. The Euler-Lotka equation

The maximum intrinsic rate of population increase, r_{max}, can be derived from the Euler-Lotka equation, across discrete time intervals:

$$\sum_{t=1}^{\omega} l_t b_t e^{-rt} = 1$$

Here, t is any given age from 1 to ω, ω is the maximum age (hereafter a_{max}), l_t is the proportion of individuals surviving to age t, b_t is the annual reproductive output (number of females per female) at age t, and r is the rate of population increase. To obtain the maximum value of r (r_{max}), we must estimate this value in the absence of density dependence (Myers et al. 1997).

From the equation above, survival across all age classes can be further broken down into juvenile and adult survival. Annual adult survival is defined as $p = e^{-M}$ for all fish of age $t \geq a_{mat}$, where a_{mat} is the age at 50% maturity and M is the population-specific natural mortality rate (detailed in the previous section). For juveniles of age $t < a_{mat}$, survival from age zero to maturity (the survival to maturity, $l_{a_{mat}}$) can be calculated

as $l_{a_{mat}} = (e^{-M})^{a_{mat}}$. Assuming that adult annual survival, p, is constant after maturity, it follows that $l_t = l_{a_{mat}} p^{t-a_{mat}}$.

From here, if we also assumed that fecundity is constant after maturity, so $b_t = b_{a_{mat}}$, we can remove survival to maturity and the annual reproductive output so the summation begins at $t = a_{mat}$:

$$l_{a_{mat}} b \sum_{a_{mat}}^{a_{max}} p^{t-a_{mat}} e^{-r_{max} t} = 1$$

We can then solve the summation and rewrite the equation as:

$$l_{a_{mat}} b = e^{r_{max} a_{mat}} - p(e^{r_{max}})^{a_{mat}-1},$$

where the term on the left, $l_{a_{mat}} b$, is the maximum annual reproductive rate $\tilde{\alpha}$ (also referred to as the maximum annual spawners per spawner), described as "the number of spawners produced by each spawner per year (after a lag of a_{mat} years, where a_{mat} is age-at-maturity)" (Myers et al. 1997, Myers 2001, Pardo et al. 2016). However, the calculation of $\tilde{\alpha}$ differs for sharks and teleosts, both detailed separately below.

A.1.4.2. The maximum annual reproductive rate

For sharks

Shark populations generally exhibit little density dependence, roughly constant litter sizes and predictable reproductive periodicities throughout their life cycles (Clarke et al. 2003, Forrest & Walters 2009, Pardo et al. 2016). Thus, we can calculate $\tilde{\alpha}$ for sharks directly as the product of survival to maturity and annual reproductive output ($l_{a_{mat}} b$; see Methods section in Chapter 1).

For teleosts

Meanwhile, for teleost, the relationship between fecundity and female size is nearly universally positive, and density dependence matters to overall population dynamics (Wootton 1998, Myers et al. 1997). Following the standard practice for teleosts

outlined in Myers *et al.* (1997), we used a derivation of the Euler-Lotka equation to estimate $\tilde{\alpha}$ from standardized measures of density-independent recruitment. The maximum annual recruitment per spawner at low spawner abundance (i.e., in the absence of density dependence), α, is approximated by the slope-at-the-origin of stock-recruitment relationships fit to timeseries data on the number of recruits 'R' as a function of the number spawners 'S' (or spawning stock biomass 'SSB') for a given species stock. All stock-recruitment data were obtained from the RAM Legacy Database and stock-recruitment relationships (in our case, Ricker models) were fit using the *FSA, FSAdata* and *nlstools* packages in R (Ricard et al. 2012, Ogle 2013 *FishR vignette*), with the exception of the pink salmon *Oncorhynchus gorbuscha*, for which measures of α were opportunitiscally obtained from literature for stocks matching those of the metabolic rate data (Pess et al. 2012). To ensure α was infered in the absence of density dependence and to limit the influence of datapoints (or lack thereof) for years of high spawner abundance, we derived α from Ricker models fit to the lowest 10 SSB years as well as fit to all SSB years, following Denney et al. (2002), and selected the highest value of α generated by either method. In a few cases, the Ricker model fit to lowest 10 SSB years yielded unrealistically high values of α. We therefore limited selection of α (i.e., if it was the higher value of the two methods described above) based on the Ricker model's peak recruitment level Rp (from the 3rd parameterization of the Ricker model; Ogle 2013 *FishR vignette*). If Rp exceeded the highest observed level of recruitment across all SSB years in the stock's timeseries, we discarded this estimate of α and opted for the α generated from a model fit across all SSB years.

For iteroparous species, the maximum annual recruitment per spawner, α, must then be standardized to account for differences in lifetime recruit production across species (based on the lifetime spawning biomass discounted for repeat spawning throughout the lifespan). As per Myers et al. (1997) and further detailed in Goodwin et al. (2006), α is standardized by the average spawning stock biomass produced per recruit over its lifetime in the absence of fishing pressure $SPR_{f=0}$ (in units of spawning biomass/recruit). We calculate the total biomass of spawners produced per recruit by multiplying the number of fish surviving to each age class (starting from the age of recruitment until the maximum observed age of the stock) by the proportion of mature fish from each age class, which we assigned as 0 prior to maturity, 0.5 at the age-at-maturity, and 1.0 for the age classes following maturity, multiplied by the weight of a

spawner in each age class (calculated from von Bertalanffy and length-weight relationships for the stock in question). From the total biomass of spawners produced per recruit in the absence of fishing pressure $SPR_{f=0}$ (SSB/recruit) and the maximum annual recruits per unit of spawning stock biomass in the absence of density dependence α (recruits/SSB), we compute the number of recruits produced per recruit over its lifetime ($\hat{\alpha}$) as:

$$\hat{\alpha} = \alpha\, SPR_{f=0}.$$

We then calculate the maximum annual spawners per spawner $\tilde{\alpha}$ from the above standardized measure of lifetime recruit production and the adult survival (p) as:

$$\tilde{\alpha} = \hat{\alpha}(1 - p).$$

For semelparous species, α represents lifetime spawning and does not need to be standardized as it does for iteroparous species (Myers 2001). Thus, for species for which R and S are in the same units (as it was for Pacific salmon species of the genus *Oncorhynchus*), α can be taken directly as $\tilde{\alpha}$. In the case of the semelparous Barents Sea capelin, *Mallotus villosus*, the units for R were number of recruits while S was in units SSB. As this spawning stock is nearly completely dominated by individuals aged 3-4 years (Gjosaeter 1998, Howell et al. 2022), we converted units of spawning stock biomass into number of spawners using the mean weight of 3 and 4 year old spawners (using von Bertalanffy and length-weight relationships) to obtain the same units for R and S, and subsequently used α as $\tilde{\alpha}$.

A.1.4.3. Natural mortality

The survival of sharks typically follows a type II Pearl survivorship curve, while teleosts typically follow a type III Pearl survivorship curve showing high natural mortality rates in their early life stages (Pearl 1928). Thus, we used shark- and teleost-specific natural mortality (*M*) estimators, following Pardo *et al.* (2016) for sharks, and Lorenzen (2000), Dureuil et al. (2021), and Then *et al.* (2015) for teleosts.

For sharks

For sharks, we calculated natural mortality as the inverse of the population-specific average lifespan (μ), where $M = 1/\mu$ (following Pardo et al. 2016). While the average lifespan of teleosts is typically less than the age-at-maturity, sharks demonstrate relatively constant natural mortality across life stages. Thus, the average lifespan of sharks is likely higher than the age-at-maturity, and was approximated following Pardo et al. (2016) as the midpoint between the age-at-maturity and maximum age, where $\mu = (a_{mat} + a_{max})/2$.

For teleosts

For teleosts, we used a juvenile stage-based estimator in the calculation of $SPR_{f=0}$ based on Lorenzen (2000, see also Dureuil et al. 2021), which was applied to determine the survival of immature fishes in age classes zero to maturity (a_{mat}), following which constant natural mortality was assumed and calculated using an invariant adult natural mortality estimator from Then et al. (2015). However, the highest-ranking estimator suggested by Then et al. (2015) sometimes resulted in implausible r_{max} values (e.g., r_{max} approaching 0), which can occur in species where high M is estimated in combination with relatively low reproductive output and later age-at-maturity (Pardo et al. 2018). We therefore opted for the second highest-ranking age-based estimator (which performed similarly to the higher ranking estimator), where $M = 5.109/a_{max}$ (Then et al. 2015). This estimator yielded slightly less conservative (lower) mortality estimates, using which yielded plausible r_{max} values for all species. Additionally, cross-checking our estimates of M against other estimates of natural mortality reported in the RAM database, stock assessments, and the literature appeared to favour the values yielded by this latter method.

Juvenile mortality was calculated following Lorenzen (2000) and Dureuil *et al.* (2021), where M_t is the mortality and L_t is the length of fish in age class t, and $M_{a_{mat}}$ and $L_{a_{mat}}$ are the mortality and length at the age-at-maturity, respectively:

$$M_t = M_{a_{mat}} \frac{L_{a_{mat}}}{L_t}$$

A.1.5. The calculation of reproductive output for teleosts

To assess whether any single of the life history trait components was driving the observed relationship between metabolic rate and r_{max} (if any), we constructed and examined models of the scaling of metabolic rate with measurement mass, measurement temperature, and any single one of the component traits of r_{max}, which included the reproductive output 'b' (see Methods section Chapter 1 and Supplementary Methods section A.1.4 above). As aforementioned, we estimate and use b directly in the calculation of r_{max} in sharks (in the lefthand term of the r_{max} equation), while we bypass the need for using b in the calculation of the lefthand term for the r_{max} of teleosts (see the above section A.1.4). Therefore, to approximate b for teleosts, we simply calculated b as:

$$b = \frac{\tilde{\alpha}}{l_{a_{mat}}}$$

using our estimates of $\tilde{\alpha}$ (section A.1.4.2) and of the survival to maturity, $l_{a_{mat}}$, which is the product of the annual survival from age class zero to a_{mat}:

$$l_{a_{mat}} = \prod_{t=0}^{a_{mat}} e^{-M_t}$$

where M_t is the natural mortality at juvenile age class t, calculated using the stage-based juvenile natural mortality estimator for teleosts (see above section A.1.4.3).

A.2. Supplementary Results

To compare the values yielded by the shark and teleost variations of the r_{max} derivations, we calculated additional r_{max} values for 5 shark species with available spawner-recruitment data from the RAM database. However, constant mortality was applied across all age classes, as is standard practice for elasmobranchs (see section A.1.4.3). We found that the r_{max} values calculated using both methods generated similar values for the 5 species (Figure A.1a), and were related to one another with a slope approaching 1:1 (where Pearson's r = 0.94, and the linear model R^2 = 0.8; Figure A.1b). Thus, although our sample size was small, our findings suggest that both methods yield fairly similar values of r_{max}.

Table A.1. Comparison of models testing whether r_{max} or any of its component life history traits (reproductive output 'RO', age at maturity 'amat', and maximum age 'amax') explained variation in metabolic rate (RMR, MMR, or AS), including or excluding a fixed factor accounting for ecological lifestyle ('LS'). Models with ecological lifestyle (_LS) are the same as those presented in Tables 1.1 and 1.2, compared to the same models but without ecological lifestyle. In all cases, models with ecological lifestyle ranked higher those than without.

a) RMR models **(N=82)**		p_{loo}	looic	$elpd_{loo}$	se_elpd_{loo}	$elpd_{diff}$	weight
RMR_null	$stdlog(M) + std(invtemp)$	22.4	179.1	-89.6	10.3	-7.0	0.012
RMR_amat	$stdlog(M) + std(invtemp) + stdlog(amat)$	15.1	174.4	-87.2	9.8	-4.7	0.178
RMR_amax	$stdlog(M) + std(invtemp) + stdlog(amax)$	18.6	177.6	-88.8	10.2	-6.3	0.000
RMR_RO	$stdlog(M) + std(invtemp) + stdlog(RO)$	22.7	181.5	-90.8	10.2	-8.2	0.000
RMR_rmax	$stdlog(M) + stdinv(temp) + stdlog(r_{max})$	20.0	179.8	-89.9	10.3	-7.4	0.000
RMR_null_LS	$stdlog(M) + std(invtemp) + LS$	20.0	167.8	-83.9	13.0	-1.4	0.000
RMR_amat_LS	$stdlog(M) + std(invtemp) + stdlog(amat) + LS$	18.0	165.1	-82.6	12.9	0.0	0.348
RMR_amax_LS	$stdlog(M) + std(invtemp) + stdlog(amax) + LS$	18.9	167.3	-83.7	13.5	-1.1	0.301
RMR_RO_LS	$stdlog(M) + std(invtemp) + stdlog(RO) + LS$	19.7	169.8	-84.9	13.0	-2.3	0.000
RMR_rmax_LS	$stdlog(M) + stdinv(temp) + stdlog(r_{max}) + LS$	19.7	168.3	-84.2	13.3	-1.6	0.162
b) MMR models **(N=49)**							
MMR_null	$stdlog(M) + std(invtemp)$	38.9	64.4	-32.2	3.7	-13.8	0.000
MMR_amat	$stdlog(M) + std(invtemp) + stdlog(amat)$	39.1	73.1	-36.6	4.2	-18.2	0.000
MMR_amax	$stdlog(M) + std(invtemp) + stdlog(amax)$	39.2	69.4	-34.7	4.1	-16.3	0.000
MMR_RO	$stdlog(M) + std(invtemp) + stdlog(RO)$	38.4	68.7	-34.4	3.8	-16.0	0.000
MMR_rmax	$stdlog(M) + std(invtemp) + stdlog(r_{max})$	34.9	69.5	-34.7	4.3	-16.4	0.000
MMR_null_LS	$stdlog(M) + std(invtemp) + LS$	30.7	46.4	-23.2	3.9	-4.8	0.213
MMR_amat_LS	$stdlog(M) + std(invtemp) + stdlog(amat) + LS$	15.3	51.9	-26.0	4.5	-7.6	0.000
MMR_amax_LS	$stdlog(M) + std(invtemp) + stdlog(amax) + LS$	27.8	51.9	-25.9	4.5	-7.6	0.000

MMR_RO_LS	$stdlog(M) + std(invtemp) + stdlog(RO) + LS$	30.0	50.1	-25.1	4.0	-6.7	0.000
MMR_rmax_LS	$stdlog(M) + std(invtemp) + stdlog(r_{max}) + LS$	21.7	36.7	-18.4	5.3	0.0	0.786

c) AS models **(N=45)**

AS_null	$stdlog(M) + std(invtemp)$	21.3	96.0	-48.0	5.9	-15.7	0.000
AS_amat	$stdlog(M) + std(invtemp) + stdlog(amat)$	17.4	102.2	-51.1	6.2	-18.8	0.000
AS_amax	$stdlog(M) + std(invtemp) + stdlog(amax)$	22.2	99.9	-49.9	6.2	-17.7	0.000
AS_RO	$stdlog(M) + std(invtemp) + stdlog(RO)$	22.0	99.5	-49.8	5.7	-17.5	0.000
AS_rmax	$stdlog(M) + std(invtemp) + stdlog(r_{max})$	17.8	98.1	-49.0	5.0	-16.8	0.000
AS_null_LS	$stdlog(M) + std(invtemp) + LS$	17.8	77.0	-38.5	7.1	-6.2	0.187
AS_amat_LS	$stdlog(M) + std(invtemp) + stdlog(amat) + LS$	12.4	75.3	-37.6	3.9	-5.4	0.186
AS_amax_LS	$stdlog(M) + std(invtemp) + stdlog(amax) + LS$	17.8	79.3	-39.6	7.6	-7.4	0.018
AS_RO_LS	$stdlog(M) + std(invtemp) + stdlog(RO) + LS$	18.0	78.8	-39.4	6.8	-7.1	0.001
AS_rmax_LS	$stdlog(M) + std(invtemp) + stdlog(r_{max}) + LS$	14.3	64.5	-32.3	6.1	0.0	0.608

Table A.2. Comparison of models testing whether the component life history traits of r_{max} (reproductive output 'RO', age at maturity 'amat', and maximum age 'amax') explain variation in (a) resting metabolic rate RMR, (b) maximum metabolic rate MMR and (c) absolute aerobic scope AS (MMR – RMR) across marine fishes, while accounting for the effect of measurement temperature ('invtemp'), measurement body mass ('M') and ecological lifestyle ('LS'). The metabolic rate dataset was based on the temperature closest to the mean of 15°C (see Methods). Models were fit in *brms* using R version 4.0.5. Metabolic rates (Watts), reproductive output (no. of offspring), age-at-maturity (years), maximum age (years), and body mass (grams) were natural log-transformed, while measurement temperature was parameterized as the inverse temperature (see Methods). All explanatory variables were standardized. All models within 2 looic of the highest-ranking model (emboldened) are highlighted in grey.

a) RMR models (N = 82)		p_{loo}	looic	$elpd_{loo}$	se_{elpd_loo}	$elpd_{diff}$	weight
RMR_null	$stdlog(M) + std(invtemp) + LS$	21.3	134.0	-67.0	10.2	-1.3	0.000
RMR_amat	$\boldsymbol{stdlog(M) + std(invtemp) + stdlog(amat) + LS}$	**15.1**	**131.5**	**-65.7**	**9.8**	**0.0**	**0.663**
RMR_amax	$stdlog(M) + std(invtemp) + stdlog(amax) + LS$	16.9	132.6	-66.3	10.2	-0.6	0.156
RMR_RO	$stdlog(M) + std(invtemp) + stdlog(RO) + LS$	17.5	134.1	-67.0	10.0	-1.3	0.182
b) MMR models (N = 49)							
MMR_null	$\boldsymbol{stdlog(M) + std(invtemp) + LS}$	**28.4**	**55.6**	**-27.8**	**4.0**	**0.0**	**0.590**
MMR_amat	$stdlog(M) + std(invtemp) + stdlog(amat) + LS$	15.0	56.9	-28.5	4.4	-0.7	0.410
MMR_amax	$stdlog(M) + std(invtemp) + stdlog(amax) + LS$	26.7	59.7	-29.8	4.6	-2.0	0.000
MMR_RO	$stdlog(M) + std(invtemp) + stdlog(RO) + LS$	28.5	57.8	-28.9	4.0	-1.1	0.000
c) AS models (N = 45)							
AS_null	$\boldsymbol{stdlog(M) + std(invtemp) + LS}$	**25.2**	**61.3**	**-30.6**	**4.6**	**0.0**	**1.000**
AS_amat	$stdlog(M) + std(invtemp) + stdlog(amat) + LS$	15.5	65.0	-32.5	5.1	-1.9	0.000
AS_amax	$stdlog(M) + std(invtemp) + stdlog(amax) + LS$	23.9	63.2	-31.6	4.9	-1.0	0.000
AS_RO	$stdlog(M) + std(invtemp) + stdlog(RO) + LS$	25.8	64.2	-32.1	4.7	-1.5	0.000

Table A.3. Comparison of models testing whether the maximum intrinsic rate of population increase, r_{max}, explained variation in (a) RMR, (b) MMR, and (c) AS across marine fishes, while accounting for the effects of measurement temperature ('invtemp'), measurement body mass ('M') and ecological lifestyle ('LS'). The metabolic rate dataset was based on the temperature closest to the mean of 15°C (see Methods). Models were fit in *brms* using R version 4.0.5. Metabolic rates (Watts), r_{max} (yr^{-1}), its component life history traits, and body mass were natural log-transformed, while measurement temperature was parameterized as the inverse temperature (see methods). All explanatory variables were standardized. All models within 2 looic of the highest-ranking model (emboldened) are highlighted in grey.

a) RMR models (N = 82)		p_{loo}	looic	$elpd_{loo}$	se_elpd_{loo}	$elpd_{diff}$	weight
RMR_amat	$\boldsymbol{stdlog(M) + std(invtemp) + stdlog(amat) + LS}$	**15.1**	**131.5**	**-65.7**	**9.8**	**0.0**	**0.378**
RMR_amax	$stdlog(M) + std(invtemp) + stdlog(amax) + LS$	16.9	132.6	-66.3	10.2	-0.6	0.214
RMR_rmax	$stdlog(M) + stdinv(temp) + stdlog(r_{max}) + LS$	17.5	133.7	-66.9	10.0	-1.1	0.409
b) MMR models (N = 49)							
MMR_null	$stdlog(M) + std(invtemp) + LS$	28.4	55.6	-27.8	4.0	-4.7	0.126
MMR_amat	$stdlog(M) + std(invtemp) + stdlog(amat) + LS$	15.0	56.9	-28.5	4.4	-5.3	0.000
MMR_rmax	$\boldsymbol{stdlog(M) + std(invtemp) + stdlog(r_{max}) + LS}$	**21.5**	**46.3**	**-23.1**	**5.0**	**0.0**	**0.874**
c) AS models (N = 45)							
AS_null	$stdlog(M) + std(invtemp) + LS$	25.2	61.3	-30.6	4.6	-0.3	0.420
AS_amax	$stdlog(M) + std(invtemp) + stdlog(amax) + LS$	23.9	63.2	-31.6	4.9	-1.3	0.000
AS_rmax	$\boldsymbol{stdlog(M) + std(invtemp) + stdlog(r_{max}) + LS}$	**20.4**	**60.6**	**-30.3**	**6.0**	**0.0**	**0.580**

Table A.4. Coefficient means and 95% Bayesian Credible Intervals (BCI, in parentheses) for all models from dataset closest to the mean of 15°C (see Methods). B' = benthic, 'BP' = benthopelagic, and 'P' = pelagic. Models (and corresponding model names) are the same as those presented in Tables A.2 and A.3, except here only the inverse temperature was standardized (i.e., centered and scaled; see Methods).

model	lifestyle	intercept	log_mass	std_inv_temp	log_rmax_or_trait	sigma
RMR_null	P	-6.91 (-7.23 to -6.58)	0.84 (0.77 to 0.91)	-0.59 (-0.74 to -0.45)	NA	0.48 (0.34 to 0.60)
	BP	-7.09 (-7.41 to -6.77)				
	B	-7.75 (-8.37 to -7.09)				
RMR_amat	P	-6.99 (-7.30 to -6.67)	0.90 (0.81 to 0.98)	-0.50 (-0.66 to -0.36)	-0.21 (-0.38 to -0.03)	0.49 (0.39 to 0.60)
	BP	-7.12 (-7.42 to -6.82)				
	B	-7.73 (-8.24 to -7.18)				
RMR_amax	P	-6.58 (-6.89 to -6.26)	0.88 (0.80 to 0.95)	-0.52 (-0.68 to -0.37)	-0.20 (-0.39 to -0.00)	0.49 (0.38 to 0.59)
	BP	-6.71 (-7.03 to -6.40)				
	B	-7.37 (-8.05 to -6.71)				
RMR_RO	P	-7.04 (-7.35 to -6.73)	0.85 (0.78 to 0.92)	-0.61 (-0.75 to -0.47)	0.05 (-0.02 to 0.11)	0.49 (0.37 to 0.60)
	BP	-7.24 (-7.55 to -6.93)				
	B	-7.89 (-8.47 to -7.27)				
RMR_rmax	P	-6.93 (-7.23 to -6.63)	0.87 (0.80 to 0.94)	-0.56 (-0.70 to -0.43)	0.16 (0.02 to 0.30)	0.49 (0.38 to 0.59)
	BP	-7.13 (-7.44 to -6.82)				
	B	-7.73 (-8.26 to -7.18)				

MMR_null	P	-5.39 (-5.79 to -4.99)	0.87 (0.79 to 0.95)	-0.40 (-0.55 to -0.24)	NA	0.30 (0.12 to 0.47)
	BP	-6.17 (-6.56 to -5.78)				
	B	-6.55 (-7.36 to -5.69)				
MMR_amat	P	-5.05 (-5.38 to -4.73)	0.90 (0.83 to 0.97)	-0.24 (-0.55 to -0.13)	-0.35 (-0.55 to -0.13)	0.37 (0.24 to 0.48)
	BP	-5.78 (-6.13 to -5.43)				
	B	-6.31 (-6.89 to -5.74)				
MMR_amax	P	-5.06 (-5.45 to -4.67)	0.88 (0.80 to 0.96)	-0.35 (-0.52 to -0.18)	-0.14 (-0.35 to 0.08)	0.33 (0.16 to 0.49)
	BP	-5.82 (-6.21 to -5.44)				
	B	-6.26 (-7.17 to -5.37)				
MMR_RO	P	-5.44 (-5.84 to -5.04)	0.87 (0.79 to 0.95)	-0.40 (-0.56 to -0.24)	0.02 (-0.07 to 0.10)	0.31 (0.14 to 0.48)
	BP	-6.24 (-6.64 to -5.84)				
	B	-6.60 (-7.45 to -5.70)				
MMR_rmax	P	-5.39 (-5.70 to -5.09)	0.94 (0.87 to 1.00)	-0.26 (-0.39 to -0.13)	0.44 (0.25 to 0.62)	0.30 (0.17 to 0.42)
	BP	-6.24 (-6.54 to -5.93)				
	B	-6.61 (-7.17 to -6.03)				
AS_null	P	-5.47 (-6.00 to -4.95)	0.83 (0.72 to 0.95)	-0.45 (-0.67 to -0.23)	NA	0.46 (0.30 to 0.65)
	BP	-6.29 (-6.82 to -5.75)				
	B	-6.79 (-7.80 to -5.76)				
AS_amat	P	-5.22 (-5.68 to -4.75)	0.89 (0.77 to 1.00)	-0.30 (-0.54 to -0.08)	-0.38 (-0.67 to -0.05)	0.51 (0.35 to 0.67)
	BP	-6.02 (-6.51 to -5.51)				
	B	-6.59 (-7.40 to -5.79)				
AS_amax	P	-5.21 (-5.74 to -4.70)	0.85 (0.73 to 0.97)	-0.42 (-0.66 to -0.18)	-0.13 (-0.43 to 0.18)	0.47 (0.30 to 0.67)

	BP	-6.02 (-6.55 to -5.48)				
	B	-6.54 (-7.71 to -5.41)				
AS_RO	P	-5.63 (-6.17 to -5.10)	0.84 (0.72 to 0.95)	-0.47 (-0.69 to -0.24)	0.04 (-0.08 to 0.16)	0.47 (0.30 to 0.66)
	BP	-6.48 (-7.02 to -5.93)				
	B	-6.93 (-7.97 to -5.84)				
AS_rmax	P	-5.57 (-5.99 to -5.14)	0.93 (0.82 to 1.03)	-0.33 (-0.52 to -0.14)	0.50 (0.23 to 0.76)	0.45 (0.32 to 0.61)
	BP	-6.48 (-6.93 to -6.02)				
	B	-6.89 (-7.64 to -6.13)				

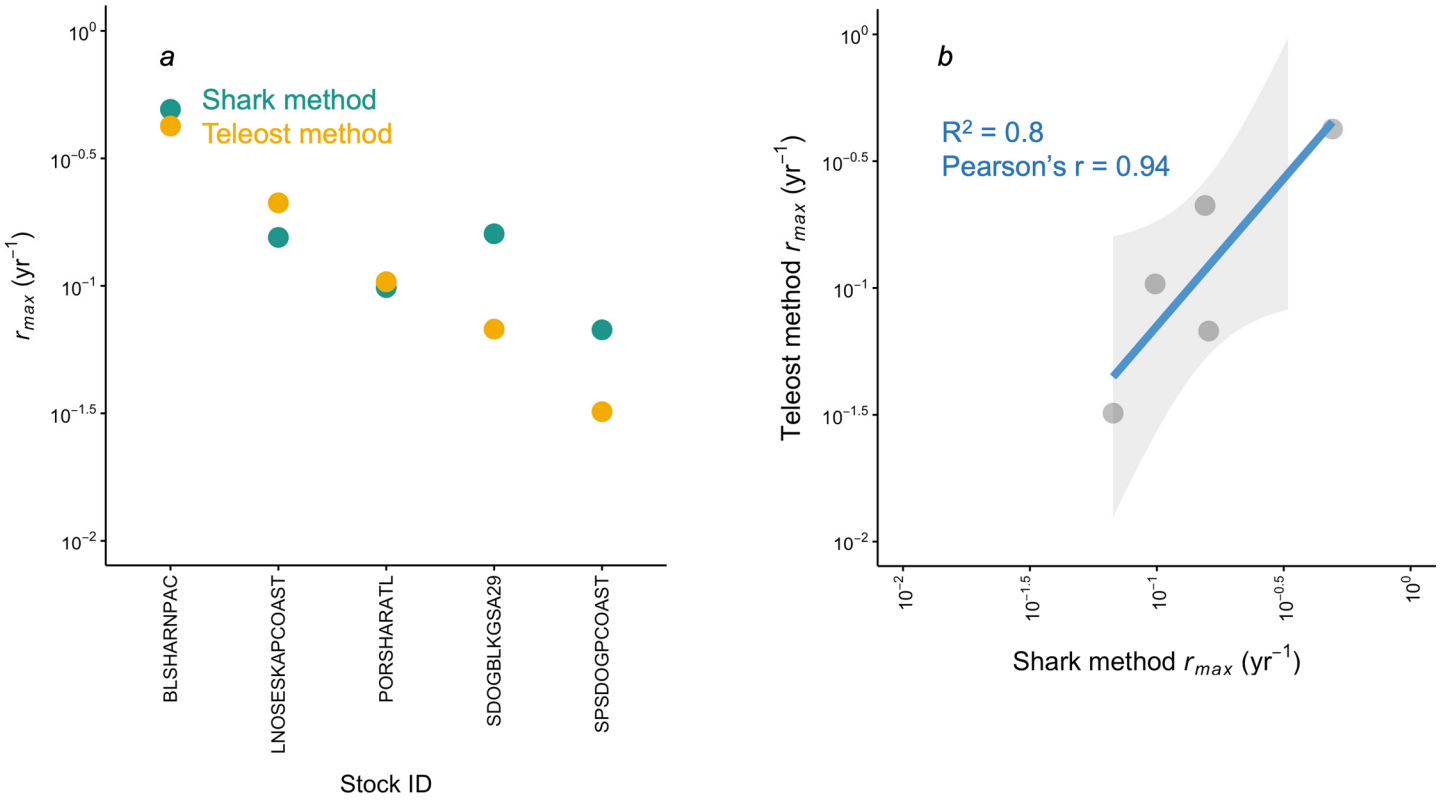

Figure A.1. **Shark and teleost r_{max} methods yielded similar values of r_{max} for 5 shark stocks.** Panel (a) shows the r_{max} values generated using both shark- and teleost-specific methods (in green and yellow, respectively) for the 5 shark species with available spawner-recruitment timeseries, shown by stock ID: BLSHARNPAC (North Pacific stock of the blue shark, *Prionace glauca*), LNOSESKAPCOAST (Northeastern Pacific stock of the longnose skate, *Beringraja rhina*), PORSHARATL (Atlantic stock of the porbeagle shark, *Lamna nasus*), SDOGBLKGSA29 (Black Sea stock of the spurdog, *Squalus acanthias*), and SPSDOGPCOAST (Northeastern Pacific stock of the Pacific spiny dogfish, *Squalus suckleyi*). Panel (b) shows the linear fit of the relationship between the two sets of r_{max} values for the 5 species, with an R^2=0.8 and Pearson's correlation coefficient of 0.94.

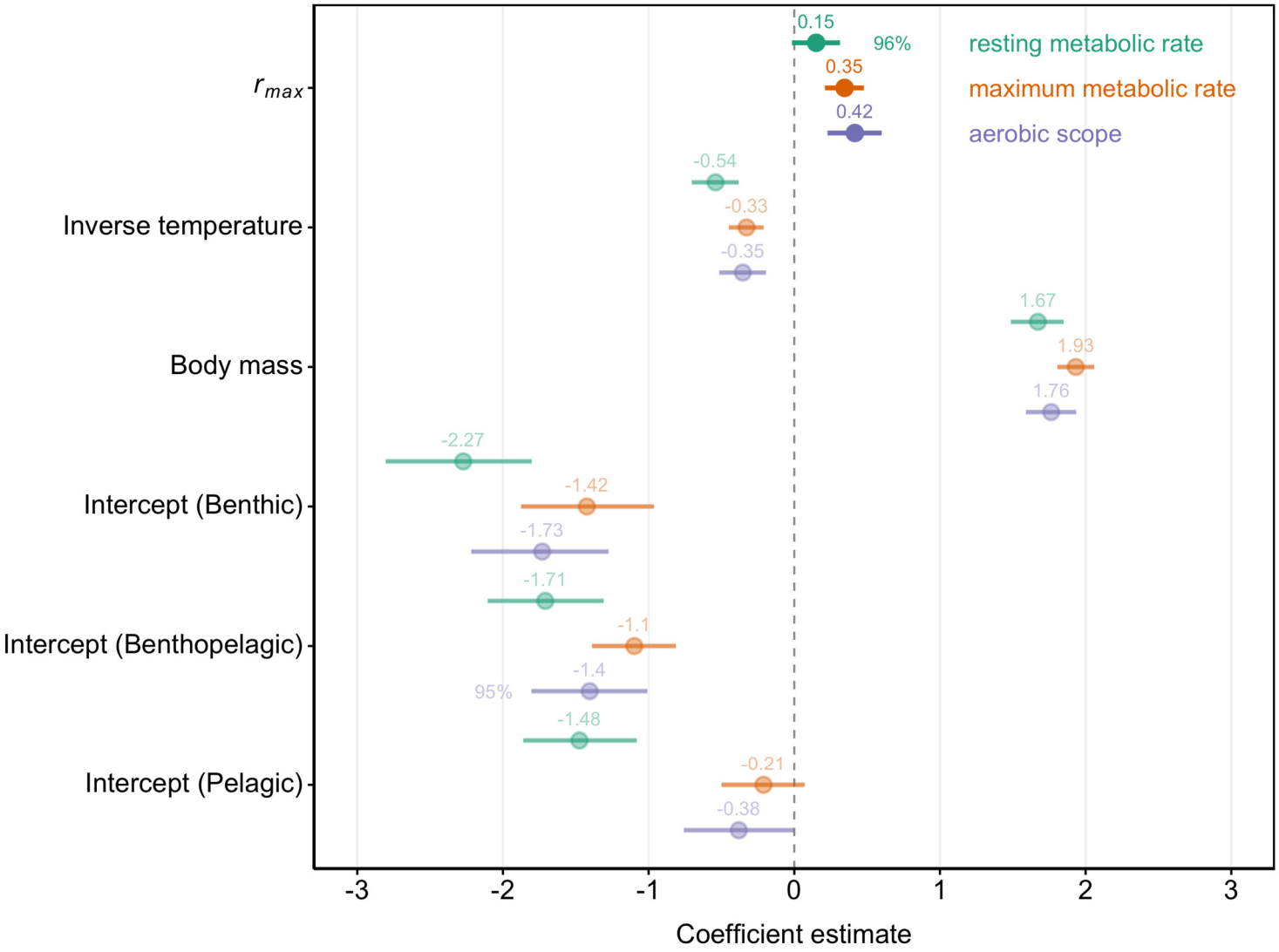
0.15
96%
0.35
0.42
resting metabolic rate
maximum metabolic rate
aerobic scope
r_{max}
-0.54
-0.33
-0.35
Inverse temperature
1.67
1.93
1.76
Body mass
-2.27
-1.42
-1.73
Intercept (Benthic)
-1.71
-1.1
-1.4
95%
Intercept (Benthopelagic)
-1.48
-0.21
-0.38
Intercept (Pelagic)
-3
-2
-1
0
1
2
3
Coefficient estimate

Figure A.2. Coefficients plot of the effects of r_{max}, measurement body mass, measurement temperature, and ecological lifestyle (with respective intercepts for 'Benthic', 'Benthopelagic', and 'Pelagic' species) on resting metabolic rate 'RMR' (in green, N=82), maximum metabolic rate 'MMR' (in orange, N=49), and aerobic scope 'AS' (in purple, N=45). The intercepts correspond to the metabolic rates of 'Benthic', 'Benthopelagic', or 'Pelagic' species at the mean body mass, temperature, and rmax. Metabolic rates and all explanatory variables were natural log-transformed, except for measurement temperature which was taken as the inverse temperature (see Methods). All explanatory variables were standardized to allow for direct comparison of variables.

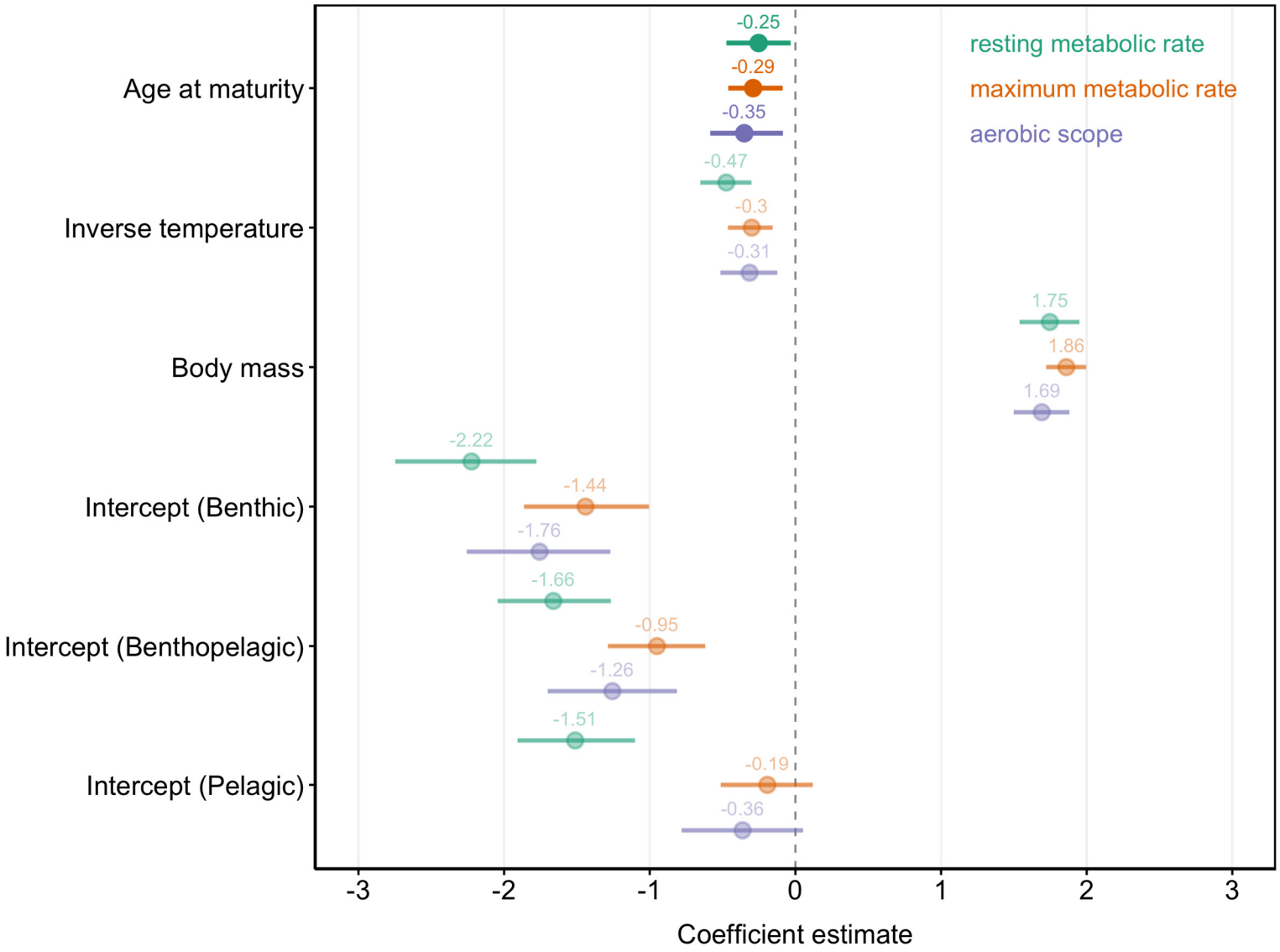
resting metabolic rate
maximum metabolic rate
aerobic scope
Age at maturity
Inverse temperature
Body mass
Intercept (Benthic)
Intercept (Benthopelagic)
Intercept (Pelagic)
-0.25
-0.29
-0.35
-0.47
-0.3
-0.31
1.75
1.86
1.69
-2.22
-1.44
-1.76
-1.66
-0.95
-1.26
-1.51
-0.19
-0.36
-3
-2
-1
0
1
2
3
Coefficient estimate

Figure A.3. Coefficients plot of the effects of age at maturity, measurement body mass, measurement temperature, and ecological lifestyle (with respective intercepts for ‘Benthic’, ‘Benthopelagic’, and ‘Pelagic’ species) on resting metabolic rate ‘RMR’ (in green, N=82), maximum metabolic rate ‘MMR’ (in orange, N=49), and aerobic scope ‘AS’ (in purple, N=45). The intercepts correspond to the metabolic rates of ‘Benthic’, ‘Benthopelagic’, or ‘Pelagic’ species at the mean body mass, temperature, and age at maturity. Metabolic rates and all explanatory variables were natural log-transformed, except for measurement temperature which was taken as the inverse temperature (see Methods). All explanatory variables were standardized to allow for direct comparison between variables.

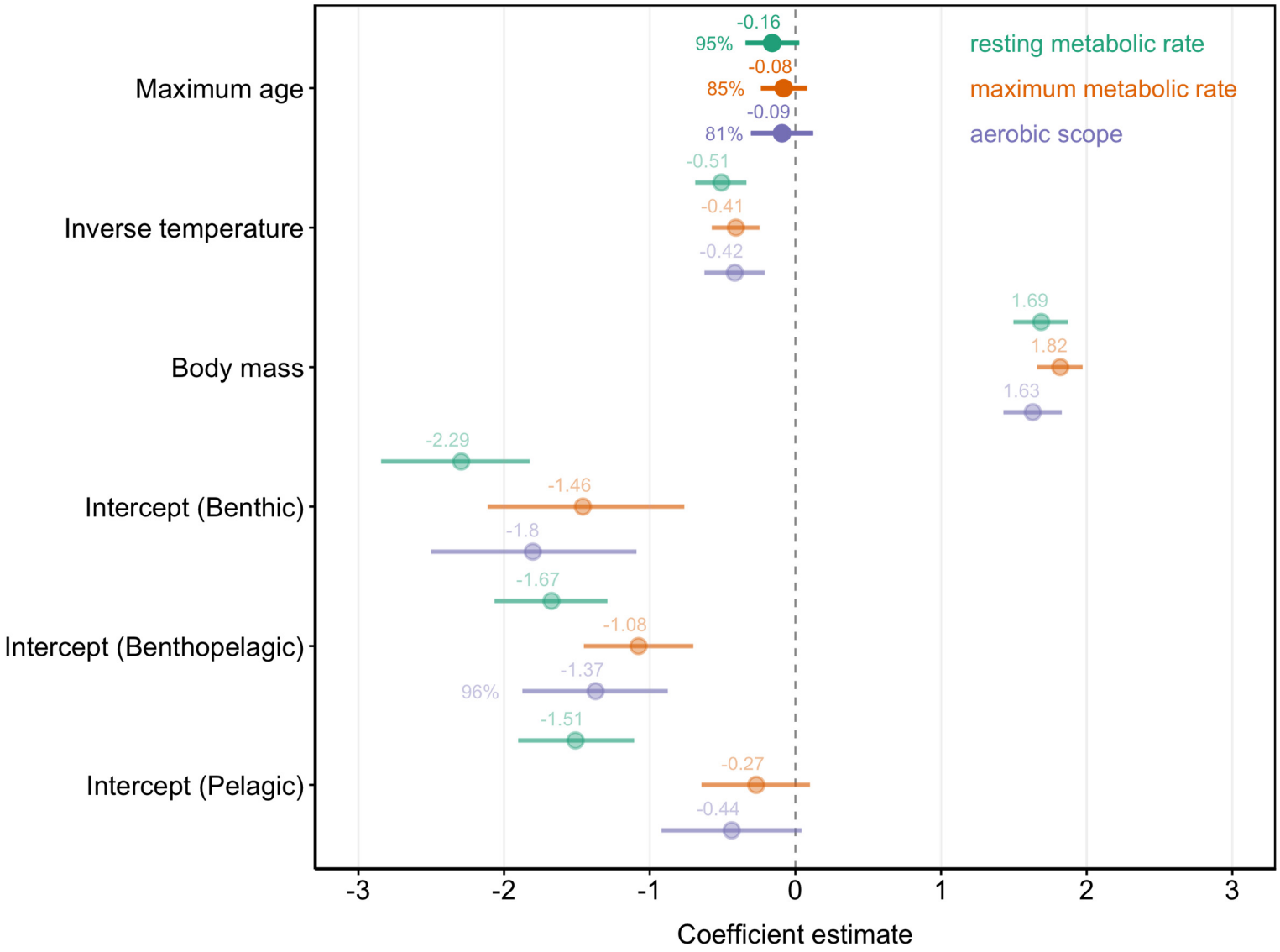
Maximum age
Inverse temperature
Body mass
Intercept (Benthic)
Intercept (Benthopelagic)
Intercept (Pelagic)
-0.16
95%
-0.08
85%
-0.09
81%
-0.51
-0.41
-0.42
1.69
1.82
1.63
-2.29
-1.46
-1.8
-1.67
-1.08
-1.37
96%
-1.51
-0.27
-0.44
resting metabolic rate
maximum metabolic rate
aerobic scope
-3
-2
-1
0
1
2
3
Coefficient estimate

Figure A.4. Coefficients plot of the effects of maximum age, measurement body mass, measurement temperature, and ecological lifestyle (with respective intercepts for ‘Benthic’, ‘Benthopelagic’, and ‘Pelagic’ species) on resting metabolic rate ‘RMR’ (in green, N=82), maximum metabolic rate ‘MMR’ (in orange, N=49), and aerobic scope ‘AS’ (in purple, N=45). The intercepts correspond to the metabolic rates of ‘Benthic’, ‘Benthopelagic’, or ‘Pelagic’ species at the mean body mass, temperature, and maximum age. Metabolic rates and all explanatory variables were natural log-transformed, except for measurement temperature which was taken as the inverse temperature (see Methods). All explanatory variables were standardized to allow for direct comparison of variables.

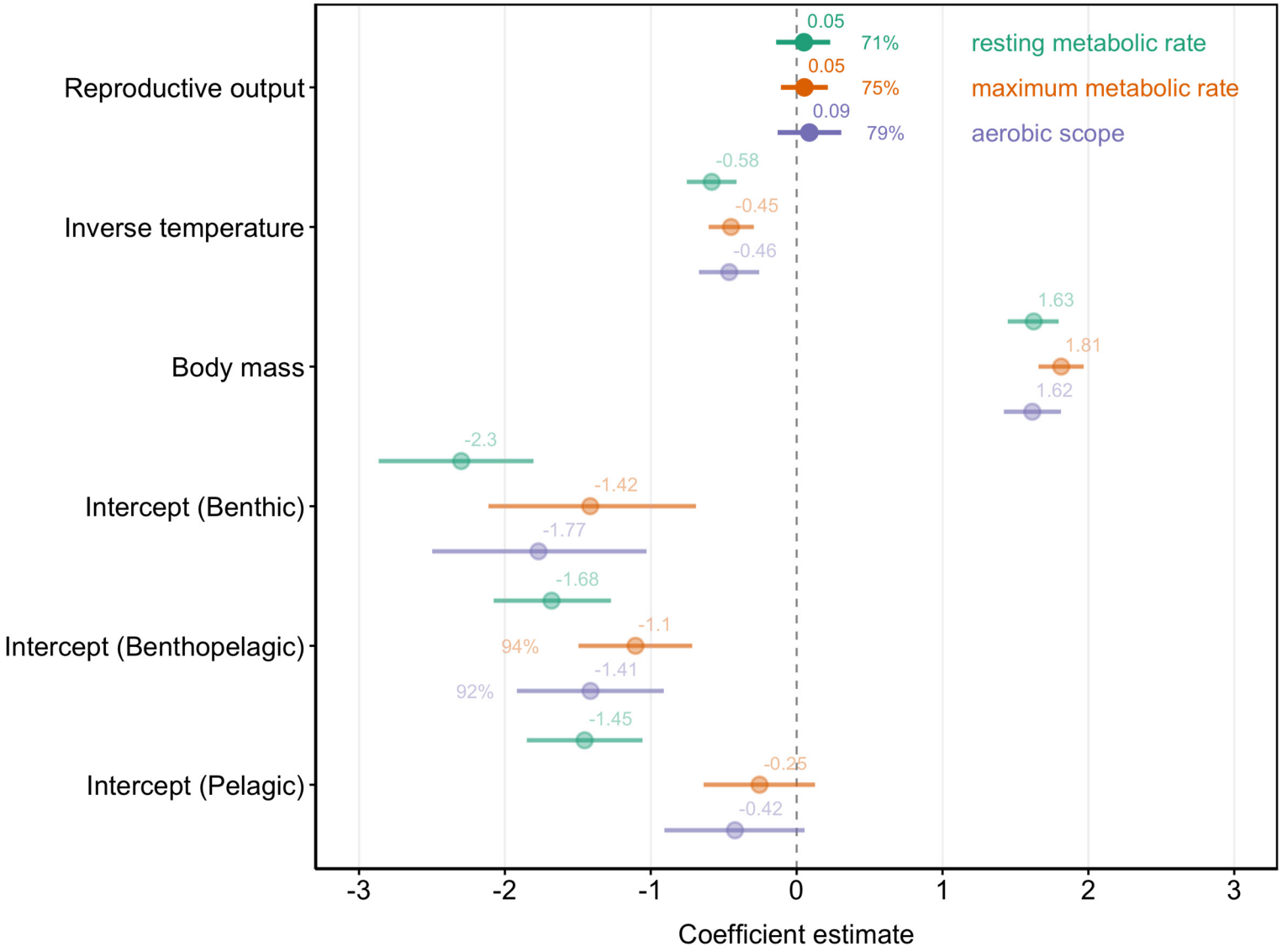
Reproductive output
Inverse temperature
Body mass
Intercept (Benthic)
Intercept (Benthopelagic)
Intercept (Pelagic)
0.05
71%
0.05
75%
0.09
79%
resting metabolic rate
maximum metabolic rate
aerobic scope
-0.58
-0.45
-0.46
1.63
1.81
1.62
-2.3
-1.42
-1.77
-1.68
-1.1
94%
-1.41
92%
-1.45
-0.25
-0.42
-3
-2
-1
0
1
2
3
Coefficient estimate

Figure A.5. Coefficients plot of the effects of reproductive output, measurement body mass, measurement temperature, and ecological lifestyle (with respective intercepts for ‘Benthic’, ‘Benthopelagic’, and ‘Pelagic’ species) on resting metabolic rate ‘RMR’ (in green, N=82), maximum metabolic rate ‘MMR’ (in orange, N=49), and aerobic scope ‘AS’ (in purple, N=45). The intercepts correspond to the metabolic rates of ‘Benthic’, ‘Benthopelagic’, or ‘Pelagic’ species at the mean body mass, temperature, and reproductive output. Metabolic rates and all explanatory variables were natural log-transformed, except for measurement temperature which was taken as the inverse temperature (see Methods). All explanatory variables were standardized to allow for direct comparison of variables.

A.3. References

Auer, S. K., Killen, S. S., & Rezende, E. L. (2017). Resting vs. active: A meta-analysis of the intra-and inter-specific associations between minimum, sustained, and maximum metabolic rates in vertebrates. *Functional Ecology*, *31*(9), 1728-1738.

Chabot, D., Steffensen, J. F., & Farrell, A. P. (2016). The determination of standard metabolic rate in fishes. *Journal of Fish Biology*, *88*(1), 81-121.

Clarke, M. W., Keely, C. J., Connolly, P. L., & Molloy, J. P. (2003). A life history approach to the assessment and management of deepwater fisheries in the Northeast Atlantic. *Journal of Northwest Atlantic Fishery Science*, *31*, 401.

Denney, N. H., Jennings, S., & Reynolds, J. D. (2002). Life–history correlates of maximum population growth rates in marine fishes. *Proceedings of the Royal Society of London. Series B: Biological Sciences*, *269*(1506), 2229-2237.

Dureuil, M., Aeberhard, W. H., Burnett, K. A., Hueter, R. E., Tyminski, J. P., & Worm, B. (2021). Unified natural mortality estimation for teleosts and elasmobranchs. *Marine Ecology Progress Series*, *667*, 113-129.

Forrest, R. E., & Walters, C. J. (2009). Estimating thresholds to optimal harvest rate for long-lived, low-fecundity sharks accounting for selectivity and density dependence in recruitment. *Canadian Journal of Fisheries and Aquatic Sciences*, *66*(12), 2062-2080.

Froese, R., and Pauly, D. 2019. FishBase World Wide Web electronic publication. www.fishbase.org (Accessed 9 January 2019).

Fry, F. E. J. (1971). The effect of environmental factors on the physiology of fish. In *Fish physiology* (Vol. 6, pp. 1-98). Academic press.

Gjøsæter, H. (1998). The population biology and exploitation of capelin (Mallotus villosus) in the Barents Sea. *Sarsia*, *83*(6), 453-496.

Goodwin, N. B., Grant, A., Perry, A. L., Dulvy, N. K., & Reynolds, J. D. (2006). Life history correlates of density-dependent recruitment in marine fishes. *Canadian Journal of Fisheries and Aquatic Sciences*, *63*(3), 494-509.

Hennemann, W. W. (1983). Relationship among body mass, metabolic rate and the intrinsic rate of natural increase in mammals. *Oecologia*, *56*, 104-108.

Howell, D., Bogstad, B., Chetyrkin, A., Fall, J. J. E., Filin, A., Godiksen, J. A., ... & Yaragina, N. (2022). Report of the Joint Russian-Norwegian Working Group on Arctic Fisheries (JRN-AFWG) 2022. *IMR/PINRO Joint Report Series*.

IUCN. (2022). The IUCN Red List of Threatened Species. Version 2022-2.

Killen, S. S., Glazier, D. S., Rezende, E. L., Clark, T. D., Atkinson, D., Willener, A. S., & Halsey, L. G. (2016). Ecological influences and morphological correlates of resting and maximal metabolic rates across teleost fish species. *The American Naturalist*, *187*(5), 592-606.

Killen, S. S., Norin, T., & Halsey, L. G. (2017). Do method and species lifestyle affect measures of maximum metabolic rate in fishes?. *Journal of Fish Biology*, *90*(3), 1037-1046.

Lorenzen, K. (2000). Allometry of natural mortality as a basis for assessing optimal release size in fish-stocking programmes. *Canadian Journal of Fisheries and Aquatic Sciences*, *57*(12), 2374-2381.

Myers, R. A., Hutchings, J. A., & Barrowman, N. J. (1997). Why do fish stocks collapse? The example of cod in Atlantic Canada. *Ecological applications*, *7*(1), 91-106.

Myers, R. A. (2001). Stock and recruitment: generalizations about maximum reproductive rate, density dependence, and variability using meta-analytic approaches. *ICES Journal of Marine Science*, *58*(5), 937-951.

Ogle, D. H. (2013). fishR Vignette-von Bertalanffy growth models. *Ashland, WI: Northland College*, *54*.

Pardo, S. A., Kindsvater, H. K., Reynolds, J. D., & Dulvy, N. K. (2016). Maximum intrinsic rate of population increase in sharks, rays, and chimaeras: the importance of survival to maturity. *Canadian journal of fisheries and aquatic sciences*, *73*(8), 1159-1163.

Pardo, S. A., Cooper, A. B., Reynolds, J. D., & Dulvy, N. K. (2018). Quantifying the known unknowns: estimating maximum intrinsic rate of population increase in the face of uncertainty. *ICES Journal of Marine Science*, *75*(3), 953-963.

Pearl, R. (1928). *The rate of living* (pp. 356-359). London: University Press.

Pess, G. R., Hilborn, R., Kloehn, K., & Quinn, T. P. (2012). The influence of population dynamics and environmental conditions on pink salmon (Oncorhynchus gorbuscha) recolonization after barrier removal in the Fraser River, British Columbia, Canada. *Canadian Journal of Fisheries and Aquatic Sciences*, *69*(5), 970-982.

RAM Legacy Stock Assessment Database. 2018. Version 4.44-assessment-only. Released 2018-12-22. DOI:10.5281/zenodo.2542919.

Ricard, D., Minto, C., Jensen, O.P. and Baum, J.K. (2012) Evaluating the knowledge base and status of commercially exploited marine species with the RAM Legacy Stock Assessment Database. Fish and Fisheries 13 (4) 380-398. DOI: 10.1111/j.1467-2979.2011.00435.x

Spalding, M. D., Fox, H. E., Allen, G. R., Davidson, N., Ferdaña, Z. A., Finlayson, M. A. X., ... & Robertson, J. (2007). Marine ecoregions of the world: a bioregionalization of coastal and shelf areas. *BioScience*, *57*(7), 573-583.

Then, A. Y., Hoenig, J. M., Hall, N. G., Hewitt, D. A., & Handling editor: Ernesto Jardim. (2015). Evaluating the predictive performance of empirical estimators of natural mortality rate using information on over 200 fish species. *ICES Journal of Marine Science*, *72*(1), 82-92.

Appendix B.

Supplementary Material Chapter 2

B.1. Supplementary Methods

B.1.1. Estimation of environmental oxygen and temperature

Species depth ranges

While other studies have used estimates of the environmental temperature at the median depth of the entire observed depth range (taken as the midpoint between the shallowest and deepest depth observed; Barrowclift-Mahon et al. 2023, Pardo & Dulvy 2022), the oxygen availability at this depth is likely not representative of the routinely-experienced conditions in many cases, particularly for species conducting deep dives such as tunas. For example, most tuna species are known to avoid low oxygen and prefer the mixed depth layer, despite occasional dives to depths sometimes exceeding 1000 metres (Arrizabalaga et al. 2015, Nikolic et al. 2017). Thus, the median of their entire observed depth range would fall within the oxygen minimum zone (OMZ), characterized by hypoxic or anoxic oxygen conditions that most tunas are known to avoid or tolerate for only short time intervals. Therefore, this depth estimate was only used when no other data was available on the species' usual depth range. However, the species for which we lacked information on usual depth range were generally either very shallow- or deep-water species, in which case the median of the usual depth ranges were close to the median of the whole depth range (exemplified in infographic Figure B.1) and had similar environmental characteristics (i.e., environmental oxygen and temperature).

Conversion of oxygen concentration to partial pressure in seawater

For the calculation of the in-situ partial pressure of O_2 in seawater at depth across species, we followed the methods of Clarke et al. (2021 supplementary code and Tayler Clarke pers. comm.), which were based on methods in Sarmiento & Gruber (2004), Garcia & Gordon (1992), and Deutsch et al. (2015) and are summarized below.

To calculate the oxygen partial pressure at depth in seawater, we require data on the oxygen concentration, temperature, salinity, density, and depth of a given grid cell. The in-situ density of seawater may be calculated using the Python "*seawater*" package, using the function *sw.dens* (https://github.com/bjornaa/seawater). In this thesis however, we used water density values from the WOA (2018) to calculate the oxygen partial pressure for each grid cell.

Constants

Constants for the saturation concentration of O_2 in seawater [cm^3/dm^3]:

b_1 = 2.00907; b_2 = 3.22014; b_3 = 4.05010; b_4 = 4.94457; b_5 = 0.256847; b_6 = 3.88767; b_7 = 0.00624523; b_8= 0.00737614; b_9 = 0.010341; b_{10}= 0.00817083; b_{11} = 0.000000488682

Gas constant [J/(mol*K)]: R = 8.31

Molar volume O_2 [L/mol]: $GSmv$ = 22.3916

Partial molar volume O_2 [m^3/mol]: pmv = 0.000032

Kelvin conversion [K]: KC = 273.15

Boltzmann constant [J/K]: k = 0.000086173

Model input variables required

Potential temperature [K]: T_{potK}

Salinity [psu]: $salinity$

Oxygen concentration [mol/kg]: $cO2$

Depth [m]: $depth$

Density [kg/m^3]: roh

Conversion of oxygen concentration to partial pressure at depth in seawater

1) Convert potential temperature T_{pot} [K to °C]:

$$T_{pot} = T_{potK} - KC$$

2) Scale T_{pot}:

$$T_{scaled} = \ln\left(\frac{298.15 - T_{pot}}{KC + T_{pot}}\right)$$

3) Calculate the saturation concentration of O_2 in seawater [mmol/m^3]:

$c_{sat\_O2} = \frac{1000}{GSmv} * e^l$, with

$l = b_1 + b_2 * T_{scaled} + b_3 * {T_{scaled}}^2 + b_4 * {T_{scaled}}^3 + b_5 * {T_{scaled}}^4 + b_6 * {T_{scaled}}^5 + salinity * (b_7 + b_8 * T_{scaled} + b_9 * {T_{scaled}}^2 + b_{10} * {T_{scaled}}^3) + b_{11} * salinity^2$

Then, to obtain units [mol/m^3]:

$c_{sat\_O2\_molm3} = \frac{c_{sat\_O2}}{1000}$

4) Calculate the solubility at the surface [mol/(m^3*atm)], i.e. at depth = 0:

$solubility_0 = \frac{c_{sat\_O2\_molm3}}{0.209}$

5) Calculate pressure correction (using water density):

$pressure\_corr = e^{\frac{\frac{depth*roh*9.81*pmv}{R}}{(T_{pot}+KC)}}$

6) Calculate the solubility at any depth [mol/(m^3*atm)]:

$solubility_{depth} = solubility_0 * pressure\_corr$

7) Finally, calculate the partial pressure of O_2 within any grid cell, at any depth [atm]:

$pO2 = \frac{cO2*roh}{solubility_{depth}}$

Table B.1. Comparison of models testing the effects of environmental oxygen concentration, environmental (measurement) temperature, and measurement body mass on metabolic rate (RMR, MMR, or AS) across marine fishes, whilst accounting for evolutionary history and ecological lifestyle. Models were fit in brms using R version 4.0.5. Whole organism metabolic rate (Watts), measurement body mass (grams), and environmental oxygen concentration (μmol/kg) were natural log transformed, while measurement temperature was taken as the inverse temperature (see Methods). All explanatory variables were standardized. All models within 2 looic of the highest-ranking model (emboldened) are highlighted in grey.

a) RMR models (N = 169)		p_{loo}	looic	$elpd_{loo}$	se_elpd_{loo}	$elpd_{diff}$	weight
RMR_mt	$stdlog(M) + std(invtemp) + LS$	36.2	261.3	-130.7	12.8	-3.6	0.068
RMR_mxt	$stdlog(M) * std(invtemp) + LS$	32.9	264.9	-132.4	12.6	-5.4	0.000
RMR_mo	$stdlog(M) + stdlog(DO) + LS$	52.6	328.6	-164.3	10.2	-37.2	0.134
RMR_mxo	$stdlog(M) * stdlog(DO) + LS$	54.5	324.6	-162.3	10.9	-35.2	0.000
RMR_mto	$\boldsymbol{stdlog(M) + std(invtemp) + stdlog(DO) + LS}$	**33.6**	**254.1**	**-127.1**	**12.1**	**0.0**	**0.395**
RMR_mxto	$stdlog(M) * std(invtemp) + stdlog(DO) + LS$	31.5	256.5	-128.3	11.9	-1.2	0.404
RMR_mxot	$stdlog(M) * stdlog(DO) + std(invtemp) + LS$	36.7	256.0	-128.0	12.2	-1.0	0.000
RMR_mtxo	$stdlog(M) + std(invtemp) * stdlog(DO) + LS$	32.3	256.2	-128.1	12.3	-1.0	0.000
b) MMR models (N = 100)							
MMR_mt	$stdlog(M) + std(invtemp) + LS$	30.7	154.8	-77.4	15.9	-20.6	0.068
MMR_mxt	$stdlog(M) * std(invtemp) + LS$	34.1	155.2	-77.6	15.3	-20.7	0.000
MMR_mo	$stdlog(M) + stdlog(DO) + LS$	65.8	143.7	-71.9	7.9	-15.0	0.134
MMR_mxo	$stdlog(M) * stdlog(DO) + LS$	69.4	148.5	-74.3	8.2	-17.4	0.000
MMR_mto	$\boldsymbol{stdlog(M) + std(invtemp) + stdlog(DO) + LS}$	**22.4**	**113.7**	**-56.8**	**7.9**	**0.0**	**0.395**
MMR_mxto	$stdlog(M) * std(invtemp) + stdlog(DO) + LS$	24.6	113.7	-56.8	8.0	0.0	0.404
MMR_mxot	$stdlog(M) * stdlog(DO) + std(invtemp) + LS$	24.3	115.6	-57.8	7.9	-1.0	0.000
MMR_mtxo	$stdlog(M) + std(invtemp) * stdlog(DO) + LS$	23.1	116.0	-58.0	8.0	-1.2	0.000

c) AS models (N = 80)

AS_mt	$stdlog(M) + std(invtemp) + LS$	31.8	149.5	-74.7	13.4	-3.5	0.000
AS _mxt	$stdlog(M) * std(invtemp) + LS$	36.2	145.5	-72.7	12.8	-1.5	0.000
AS _mo	$stdlog(M) + stdlog(DO) + LS$	56.9	146.4	-73.2	9.3	-1.9	0.273
AS _mxo	$stdlog(M) * stdlog(DO) + LS$	57.2	149.6	-74.8	9.3	-3.5	0.000
AS _mto	$stdlog(M) + std(invtemp) + stdlog(DO) + LS$	23.4	144.7	-72.4	15.0	-1.1	0.000
AS _mxto	$\boldsymbol{stdlog(M) * std(invtemp) + stdlog(DO) + LS}$	**29.4**	**142.6**	**-71.3**	**15.5**	**0.0**	**0.727**
AS _mxot	$stdlog(M) * stdlog(DO) + std(invtemp) + LS$	23.9	147.2	-73.6	14.7	-2.3	0.000
AS _mtxo	$stdlog(M) + std(invtemp) * stdlog(DO) + LS$	25.3	146.2	-73.1	15.1	-1.8	0.000

Table B.2. Comparison of models testing the effects of environmental oxygen concentration, environmental temperature, and maximum body mass on r_{max} across marine fishes, whilst accounting for evolutionary history. Models were fit in *brms* using R version 4.0.5. The maximum intrinsic rate of population increase r_{max} (yr^{-1}), maximum body mass (grams), and environmental oxygen concentration (μmol/kg) were natural log transformed, while measurement temperature was taken as the inverse temperature (see Methods). All explanatory variables were standardized. All models within 2 looic of the highest-ranking model (emboldened) are highlighted in grey.

r_{max} models (N = 80)		p_{loo}	looic	$elpd_{loo}$	se_elpd_{loo}	$elpd_{diff}$	weight
rmax_m	$stdlog(M)$	14.5	197.0	-98.5	8.6	-15.3	0.000
rmax_mt	$stdlog(M) + std(invtemp)$	19.2	185.2	-92.6	8.8	-9.4	0.000
rmax_mxt	$stdlog(M) * std(invtemp)$	19.9	187.2	-93.6	8.9	-10.4	0.000
rmax_mo	$stdlog(M) + stdlog(DO)$	13.7	174.1	-87.0	7.7	-3.8	0.000
rmax_mxo	$stdlog(M) * stdlog(DO)$	14.7	176.0	-88.0	7.7	-4.7	0.000
rmax_mto	$\boldsymbol{stdlog(M) + std(invtemp) + stdlog(DO)}$	**16.4**	**166.5**	**-83.2**	**7.9**	**0.0**	**0.808**
rmax_mxto	$stdlog(M) * std(invtemp) + stdlog(DO)$	16.7	167.3	-83.6	7.6	-0.4	0.000
rmax_mxot	$stdlog(M) * stdlog(DO) + std(invtemp)$	17.5	168.0	-84.0	8.1	-0.8	0.000
rmax_mtxo	$stdlog(M) + std(invtemp) * stdlog(DO)$	19.6	169.0	-84.5	7.7	-1.3	0.192

Table B.3. Comparison of models testing the effects of environmental oxygen partial pressure, environmental (measurement) temperature, and measurement body mass on metabolic rate (RMR, MMR, or AS) across marine fishes, whilst accounting for evolutionary history and ecological lifestyle. Environmental oxygen partial pressure and temperature were estimated at the lower (deepest) limit of the usual depth range for each species across grid cells overlapping with its core distribution. Models were fit in brms using R version 4.0.5. Whole organism metabolic rate (Watts), measurement body mass (grams), and environmental oxygen partial pressure (atm) were natural log transformed, while measurement temperature was taken as the inverse temperature (see Methods). All explanatory variables were standardized. All models within 2 looic of the highest-ranking model (emboldened) are highlighted in grey.

a) RMR models (N = 169)		p_{loo}	looic	$elpd_{loo}$	se_elpd_{loo}	$elpd_{diff}$	weight
RMR_mt	$stdlog(M) + std(invtemp) + LS$	37.4	264.4	-132.2	12.8	-2.1	0.432
RMR_mxt	$stdlog(M) * std(invtemp) + LS$	35.2	268.7	-134.3	12.6	-4.2	0.000
RMR_mo	$stdlog(M) + stdlog(PO2) + LS$	52.5	326.0	-163.0	10.7	-32.9	0.000
RMR_mxo	$stdlog(M) * stdlog(PO2) + LS$	54.1	318.3	-159.1	10.6	-29.1	0.038
RMR_mto	$stdlog(M) + std(invtemp) + stdlog(PO2) + LS$	34.7	265.7	-132.8	12.3	-2.8	0.000
RMR_mxto	$stdlog(M) * std(invtemp) + stdlog(PO2) + LS$	32.4	268.5	-134.3	12.0	-4.2	0.000
RMR_mxot	$\boldsymbol{stdlog(M) * stdlog(PO2) + std(invtemp) + LS}$	**37.1**	**260.2**	**-130.1**	**12.3**	**0.0**	**0.529**
RMR_mtxo	$stdlog(M) + std(invtemp) * stdlog(PO2) + LS$	34.3	268.2	-134.1	12.4	-4.0	0.000
b) MMR models (N = 100)							
MMR_mt	$stdlog(M) + std(invtemp) + LS$	28.1	156.3	-78.2	14.8	-13.8	0.151
MMR_mxt	$stdlog(M) * std(invtemp) + LS$	30.4	159.0	-79.5	14.9	-15.2	0.000
MMR_mo	$stdlog(M) + stdlog(PO2) + LS$	53.8	162.1	-81.0	7.6	-16.7	0.056
MMR_mxo	$stdlog(M) * stdlog(PO2) + LS$	55.9	162.9	-81.5	7.7	-17.1	0.000
MMR_mto	$\boldsymbol{stdlog(M) + std(invtemp) + stdlog(PO2) + LS}$	**20.0**	**128.7**	**-64.3**	**8.4**	**0.0**	**0.793**
MMR_mxto	$stdlog(M) * std(invtemp) + stdlog(PO2) + LS$	21.3	130.9	-65.4	8.3	-1.1	0.000
MMR_mxot	$stdlog(M) * stdlog(PO2) + std(invtemp) + LS$	21.8	131.5	-65.8	8.5	-1.4	0.000

MMR_mtxo	$stdlog(M) + std(invtemp) * stdlog(PO2) + LS$	21.1	131.2	-65.6	8.3	-1.3	0.000
c) AS models (N = 80)							
AS_mt	$stdlog(M) + std(invtemp) + LS$	23.0	153.4	-76.7	13.1	-2.8	0.000
AS _mxt	$stdlog(M) * std(invtemp) + LS$	25.1	154.1	-77.1	13.0	-3.1	0.000
AS _mo	$stdlog(M) + stdlog(PO2) + LS$	36.1	167.3	-83.6	9.6	-9.7	0.122
AS _mxo	$stdlog(M) * stdlog(PO2) + LS$	35.3	170.7	-85.4	9.5	-11.4	0.000
AS _mto	$\boldsymbol{stdlog(M) + std(invtemp) + stdlog(PO2) + LS}$	**19.1**	**147.9**	**-73.9**	**15.3**	**0.0**	**0.639**
AS _mxto	$stdlog(M) * std(invtemp) + stdlog(PO2) + LS$	21.7	148.5	-74.2	15.3	-0.3	0.238
AS _mxot	$stdlog(M) * stdlog(PO2) + std(invtemp) + LS$	19.7	150.4	-75.2	15.1	-1.3	0.000
AS _mtxo	$stdlog(M) + std(invtemp) * stdlog(PO2) + LS$	20.0	149.9	-74.9	15.8	-1.0	0.000

Table B.4. Comparison of models testing the effects of environmental oxygen partial pressure, environmental temperature, and maximum body mass on population growth rate r_{max} across marine fishes, whilst accounting for evolutionary history. Environmental oxygen partial pressure and temperature were estimated at the lower (deepest) limit of the usual depth range for each species across grid cells overlapping with its core distribution. Models were fit in brms using R version 4.0.5. The maximum intrinsic rate of population increase r_{max} (yr^{-1}), maximum body mass (grams), and environmental oxygen partial pressure (atm) were natural log transformed, while measurement temperature was taken as the inverse temperature (see Methods). All explanatory variables were standardized. All models within 2 looic of the highest-ranking model (emboldened) are highlighted in grey.

r_{max} models (N = 80)		p_{loo}	looic	$elpd_{loo}$	se_elpd_{loo}	$elpd_{diff}$	weight
rmax_m	$stdlog(M)$	14.5	196.8	-98.4	8.6	-11.3	0.000
rmax_mt	$stdlog(M) + std(invtemp)$	19.4	185.9	-92.9	8.4	-5.9	0.056
rmax_mxt	$stdlog(M) * std(invtemp)$	20.1	187.9	-93.9	8.5	-6.9	0.000
rmax_mo	$stdlog(M) + stdlog(PO2)$	13.9	179.3	-89.7	7.6	-2.6	0.000
rmax_mxo	$stdlog(M) * stdlog(PO2)$	15.5	181.2	-90.6	7.8	-3.5	0.000
rmax_mto	$\boldsymbol{stdlog(M) + std(invtemp) + stdlog(PO2)}$	**16.9**	**174.2**	**-87.1**	**7.7**	**0.0**	**0.411**
rmax_mxto	$stdlog(M) * std(invtemp) + stdlog(PO2)$	17.2	175.3	-87.6	7.5	-0.5	0.000
rmax_mxot	$stdlog(M) * stdlog(PO2) + std(invtemp)$	18.3	174.2	-87.1	7.9	0.0	0.533
rmax_mtxo	$stdlog(M) + std(invtemp) * stdlog(PO2)$	17.9	176.7	-88.3	8.4	-1.3	0.000

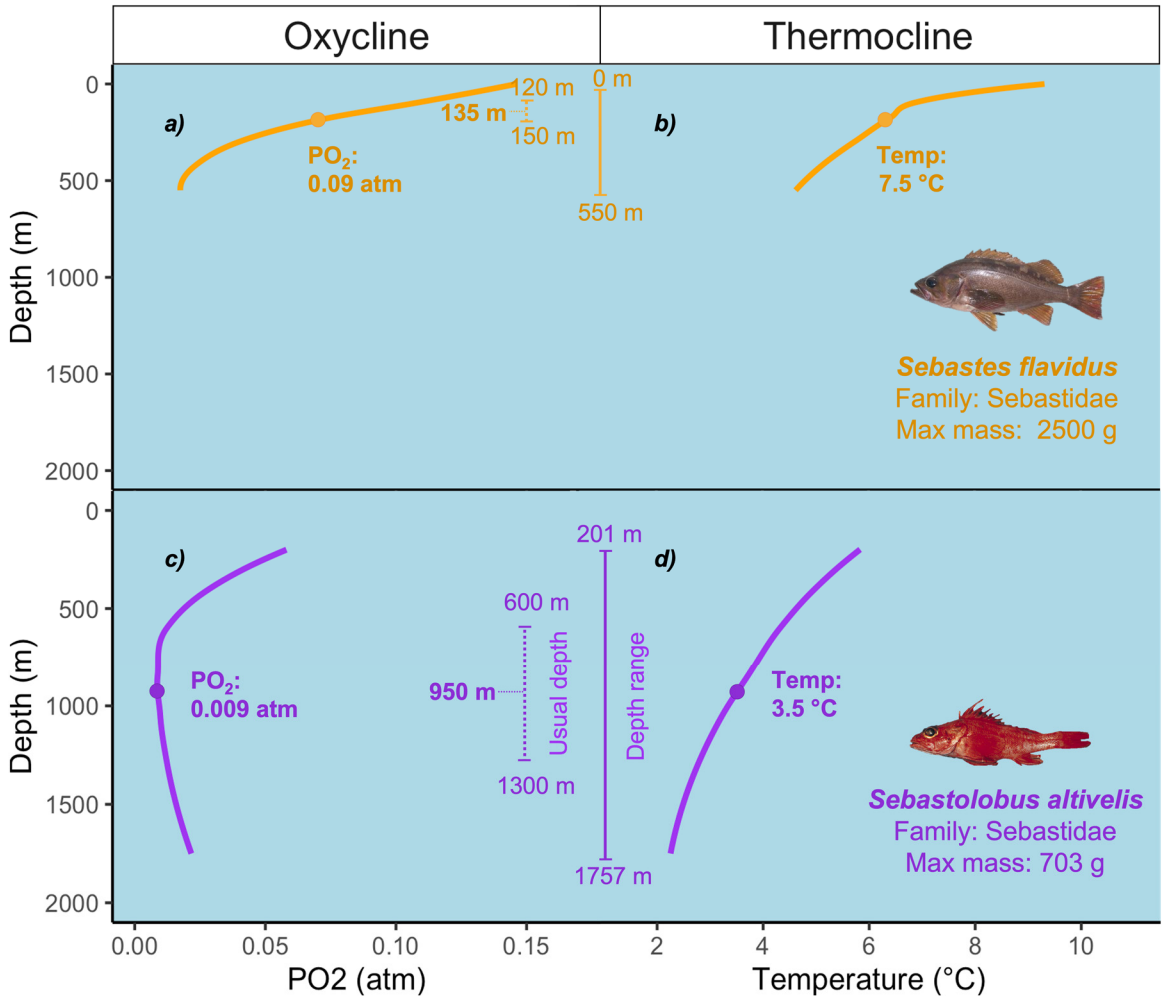

Figure B.1. Estimating mean environmental oxygen partial pressure (atm) and temperature (°C) at usual depth: examplary cases for two rockfish species from the family *Sebastidae*. Oxyclines and thermoclines for the yellowtail rockfish, *Sebastes flavidus* (in orange; *a,b*) and the longspine thornyhead, *Sebastolobus altivelis* (in purple; *c,d*), showing changes in the mean oxygen partial pressure (*a,c*) or temperature (*b,d*) with depth across the core distribution of each species. The circle on each cline marks the mean oxygen or temperature at the median usual depth. The full depth ranges are shown by solid vertical lines, and the usual depth ranges by dotted lines, along with the median of the usual depth range. This figure shows that for intermediate depth species, the environmental oxygen and temperature at median usual depth might be quite different (e.g. for *Sebastes flavidus*, in orange), while for very shallow-water or very deep-sea species (e.g., *Sebastolobus altivelis*, in purple) the environmental conditions at the median of the full depth range often resemble those at the median of their usual depth range, and thus is generally a good proxy of the median usual depth for these species.

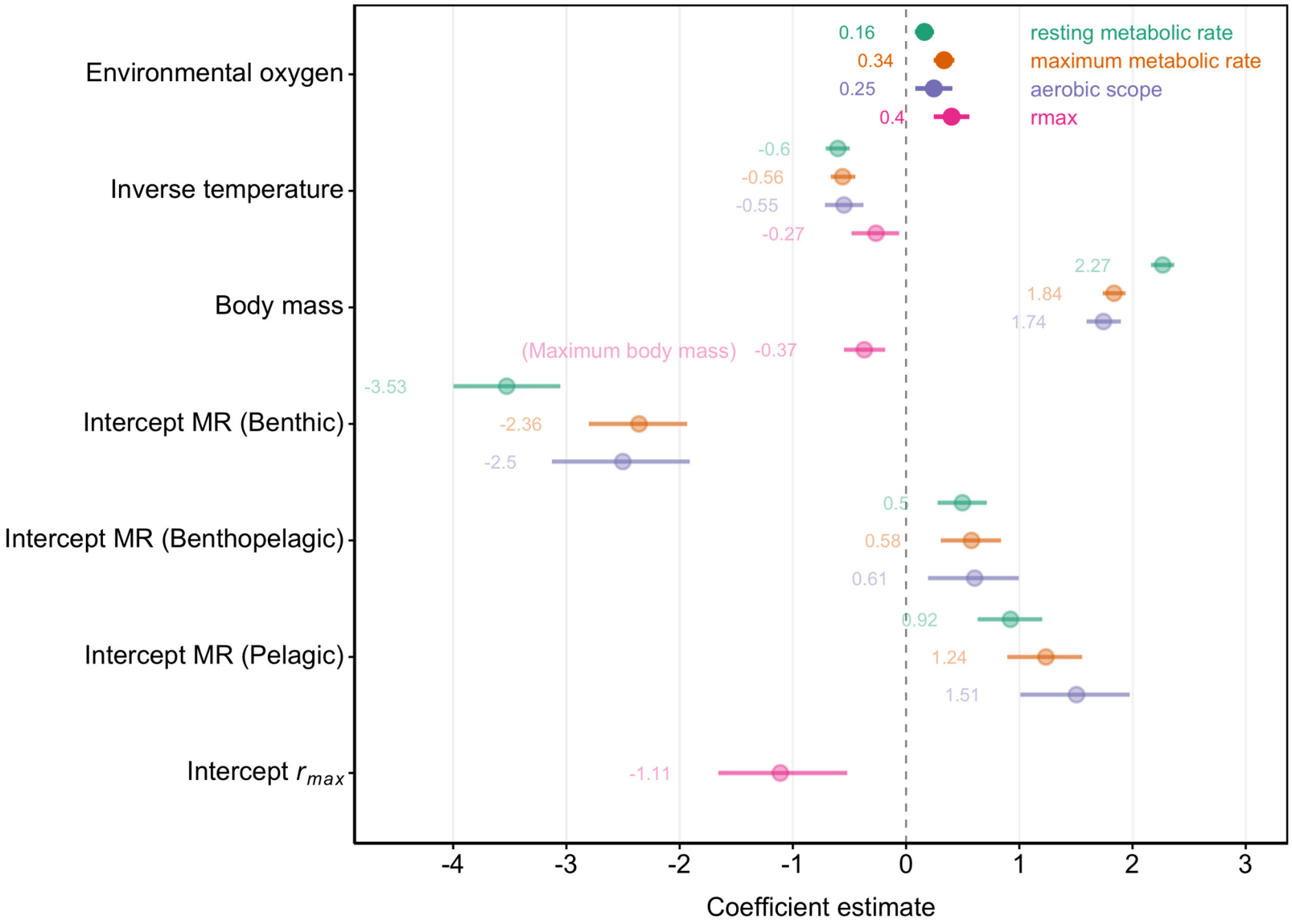
Environmental oxygen
Inverse temperature
Body mass
Intercept MR (Benthic)
Intercept MR (Benthopelagic)
Intercept MR (Pelagic)
Intercept r_{max}
0.16
0.34
0.25
0.4
resting metabolic rate
maximum metabolic rate
aerobic scope
rmax
-0.6
-0.56
-0.55
-0.27
2.27
1.84
1.74
(Maximum body mass)
-0.37
-3.53
-2.36
-2.5
0.5
0.58
0.61
0.92
1.24
1.51
-1.11
-4
-3
-2
-1
0
1
2
3
Coefficient estimate

Figure B.2. Environmental oxygen is a key factor in shaping metabolic rate (particularly MMR and AS) and r_{max} across fishes. Coefficients plot of the effects of environmental oxygen and temperature on resting metabolic rate 'RMR' (in green, N=169), maximum metabolic rate 'MMR' (in orange, N=100), and aerobic scope 'AS' (in purple, N=80), and r_{max} (in pink, N=80), whilst accounting for effects of environmental temperature, body mass, evolutionary, and ecological lifestyle (for metabolic rates). The metabolic rate intercepts (Intercept MR) correspond to the metabolic rates of 'Benthic', 'Benthopelagic', or 'Pelagic' species at the mean body mass, temperature, and r_{max} of the dataset. Metabolic rates and all explanatory variables were natural log-transformed, except for measurement temperature which was taken as the inverse temperature (see Methods). For metabolic rate, body mass was the measurement body mass and temperature was the measurement temperature, taken at the closest temperature to environmental temperature (the relationship between measurement and environmental temperature having Pearson's r ~0.95). For r_{max}, body mass was the maximum observed body mass and temperature was the environmental temperature. All explanatory variables were standardized to allow for the direct comparison between the explanatory variables of a given model.

B.2. References

Arrizabalaga, H., Dufour, F., Kell, L., Merino, G., Ibaibarriaga, L., Chust, G., ... & Bonhomeau, S. (2015). Global habitat preferences of commercially valuable tuna. *Deep Sea Research Part II: Topical Studies in Oceanography*, *113*, 102-112.

Barrowclift, E., Gravel, S. M., Pardo, S. A., Bigman, J. S., Berggren, P., & Dulvy, N. K. (2023). Tropical rays are intrinsically more sensitive to overfishing than the temperate skates. *Biological Conservation*, *281*, 110003.

Clarke, T. M., Wabnitz, C. C., Striegel, S., Frölicher, T. L., Reygondeau, G., & Cheung, W. W. (2021). Aerobic growth index (AGI): An index to understand the impacts of ocean warming and deoxygenation on global marine fisheries resources. Progress in Oceanography, 195, 102588.

Garcia, H. E., & Gordon, L. I. (1992). Oxygen solubility in seawater: Better fitting equations. *Limnology and oceanography*, *37*(6), 1307-1312.

Nikolic, N., Morandeau, G., Hoarau, L., West, W., Arrizabalaga, H., Hoyle, S., ... & Fonteneau, A. (2017). Review of albacore tuna, Thunnus alalunga, biology, fisheries and management. *Reviews in fish biology and fisheries*, *27*, 775-810.

Pardo, S. A., & Dulvy, N. K. (2022). Body mass, temperature, and depth shape the maximum intrinsic rate of population increase in sharks and rays. *Ecology and Evolution*, *12*(11), e9441.

Sarmiento, J. L., & Gruber, N. (2004). Oceanic carbon cycle, atmospheric CO2, and climate. *Ocean Biogeochemical Dynamics*, 1-99.